

Oil Upgrading by Molecular Rearrangement and Cracking: A Study Using Model Compounds
and Natural Chabazite

by

Gonzalo Rocha Aguilera

A thesis submitted in partial fulfillment of the requirements for the degree of

Doctor of Philosophy

In Chemical Engineering

Department of Chemical and Materials Engineering
University of Alberta

© Gonzalo Rocha Aguilera, 2015

Abstract

As demand for fuel increases, new technologies that can convert heavy oil and bitumen into light fuels are needed. Natural zeolites have been proven to catalyze reactions that decrease molecular weight, density, nitrogen, and metals content as well as vacuum residue content when mixed with raw oil sands at cracking conditions. Chabazite is an abundant and inexpensive natural zeolite with high acidity and a platy morphology that could be used for a new upgrading process for bitumen and heavy oils.

In this work, model compounds were used to determine the mode of action of the chabazite towards nitrogen compounds, porphyrins, alkanes and substituted aromatics. Sulfur compounds were not studied here since previous studies suggest that the chabazite is not highly active towards such compounds. Indole and octaethylprophyrin (OEP) (in Ni and vanadyl form) were used as model compounds for nitrogen and metals. Both compounds were used in solution with 1-methylnaphthalene as solvent.

Using indole as model compound, 43% indole removal and 17% nitrogen removal was achieved. Ni and vanadyl octaethylprophyrin were also used and the chabazite was able to remove up to 47.5% vanadium. Hexadecane was also used and a conversion up to 10.1% was achieved. All those reactions were done at 400 °C for 1 hr using a catalyst load of 10%. Cumene was reacted at 300 °C for 4 hr giving a maximum conversion of 25.1%. Up to 90% nickel removal was obtained at room temperature at equilibrium.

The main reaction observed in those systems was transalkylation. Cumene, indole, OEP and the solvent underwent transalkylation reactions. Other reactions observed were opening of the pyrrolic ring, demetalation of porphyrins and cracking. With this observation, reactions were made using artificial oil sands. The addition of 2,2,4-trimethylpentane as methyl groups donor increased the conversion of the vacuum residue contained in the artificial oil sands

Reaction paths for the nitrogen and metals removal were proposed. For indole, the non-basic nitrogen was converted to basic nitrogen (aniline) and then adsorbed into the surface of the chabazite. Metals were removed through demetalation of the porphyrin and adsorption.

During this study, it was also observed that chabazite is more active than zeolite Y for cumene cracking while zeolite Y is more active towards hexadecane cracking. It was also observed that both Lewis and Brønsted-Lowry acid sites play different roles. Indole seems to preferentially adsorb into Brønsted-Lowry acid sites preventing them from participating in further reactions. Cumene-indole conjugated products, however, were observed.

The role of the water was also studied but no definitive conclusions were drawn. Water seems to affect preferentially the Brønsted-Lowry acid sites. It also seems to adsorb competitively thus preventing some molecules from adsorption. It also increases the dispersion of the catalyst and reduces coke formation.

The results presented in this study opens the possibility to create a new oil upgrading process through simultaneous cracking and molecular rearrangement using cheap and abundant material such as natural zeolites. More studies on the addition of alkyl-donating molecules to increase the

activity of the zeolite are recommended. It is also suggested to study the activity of the chabazite towards different feeds including vacuum residue, asphaltenes and heavy gas oil.

Preface

I designed the experiments, collected the data, and analyzed the results for the majority of the work continued in this thesis. This thesis contains, however, a small amount of work by Dr. Abu S. M. Junaid and MSc Vikas Gupta. Chapter 2 was published as Rocha Aguilera, G; Gupta, VG; Yang, SF; Kuznicki, SM; McCaffrey, WC; *Energy & Fuels*, 28 (10), 2014, 6570-6578. In this paper I was responsible for experimental design, most of the data collection, interpretation and of all the manuscript composition. Data on quinoline reactions was collected and analyzed by MSc Vikas Gupta and reinterpreted by myself. Some data on indole was collected by Dr. Shaofeng Yang. Dr. William C. McCaffrey and Dr. Steven M. Kuznicki were the supervisory authors.

Chapter 3 was submitted for publication and is currently under review and Chapter 4 will be sent for publication in a near future. In both papers I was responsible for most of the data collection, interpretation and all the manuscript composition. Some of the data was collected by Dr. Shaofeng Yang and MSc David Dhin. Experiments on the artificial oil sands were designed in collaboration with MSc David Dhin. Dr. William C. McCaffrey and Dr. Steven M. Kuznicki were the supervisory authors. Data on metals removal from raw oil sands was collected and analyzed by Dr. Abu S. M. Junaid.

Data from chapters 2, 3 and 4 was used to file for Kuznicki, S.M., McCaffrey, W.C., Junaid A.S.M., Rocha Aguilera, G. U.S. patent 62/148,122, filed on April, 2015.

Acknowledgments

The author wish to acknowledge the following organization for the financial support

- National Council for Science and Technology (CONACyT) – Mexico
- Centre for Oil Sands Innovation (COSI)
- Department of Chemical and Materials Engineering at the University of Alberta
- Helmholtz-Alberta Initiative (HAI)

The author also want to thanks Dr. William C. McCaffrey and Dr. Steven M. Kuznicki for their support during this work. Also, thanks to Dr. Jeff Stryker for his invaluable comments.

The author acknowledges the support of Dr. Shaofeng Yang and MSc. David Dhin in the gathering of data.

The work presented here contains data gracefully provided by Dr. Abu S. M. Junaid and MSc Vikas Gupta.

The author thanks the members of the committee: Dr. Rajender Gupta, Dr. John Shaw and Dr. Kevin Smith for their time and comments.

Also, the author acknowledges the technical support from the NMR spectroscopy facility from the Department of Chemistry at the University of Alberta, The Alberta Centre for Surface Engineering and Science (ACSES), Dr. Wayne Moffat, Andree Koenig and Dr. Richard Rothery.

Contents

ABSTRACT	II
PREFACE.....	V
ACKNOWLEDGMENTS	VI
CONTENTS.....	VII
LIST OF FIGURES	X
LIST OF TABLES	XIII
ABBREVIATIONS	XV
1 INTRODUCTION.....	1
2 PYRROLIC RING OPENING AND NITROGEN REMOVAL FROM SOLUTION WITHOUT HYDROGENATION: NATURAL CHABAZITE AS A CRACKING CATALYST.....	16
2.1 PREFACE	16
2.2 INTRODUCTION	17
2.3 EXPERIMENTAL SECTION	21
2.3.1 <i>Materials</i>	21
2.3.2 <i>Reactions</i>	21
2.3.3 <i>Product recovery and analysis</i>	22
2.3.4 <i>Adsorption Studies</i>	23
2.4 RESULTS	24
2.4.1 <i>Quantification of reaction products</i>	24
2.4.2 <i>Identification of products</i>	27
2.4.3 <i>Spent Catalyst Characterization</i>	29
2.4.4 <i>Chemical resistance tests</i>	30
2.4.5 <i>Aniline adsorption</i>	31
2.5 DISCUSSION	31

2.5.1	<i>Reaction Path</i>	31
2.5.2	<i>Nitrogen Removal</i>	37
2.5.3	<i>Effect of Surface Acidity and Water Addition</i>	38
2.5.4	<i>Chemical Resistance</i>	39
2.5.5	<i>Industrial Applications</i>	40
2.6	CONCLUSIONS	40
3	NI AND V REMOVAL FROM OIL AND MODEL COMPOUNDS WITHOUT HYDROGENATION: NATURAL CHABAZITE AS SOLID ACID.....	42
3.1	PREFACE	42
3.2	INTRODUCTION	42
3.3	EXPERIMENTAL.....	45
3.3.1	<i>Materials</i>	45
3.3.2	<i>Reactions</i>	48
3.3.3	<i>Product analysis</i>	49
3.4	RESULTS	50
3.5	DISCUSSION	55
3.6	CONCLUSIONS.....	63
4	CRACKING AND TRANSALKYLATION OF OIL AND MODEL COMPOUNDS: NATURAL CHABAZITE AS SOLID ACID.....	64
4.1	PREFACE	64
4.2	INTRODUCTION	65
4.3	EXPERIMENTAL SECTION	71
4.3.1	<i>Materials</i>	71
4.3.2	<i>Artificial Oil Sands</i>	71
4.3.3	<i>Reactions</i>	71
4.3.4	<i>Analysis</i>	72
4.4	RESULTS	74
4.5	DISCUSSION	82

4.6	CONCLUSIONS.....	88
5	GENERAL CONCLUSION.....	89
6	RECOMMENDATIONS.....	91

List of Figures

<i>Figure 1. β-scission of a linear alkane</i>	6
<i>Figure 2. Schematic of a visbreaking process.</i>	8
<i>Figure 3. Schematic of a delayed coking process.</i>	9
<i>Figure 4. Schematic of the fluid coking</i>	10
<i>Figure 5. Schematic of a typical ebullating bed hydroconversion unit.</i>	11
<i>Figure 6. Numbering convention for indole</i>	19
<i>Figure 7. Conversion of 2, 3 dihydroindole using different types of zeolites. ♦ Clinoptilolite, ■ Chabazite, ▲ Zeolite Y. 1 h reaction, 10% catalyst loading.</i>	26
<i>Figure 8. Major reaction products for indole and 1-methynaphthalene reactions</i>	28
<i>Figure 9. Typical XPS results N 1s region after 1 h reaction at 400 °C. (10% Ca-chabazite loading, 0.2% nitrogen solution added as indole)</i>	30
<i>Figure 10. Indole reactions to form a dimer and trimer⁶⁴</i>	33
<i>Figure 11. Trimer cracking for direct aniline/toluidine formation</i>	34
<i>Figure 12. Possible reaction network for indole cracking in presence of chabazite.</i>	36
<i>Figure 13. Structures of (A) vanadyl deoxophylloerythroetioporphyrin and (B) vanadyl etioporphyrin</i>	44
<i>Figure 14. Structures of (A) 2,3,7,8,12,13,17,18-Octaethyl-21H,23H-porphine vanadium(IV) oxide and (B) 2,3,7,8,12,13,17,18-Octaethyl-21H,23H-porphine nickel(II)</i>	48
<i>Figure 15. EPR spectra for OEP-VO in 1-methylnaphthalene solution after 1 hr reaction at 400 °C with 10% loading of Ca-chabazite. Initial concentration of vanadium was 140 ppm. ...</i>	52
<i>Figure 16. EPR spectra for spent Ca-chabazite after 1 hr reaction with a solution of OEP-VO in 1-methylnaphthalene at 400 °C. Initial concentration of vanadium in the solution was 140 ppm.</i>	53

Figure 17. XPS spectra, N 1s region. A) Ca-chabazite impregnated with OEP-VO solution (reference sample); B) Ca-chabazite impregnated with OEP-Ni solution (reference sample); C) 1H-chabazite after reaction with OEP-V, 400 °C, 1 hr , 1% water added; D) Ca-chabazite after reaction with OEP-Ni, 400°C, 1 hr, no water added.....	60
Figure 18. Possible reaction network for OEP in presence of chabazite. Dashed lines indicate demetalation and full lines indicate dealkylation.	62
Figure 19. Main reactions network for cracking process of hydrocarbon molecules ¹³⁷	67
Figure 20: Possible reaction path of cumene over zeolites ¹³⁸	69
Figure 21. SimDist results for oil sands reactions: *Unreacted oil sands (reference), ^X thermal reaction, ⁺ Ca-chabazite 10% loading, ⁻ Ca-Chabazite 10% loading plus 0.03g water plus 0.3g TMP. All reactions performed at 380 °C for 1 h.	74
Figure 22. Hexadecane conversion after reaction at 400 °C, 1 hour, 10% catalyst loading. No-added water in black, 0.1% water added in white. Average standard deviation: 3.9% standard deviation. Thermocracking with 0.1% water was not determined.	75
Figure 23. Terminal / Internal olefin ratio in hexadecane after reaction at 400 °C, 1 hour, 10% catalyst loading.....	77
Figure 24. Produced olefin / produced paraffin ratio in hexadecane after reaction at 400 °C, 1 hour, 10% catalyst loading.....	77
Figure 25. Cumene conversion after reaction at 300 °C, 4 hours, 10% catalyst loading. No-added water in black, 0.1% water added in white. 6.7% standard deviation.	78
Figure 26. Cumene conversion in the presence of indole. x no water added, ● 1% water added. 420 °C, 1h, 10% Ca-chabazite loading.....	80
Figure 27. Gas production for cumene cracking reactions as a function of initial indole concentration. 10% Ca-chabazite as catalyst, 420 °C, 1 hour, no water added.	81
Figure 28. Selectivity (percentage) towards benzene (black) and cymene (white). 10% catalyst loading (calcium chabazite unless otherwise noted), 420 °C, 1 hour reaction. 2.5% w/w initial concentration of indole.....	81

Figure 29. Solubility parameter of various substituted aromatics vs number of aliphatic carbons. n-Heptane shown as reference. Blue line indicates the value for n-heptane. The red line indicates the value for toluene. Orange dots for Hildebrand parameter, Blue dots for Hansen parameter..... 87

List of Tables

<i>Table 1. Typical properties of Athabasca bitumen⁵</i>	<i>2</i>
<i>Table 2. Distillation products of Athabasca bitumen⁵</i>	<i>2</i>
<i>Table 3. Worldwide process capacity for heavy oil and residue processing¹⁶</i>	<i>5</i>
<i>Table 4. Comparison of thermal vs catalytic cracking products. Adapted from ¹⁹</i>	<i>6</i>
<i>Table 5. Indole and nitrogen removal from a 0.2% w/w nitrogen solution at 400 °C, 1 h reaction, 10 % chabazite catalyst loading.</i>	<i>24</i>
<i>Table 6. Nitrogen balance of indole reaction over Ca-chabazite. Based on 7.5 mg of initial nitrogen. (0.2% w/w nitrogen solution at 400 °C, 1 h reaction, 10% ca-chabazite loading, no added water)</i>	<i>25</i>
<i>Table 7. Conversion of quinoline using clinoptilolite (0.2 % w/w nitrogen solution, 1 h reaction, 10% catalyst loading)</i>	<i>26</i>
<i>Table 8. Results for ¹H-NMR and IR spectroscopies for non-volatile products after reaction</i>	<i>27</i>
<i>Table 9. XPS results after 1 h reaction at 400 °C, 0.2 % w/w nitrogen (added as indole), 10% chabazite catalyst loading</i>	<i>29</i>
<i>Table 10. Indole removal from a 2.0% w/w nitrogen solution at 400 °C, 1 h reaction, 10 % catalyst loading</i>	<i>31</i>
<i>Table 11. Composition of untreated oil sands and extracted bitumen</i>	<i>47</i>
<i>Table 12. Vanadium concentration (ppm) for whole oil sands for both starting oil sands and after reaction at 350 °C for 1 hr, 10% catalyst loading.....</i>	<i>51</i>
<i>Table 13. Vanadium and nitrogen removal (percentage from initial concentration) from OEP-VO solutions after 1 hr at 400 °C, 10% catalyst loading, 140 ppm initial vanadium concentration, 154.0 ppm initial nitrogen concentration.</i>	<i>53</i>
<i>Table 14. Vanadium concentration in spent catalyst after 1 hr at 400 °C, 10% catalyst loading, 140 ppm initial vanadium concentration using OEP-VO.....</i>	<i>54</i>

<i>Table 15. C 1s XPS bands for spent catalyst of OEP-VO solution after 1 hr at 400 °C, 10% catalyst loading, 140 ppm initial vanadium concentration. Position in eV.....</i>	<i>55</i>
<i>Table 16. N 1s XPS bands for spent catalyst for OEP-Ni solution after 1 hr at 400 °C, 10% catalyst loading, 140 ppm initial vanadium concentration. Position in eV.....</i>	<i>55</i>
<i>Table 17. C 1s XPS bands for spent catalyst of OEP-Ni solution after 1 hr at 400 °C, 10% catalyst loading, 66 ppm initial nickel concentration. Position in eV.....</i>	<i>56</i>
<i>Table 18. N 1s XPS bands for spent catalyst of OEP-Ni solution after 1 hr at 400 °C, 10% catalyst loading, 66 ppm initial nickel concentration. Position in eV.....</i>	<i>57</i>
<i>Table 19. Summary of the main cumene acid catalysed reaction products¹³⁸.....</i>	<i>68</i>
<i>Table 20. Parameters for GC analysis of cumene and n-hexadecane reaction products.....</i>	<i>73</i>
<i>Table 21. Integration ranges for ¹H-NMR spectroscopy of hexadecane reaction products.....</i>	<i>76</i>
<i>Table 22. Liquid reaction products for chabazite and zeolite Y catalysed cracking of cumene... </i>	<i>79</i>
<i>Table 23. Hexadecane / cumene conversion ratio. 10% catalyst loading. For hexadecane, 400 °C, 1 hour reaction. For cumene, 300 °C, 4 hours reaction.....</i>	<i>83</i>
<i>Table 24. Solubility parameters of selected aromatic molecules. n-Heptane solubility included as reference¹⁵⁶.....</i>	<i>86</i>

Abbreviations

$^1\text{H-NMR}$	Proton Nuclear Magnetic Resonance
AMW	Average Molecular Weight
DSC	Differential Scanning Calorimetry
EPR	Electron Paramagnetic Resonance
FCC	Fluid Catalytic Cracking
FID	Flame Ionization Detector
FWHM	Full Width at Half Maximum
GC	Gas Chromatograph
HDM	Hydrodemetalization
HDN	Hydrodenitrogenation
HDS	Hydrodesulfurization
INAA	Instrumental Neutron Activation Analysis
IPA	iso-Propylamine
IR	Infrared
MS	Mass Spectroscopy
NMR	Nuclear Magnetic Resonance
NNN	Next Nearest Neighbor
OEP	2,3,7,8,12,13,17,18-Octaethyl-21H,23H-porphine
OEP-Ni	2,3,7,8,12,13,17,18-Octaethyl-21H,23H-porphine nickel(II)

OEP-VO	2,3,7,8,12,13,17,18-Octaethyl-21H,23H-porphine vanadium(IV) oxide
PFPD	Pulsed Flame Photometric Detector
SARA	Saturates, Aromatics, Resins and Asphaltenes
SCR	Selective Catalytic Reduction
TBP	True Boiling Point
TGA	Thermo-Gravimetric Analysis
TMP	2,2,4 trimethylpentane
UV	Ultraviolet
VR	Vacuum Residue
XPS	X-Ray Photoelectron Spectroscopy
XRD	X-Ray Diffraction

1 Introduction

In 2010, oil products supplied 32% of the energy consumed worldwide and this percentage has not change significantly since 1990¹. Being the third biggest reserves, Canadian oil sands situated in Alberta, are an important energy source; however, they present very complex technical issues from the extraction to the processing and transport. It is estimated that 2/3 of the oil sands are either too shallow to be extracted by steam injection or too deep for surface mining². In addition to that, the high viscosity and density ($> 10^4$ mPa s and < 10 °API)³ and the large concentration of heteroatoms makes the oil sands difficult to process.

The most accepted theory about the origin of the Alberta oil sands, is that they started as an organic-rich shale in western portion of the province. The organic material contained in the shale polymerized to form a matrix called kerogen. Subjected to high pressures and heating rates between 1-25 °C/Ma, the kerogen transformed into crude oil. The oil formed in southwestern Alberta migrated north. During this migration, the oil was heavily biodegraded losing the light components and became enriched in high molecular weight material⁴.

The amount of bitumen found in the oil sands is variable. The ores are considered to be low grade if the amount of bitumen is between 6 -9 %, an average ore contains 9 – 12 % oil and more than 12% bitumen, high grade³. Sand and clay comprise 80 to 85 % of the oil sand and 4 – 6 % water is also found⁵. The structure of the oil sands is dense with small voids. It has been suggested that the oil components bind the grains together. The position of the water is still under discussion. Different theories say that the water is present at the grain to grain contact points, as a thin layer around the sand grains or within the fines⁶.

The bitumen composition is highly complex and its composition and properties vary from reservoir to reservoir and even within the reservoir. For example, it is known that the asphaltene content increases with increasing depth within the reservoir³. Table 1 illustrates some typical properties of Athabasca bitumen. It terms of boiling points, bitumen contains few low temperature boiling compounds and more than 50% vacuum residue.

Table 2 shows the distilled product yields for Athabasca bitumen.

Table 1. Typical properties of Athabasca bitumen⁵.

Property	Value
Density at 15 °C (g/ml)	0.9931
API gravity	11.0
Sulfur (wt %)	4.40
Nitrogen (wppm)	5390
Hydrogen (wt %)	10.45
Carbon (wt%)	82.82
H/C atomic ratio	1.53
Viscosity at 20 °C (m ² /s)	0.025

Table 2. Distillation products of Athabasca bitumen⁵

Product	Yield (vol %)
Virgin LGO	13.5
Vacuum LGO	6.3
Vacuum HGO	23.8
Vacuum residue	56.4

Determining the composition of the bitumen is very complex due to the wide variety of molecules that are present. The most popular methods for oil characterization are based either on boiling point as the true boiling point method (TBP) (ASTM D2892), simulated distillation (ASTM D2887) and vacuum distillation (ASTM D1160); or in solubility / adsorption as the SARA (ASTM D4124) method (saturates, aromatics, resins and asphaltenes) or the USBM-API-60 method. While both, boiling point and solubility / adsorption methods are critical for the industry, they give limited information from the chemical point of view. The SARA method is

more popular than the USBM-API-60 due to its simplicity and consist in the separation of the asphaltenes by precipitation with n-heptane followed by a chromatographic separation over alumina to obtain the saturates, aromatics and resins fractions.

The saturates fraction is the most valuable one. Athabasca bitumen contains 22 to 25 % saturates and 90% of these molecules are polycyclic hydrocarbons⁷. Analysis of Athabasca bitumen from a strip mine operation shows no acyclic saturates⁷, while the same analysis for Cold Lake bitumen from in-depth collection shows measurable amounts of both straight chain and branched saturated hydrocarbons⁸.

The aromatic fraction accounts for 64% of the maltene (pentane soluble) fraction. This fraction contains 80% of molecules with less than 50 carbon atoms. This fraction tends to be non-polar and contains low oxygen and nitrogen concentration, high H/C ratio and moderate sulfur content. Sulfur in this fraction is mainly present as aromatic thiophenes and the rest of the sulfur is in form of saturated sulfides. Straight hydrocarbon chains are usually not present in this fraction and the molecules contain at least one aromatic ring⁹.

Resins, sometimes referred to as polar fraction, are similar to the asphaltene fraction but, contrary to the asphaltenes, they are soluble in pentane. This fraction is hard to characterize not only because of the wide range of structures present, but also because of their physical and chemical properties. It is known that resins can adsorb on the asphaltenes making the quantification of both fractions unreliable. They also can form aggregates that are hard to break, leading to undependable molecular weight determination¹⁰. Five major classes of compounds can be identified in the polar fraction¹¹

1. Neutral nitrogen compounds, mainly methylated carbazoles
2. Fluorenes (the least abundant class), mainly five member rings containing carbonyl groups, fused between two aromatic rings.
3. Fluorenols, aromatic tertiary alcohols
4. Carboxylic acids (most abundant), molecules containing 1 to 5 saturated rings attached to carboxylic groups
5. Sulfoxides (second most abundant), mostly saturated cyclic rings.

While saturates and aromatics fractions gives plenty of information about the chemistry of the oil, resins and asphaltenes contains a wide variety of compounds so that gathering chemical information from them is nearly impossible. Asphaltenes are defined as the fraction of the oil that is insoluble in n-pentane but soluble in toluene. Asphaltene can also be defined as an amorphous, thermolabile, friable dark solid that decomposes upon heating with intumescence without a sharp melting point. While most of the authors agree that asphaltenes are random, organic geomacromolecules, a few authors suggest that, in spite of their complexity, they might follow a certain, very complex pattern not yet elucidated³.

In an effort to understand the structure of the asphaltene, two structural models have been proposed. One is the continental model in which the asphaltene is composed of one or two polycyclic aromatics per molecule that may be alkyl-substituted. The second model is the archipelago model in which the asphaltene is composed of several small fused ring systems connected by alkyl chains. Recent views suggest that the asphaltene exist in a continuum between the archipelago and the continental model¹². One of the most recent models, the Yen-Mullins model, indicates that the archipelago architecture is dominant in the Athabasca asphaltenes^{13,14}.

Asphaltenes have been the focus of several studies not only because there is not a complete understanding of their structure, but also due to the challenges that present during oil upgrading. Asphaltenes contains heteroatoms such nitrogen, oxygen, sulfur, nickel and vanadium that are known to poison the catalysts used during oil upgrading. Additionally, asphaltenes tend to form aggregates that can cause plugging of processing, transport and storage equipment¹². As the light crude oil reserves diminishes, upgrading processes that are able to deal with high asphaltene concentration are needed.

Around 90% of the oil produced is converted into fuels. Since heavy oil and bitumen have low concentration of the fractions that become fuels, they need to be chemically transformed in order to meet the demand for fuels. Additionally, bitumens need to be treated in order to meet viscosity, and density specifications to be transported by pipelines⁴. To achieve these goals, different upgrading methods have been developed. These methods can be classified in three

categories: hydrogen addition processes, separation processes, and thermal rearrangement and carbon rejection¹⁵. *Table 3* shows a summary of the processes used worldwide for heavy oil and residue processing.

Table 3. Worldwide process capacity for heavy oil and residue processing¹⁶

Process	Capacity (Mbbbl/d)	% of total capacity
Carbon rejection	9397	56.58
Hydrogen addition	6755	40.66
Deasphalting	458	2.76

Separation processes are used mainly to remove some of the asphaltenes present in the heavy oils¹⁷. Due to its properties, asphaltenes largely contributes to the high density, viscosity and molecular weight of the oil. Additionally, asphaltene content in the oil is correlated to its coke forming tendency⁴. The most common solvents are C3 to C6 hydrocarbons¹⁸ and they are recovered through a supercritical operations¹⁵.

Thermal rearrangement and carbon rejection processes uses high temperatures and, sometimes, acid catalyst to increase the H/C ratio and to reduce the molecular weight of the heavy oil. These goals are achieved through a complex net of reactions. Those reactions occur mainly through free radicals in the case of thermal cracking and through ionic reactions in the case of catalytic cracking. It is important to mention that the term “carbon rejection” can be confusing since both products and rejected material have the same carbon concentration; however, the H/C ratio is increased by the removal of heteroatoms giving a rejected material with lower H/C ratio and higher heteroatoms content.

Cracking occurs through a very complex free-radical chain mechanism in which the propagation step is called β -scission and it is the important bond breaking step. In this step, the hydrocarbon breaks at the β position to the radical centre to give an olefin and a small alkyl radical. *Figure 1* shows the β -scission of a linear alkane.

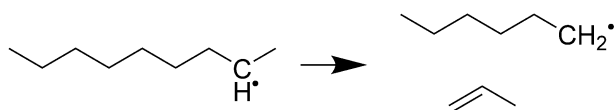


Figure 1. β -scission of a linear alkane

In addition to the β -scission, addition reactions can occur during thermal cracking especially in the liquid phase and when the olefin concentration is high. Coke formation occurs when portions of the oil became insoluble due to cracking of side chains of aromatic molecules and dehydrogenation reactions. Addition reactions can also contribute to the coke formation by increasing the molecular weight of the products⁴.

Catalytic cracking gives a different set of products indicating that the mechanism for this operation should be different that the one for thermal cracking. Table 4 shows the main differences between the products of thermal and catalytic cracking.

Table 4. Comparison of thermal vs catalytic cracking products. Adapted from ¹⁹

Hydrocarbon	Thermal cracking products	Catalytic cracking products
n-Alkanes	C ₂ is the major product Large amounts of C ₁ C ₄ to C ₁₅ olefines No branched chain products	C ₃ to C ₆ as major products No olefins larger than C ₄ Branched paraffins
Aliphatics	Little aromatization at 500 °C	Significant aromatization at 500 °C
Alkylaromatics	Side chain cracking	Dealkylation
n-Olefins	Slow double bond isomerization Little skeletal isomerization	Rapid skeletal and double bond isomerisation
Naphtenes	Slower cracking	Cracking rates comparable to those of paraffins

It is generally accepted that catalytic cracking reactions start by the formation of a carbonium ion. These ions are formed by protonation of a carbon or by extraction of a proton either by Lewis or Brønsted-Lowry acids. Carbonium ion formation has been extensively studied and it is possible to predict the type of carbonium ions will be formed in a reacting system, the stability of such ions and the paths the reactions might follow. A general rule states that the energy required to form a carbonium ion increases with an increase in hydrogen atoms attached to the carbon in which the positive charge will appear. Carbenium ions also play an important role in the catalytic cracking. These ions are formed by hydride abstraction and can react with carbonium ions causing them to undergo β -scission. Carbonium ion formation is the predominant mechanism for linear hydrocarbons while carbenium ions are predominant for branched molecules²⁰.

Once the carbonium ion is formed, there are five main possible reactions that can follow. These reactions are carbonium ion isomerization, hydride transfer, alkyde transfer, formation and breaking of carbon-carbon bonds, and chain isomerization. From these reactions, two are highly important for the catalytic cracking: hydride transfer and formation and breaking of carbon-carbon bonds.

In catalytic cracking, hydride transfer is a very fast reaction and it is responsible for a chain process that follows the carbonium ion formation and the neighboring groups can accelerate the transfer by stabilization of the resultant ion. The breaking of carbon-carbon bonds is the main responsible for the production of most of the motor fuels from crude oil. Reactions that involve both breaking and formation of carbon-carbon bonds (disproportionation) are also important in the cracking of substituted aromatic hydrocarbons¹⁹.

Different processes for oil upgrading are based on cracking reactions. The most important are visbreaking, delayed coking and fluid coking. Visbreaking is a process aimed to reduce the viscosity through mild thermal cracking. Typical conditions for visbreaking are 500 °C with a 1 to 3 minutes residence time. Figure 2 shows a schematic of the visbreaking process. Delayed coking uses long reaction times and temperatures up to 500 °C to convert the residue into gases, distillates and coke. Figure 3 shows a schematic of a typical delayed coking process. Fluid coking is a continuous process that uses hot coke particles to increase the temperature of oil. It is

a short reaction time process at temperatures around 530 °C.⁴ Figure 4 shows a schematic of the fluid coking process.

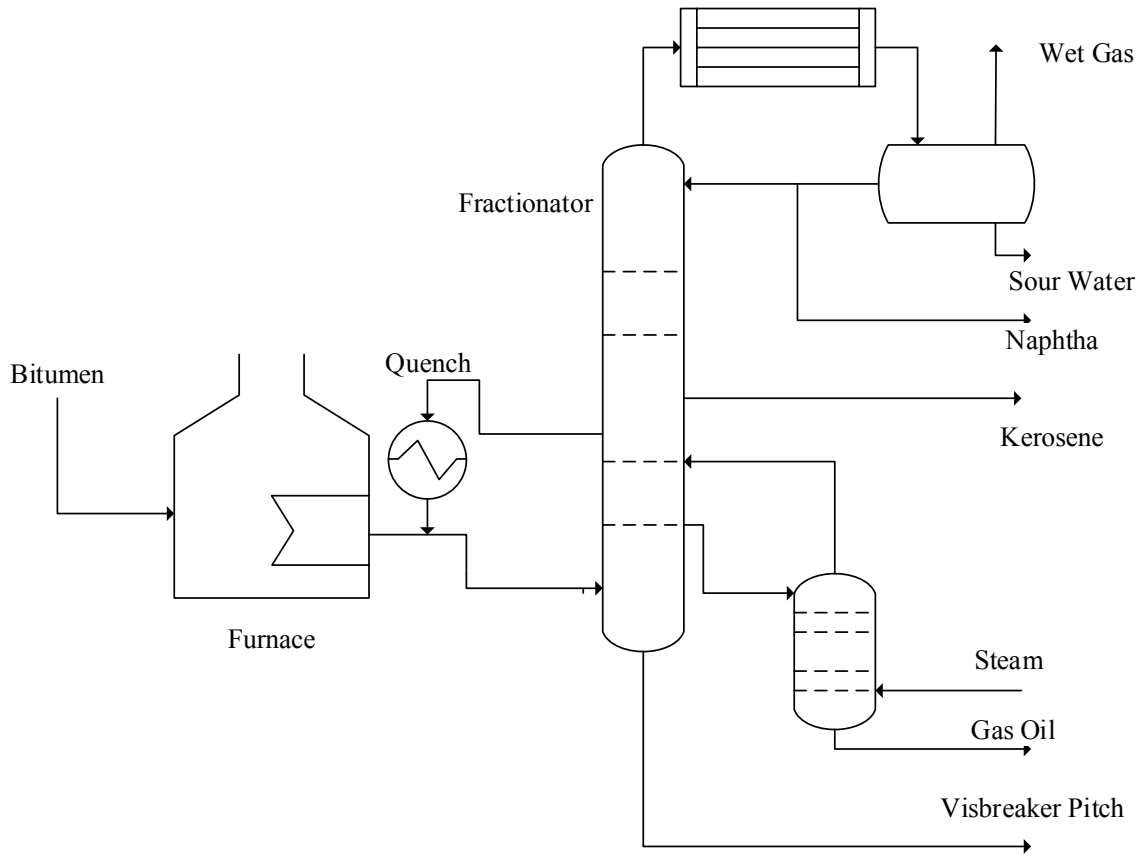


Figure 2. Schematic of a visbreaking process.

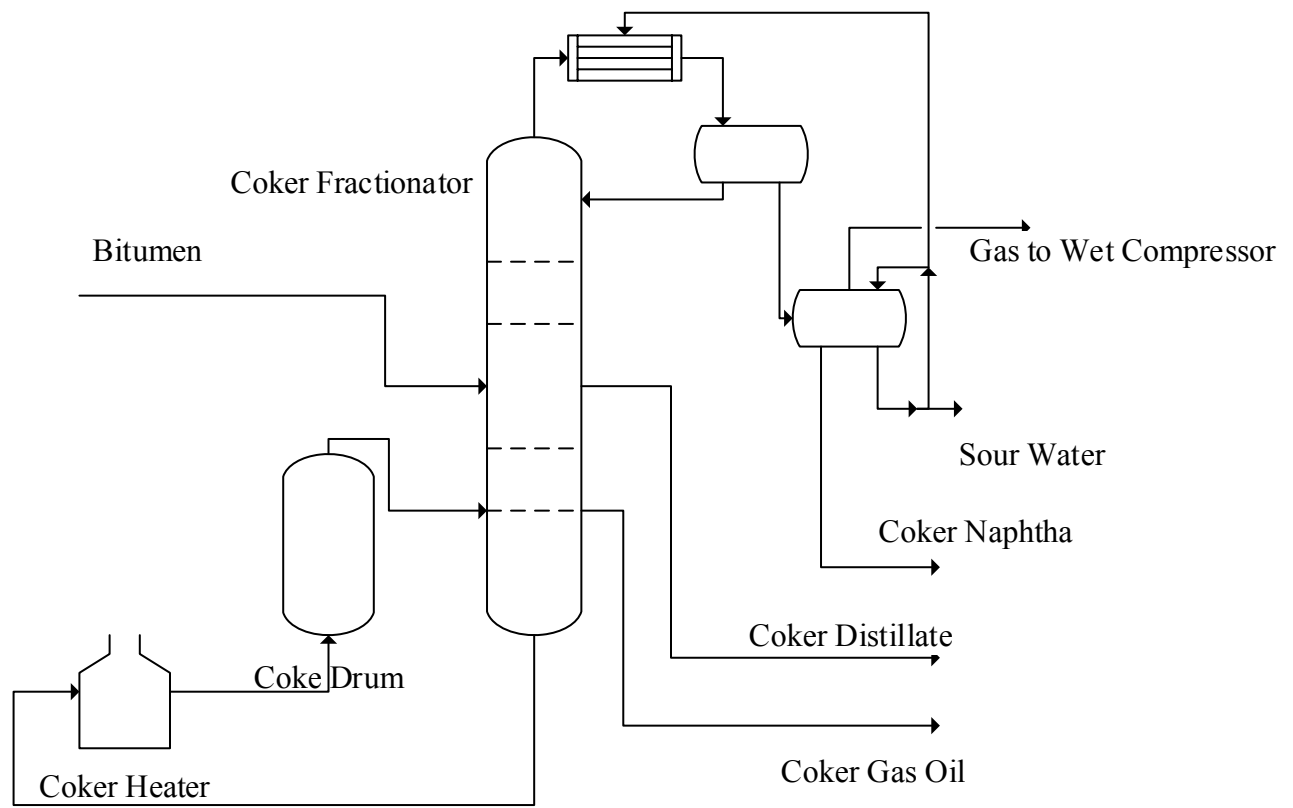


Figure 3. Schematic of a delayed coking process.

Hydrogen addition processes involves several different operations and the terminology used can be confusing. An easy way to understand these processes is by dividing them into three groups: hydroconversion, hydrotreating and hydrocracking. Hydroconversion uses high temperatures to promote thermal cracking while the catalyst have a predominant hydrogenation function while for hydrocracking, the catalyst has a double duty of hydrogenation and acid cracking and is usually the second part of a two stages process being hydrotreating the first step²¹. A schematic of a typical fixed bed hydroprocessing unit is found in Figure 5

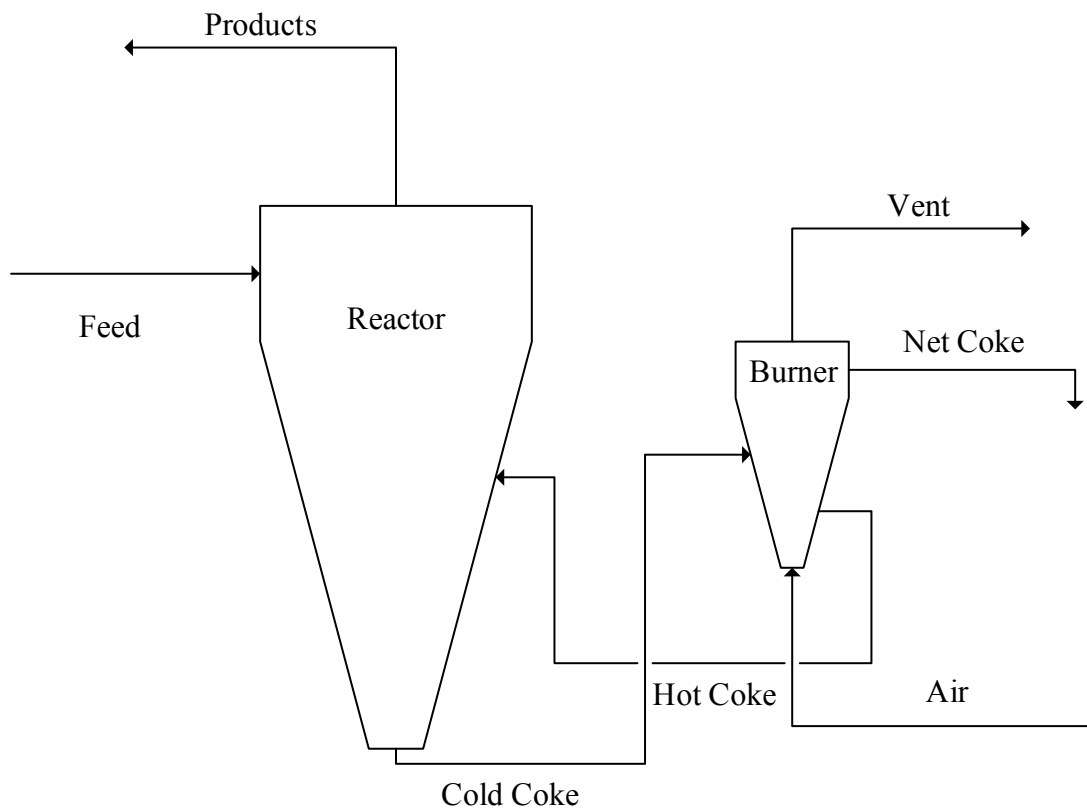


Figure 4. Schematic of the fluid coking

The main purpose of hydrotreating is to eliminate heteroatoms (N, O and S) and metals (Ni, V and sometimes Fe). Hydrotreating processes also hydrogenate olefins and aromatics²². Hydrogenation reactions that lead to S, N, O and metals removal are the same for all the hydrogen addition processes and the main difference is the selectivity of heteroatoms and metals removal.

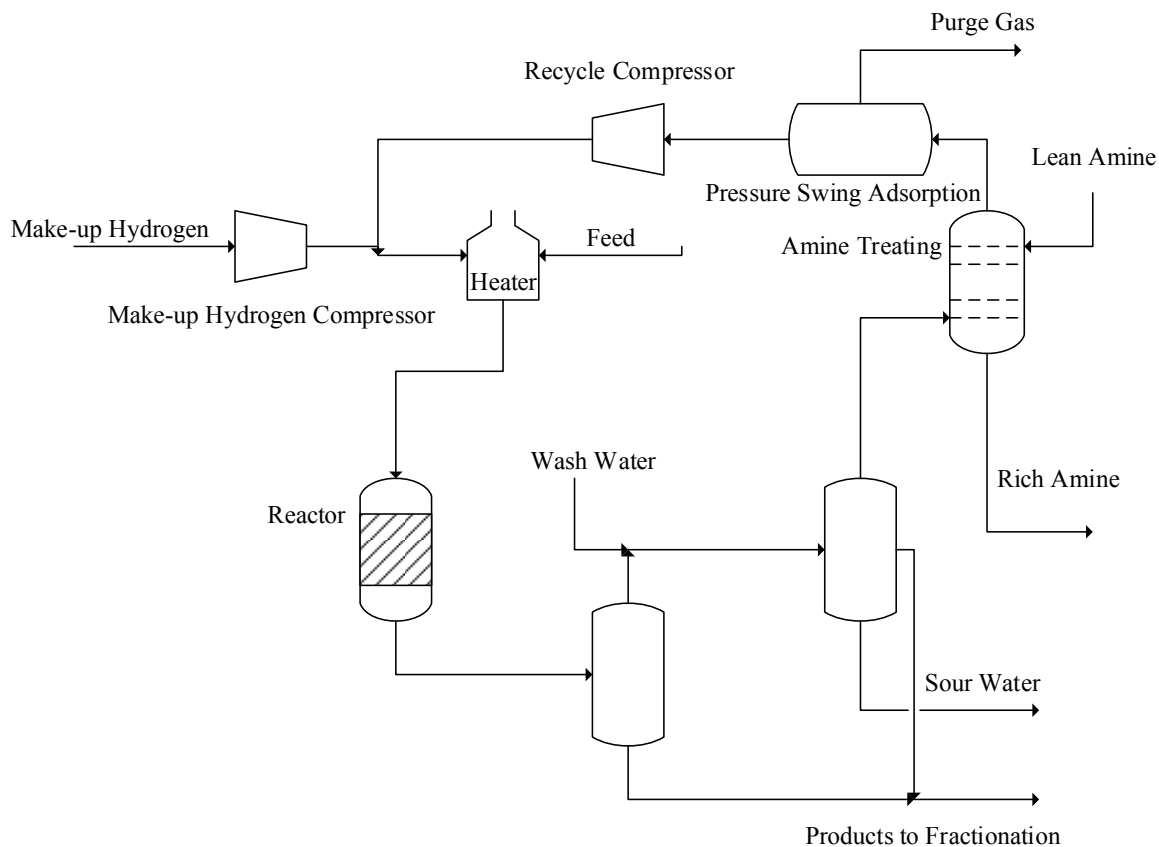


Figure 5. Schematic of a typical ebullating bed hydroconversion unit.

Sulphur removal has been widely studied. It has been proven that larger aromatic rings adsorb strongly on the surface of the catalyst making them faster to react; on the other hand, the presence of alkyl groups reduce the reactivity mainly by steric hindrance²³.

Nitrogen compounds are harder to remove than sulfur compounds and require more hydrogen. While some sulfur compounds undergo direct removal of the sulfur atom, nitrogen requires the aromatic ring to be saturated before the nitrogen is removed. As in sulfur, steric hindrance reduce the reactivity of nitrogen-containing molecules²⁴.

Since oxygen removal is not as important as nitrogen and sulfur removal for refineries, it has not been widely studied. It is suggested that oxygen removal behaves similarly to the sulfur and it is an intermediate between nitrogen and sulfur in terms of reactivity²⁵.

Metals removal is important, not only due to the deleterious effects of such contaminants in the products but also due to the impact in the catalyst and processing equipment. It is known that one of the most important processes of hydroprocessing catalyst deactivation is the accumulation of metals that leads to pore blockage²⁶. The reaction networks involved in HDM have not been widely studied; however, it is known that the metals are deposited on the surface of the catalyst as metal sulfides²⁷ and vanadyl porphyrins are more reactive than nickel porphyrins. The HDM reactions are pseudo first order at temperatures over 350 °C and lower order at lower temperatures. Both temperature and hydrogen pressure increases the rate of reaction and decreases with porphyrin concentration below 350 °C. Analysis shows that the HDM can follow a direct route forming metal sulfides, aromatics and ammonia or it can follow a more complex route involving partially hydrogenated metal porphyrins and dipyrroles²⁸.

Zeolites have received a lot of attention due to its properties as catalyst in the oil refining industry. Since its introduction in the mid 1960's as a fluid catalytic cracking (FCC) catalyst, zeolites have allowed increased conversion and gasoline yield²⁹. Additionally, there have been interest in the zeolites as support for hydroprocessing catalysts³⁰; however, zeolites have not been used industrially for primary upgrading of heavy oils. Zeolites are crystalline aluminosilicates with a well-defined framework formed by AlO_4 and SiO_4 tetrahedra linked together by sharing all the oxygens. The structure of this framework includes channels that interconnect voids occupied by cations of group I and II elements and water molecules. These cations are highly mobile and can be exchanged by other cations³¹. Zeolites have been widely researched as catalyst for several reasons. Both zeolites and amorphous silica have similar characteristics including similar activation energies towards several reactions, and similar response towards promoters and poisons; however, zeolites are more active than amorphous silica due to a higher density of active sites and a higher potential of adsorption due to the narrow pores³². Zeolites have also been widely used as adsorbents. The network of channels and cages greatly increase the surface area for adsorption³³. Natural zeolites have not found a widespread use as catalyst since they are rarely found in high purity. On the other hand, seven groups of zeolites can be considered a viable mineral resource since they occur in sufficient quantity and are easily accessible for mining. Those zeolites are mordenite, clinoptilolite, ferrierite, chabazite,

erionite, philipsite and analcime. The world's natural zeolites deposits have not been well defined but there are approximately 120 million tonnes of clinoptilolite, chabazite, erinite, mordenite and philipsite near surface in the U.S. but it is estimated that the possible U.S. resources can reach 10 trillion tons. The cost of the natural zeolites also makes them attractive. While catalyst grade synthetic zeolites cost around US \$ 45 / Kg, the cost of natural zeolites ranges between US \$20 to 267 per tonne³⁴.

For this particular study, calcium chabazite (Ca-chabazite) was chosen due to its platy morphology that allows for a large external surface area and acid strength³⁵. It was also selected due to its high acidic strength³⁶. The acid sites of the zeolite are caused by the presence of Al in the framework and the strength is highly dependent on the number of Al in the next nearest neighbour position (NNN). Al with zero Al in the NNN position have the highest acidic strength. Also, the acid site density is important. Higher acid site density will promote bimolecular reactions over monomolecular reactions. The general formula for Ca-chabazite is



and is composed of an hexagonal crystal system in which 47% of the space is void. The channels are 3.7 x 4.2 Å and the ion exchange capacity is 3.81 meq/g³⁴.

Since the chabazite is hydrophilic, water is usually present in systems that contain the zeolite. The effect of the water in reactive systems, especially with zeolites, has been studied but a complete understanding of the role of the water is still out of reach. For the sulfated zirconia catalyst, it was proposed that water converts Lewis acid sites to Brønsted acid sites. This idea was later refuted^{37,38} but the discrepancies continued. While some authors³⁹ said that the water acts as a poison and no evidence of Brønsted acid sites generation were found, others propose that water does convert Lewis acid sites into Brønsted acid sites but these sites are either not strong enough to protonate the probe molecules used in the study or they are inactive for n-butane isomerization⁴⁰. It has been also shown that different experimental methods can lead to conflicting conclusions about the water phenomena with respect to the same catalyst. Also for sulfated zirconia catalysts, IR studies with NH₃ as probe molecule shows that the NH₄⁺ band increases at expense of NH₃ bands in the presence of water. Studies with pyridine also showed

an increase in Brønsted acidity, but no increase in catalytic activity. In the same study, IR spectroscopy showed an increase in Brønsted acidity over TiO₂ in the presence of water, but TPD studies conducted with isopropylamine (IPA) only showed displacement of adsorbed molecules due to water adsorption, especially when the probe molecules are adsorbed on Lewis acid sites³⁷.

Using a commercial cracking catalyst, Matsushita and Emmet⁴¹ claimed that water may be promoting additional processes for hydrogen exchange. In their paper, they reported the optimum amount of water for the cracking of different compounds. For triptane, the optimum amount of water was between 0.1 and 0.2 % and for 2-methylpentane and n-heptane, the optimum amount is 0.15%. It is also shown in the same paper that water increases the amount of propylene produced from n-heptane cracking. Matsushita and Emmet⁴¹ also made studies with n-heptane-1-¹⁴C identifying three types of chemisorption based in the exchange ability of non-radioactive n-heptane. Water seems to increase what they called “instantaneous-exchangeable” adsorption while leaving untouched the “slowly exchangeable” adsorption and the irreversible adsorption. Kinetic studies of hexadecane cracking conducted by Corma *et al.*³⁸ shows that there is an increase in observed kinetics when water vapor is used in place of nitrogen gas as a carrier. Notably, the same study shows that there is no change in the intrinsic kinetic rate constant when nitrogen gas is added instead of water vapor. These data suggest that the water does not interact with the surface of the zeolite catalyst, at least not to the point of changing the intrinsic rate constant or the concentration of acid sites in the catalyst. Also, olefin to paraffin ratio of the products, coke yield and heat of adsorption of n-hexadecane on the zeolite remain unchanged if nitrogen gas is used instead of water vapor as a carrier. The increase in the observed kinetic rate constant with water vapor is proposed to be due to enhanced transport properties between the feed and the catalyst when compared to nitrogen gas. Alberti and Martucci⁴², however, propose that the enhanced rate in the presence of water is due to a chemical effect rather than enhanced transport properties. Using Neutron Rietveld Refinement (Neutron diffraction), they find evidence of proton transfer in synthetic low silica ferrierite. That same paper by Aberti and Martucci recalls that proton transfer promotion by water has been proposed as early as in 1806 and supported with experimental evidence. For H-ZSM-5, a synthetic zeolite, the apparent

activation energy of proton migration in the presence of nitrogen gas is reported to be 118 KJ/mol. This value reduces to 17 KJ/mol when the reaction is conducted in the presence of water in amounts as low as 1 ppm. A similar reduction from 81 KJ/mol to 30 KJ/mol with water addition was found for proton chabazite, a natural zeolite.

In a previous study, chabazite demonstrated to have the ability to catalyze reactions that lowered the density, molecular weight, and nitrogen and metals content in raw oil sands and it was determined that the presence of water in the reacting system affects the reactions³⁵. In the present study; the properties of chabazite were studied using four model compounds: indole for nitrogen removal, octaethylporphyrin for nickel and vanadium removal, hexadecane for cracking of the saturate fraction and cumene for transalkylation reactions of the aromatic fraction. By observing the reactions of the four compounds in presence of ca-chabazite and the adsorption capabilities for nitrogen and metals, a general reaction path for the oil in presence of natural zeolites can be proposed and, with that knowledge, novel and improved processes can be envisioned for the upgrading of oil and oil products.

2 Pyrrolic Ring Opening and Nitrogen Removal from Solution without Hydrogenation: Natural Chabazite as a Cracking Catalyst

2.1 Preface

As stated before, bitumen and some heavy oils need to be upgraded in order to be transported and processed. The goals of the upgrading processes include reduction in viscosity, molecular weight and density, removal of nitrogen, sulfur and metals and increase in the H/C ratio. In this thesis, the properties of the chabazite as an upgrading catalyst were explored focusing in nitrogen and metals removal and activity towards alkanes and substituted aromatics. The papers in which this document is based are presented in chronological order of publication since each paper makes reference to the previous ones. Sulfur was not included in this study since previous studies show that the chabazite has no significant activity towards sulfur compounds.

This chapter deals with nitrogen removal using model compounds. Nitrogen compounds can poison the catalyst of subsequent operations (FCC, hydrotreating, etc.). Removal of such compounds improves the life of such catalyst reducing the operating costs. Previous studies show that chabazite removes up to 74% of the nitrogen present in raw oil sands⁴³; however, the complexity of the raw oil sands – chabazite system makes the elucidation of the zeolite's mode of action nearly impossible. Indole was chosen as a model compound since its derivatives have been proven to be very difficult to remove through conventional upgrading processes. Since the objective of this project is to develop a process with a low cost catalyst, the chabazite was used in raw form. No metals were deposited on the zeolite and hydrogen was not added to the reaction. The scope of this chapter is to present quantification data in removal of both indole and nitrogen from solution. Also, nitrogen products were identified and a reaction path for the formation of such products is suggested. A version of this paper was published in the Energy & Fuels Journal.

2.2 Introduction

The activity and poisoning of refinery catalysts by various organonitrogen compounds directly impacts the profitability of petroleum refineries. With this concern in mind, continuous research on improved process for oil upgrading is being conducted worldwide. Increase in yield by minimizing byproducts and reducing the use of expensive chemicals like hydrogen are important areas of opportunity. The focus of this research is to provide a possible path to reduce the need of hydrogen addition by transforming nitrogen-bearing compounds that are hard to crack and require large amounts of hydrogen into compounds that are easier to crack and require less hydrogen.

In order to meet current and proposed stringent fuel specifications, high severity hydrotreating must be used. Unwanted side effects of high severity processing typically include yield losses, high hydrogen consumption and higher capital and operating costs. To further complicate the production of high quality products, a current trend in petroleum refining is the increased availability of heavy oils. One issue with these feeds is their elevated levels of undesirable compounds, such as sulfur, nitrogen, and metals. Nitrogen is particularly problematic to refineries and can be present in concentrations up to 4000 ppm in heavy oils⁴. These nitrogen bearing compounds, naturally present in petroleum feed stocks, have multiple negative effects such as poisoning of FCC catalysts⁴⁴ which reduces gasoline yield, increased sediment formation during storage⁴⁵ and increased toxic emissions⁴⁶ from transportation fuels, among others. Hydrodenitrogenation (HDN) is the main commercial method used to remove nitrogen from oil fractions and is performed in a single processing step together with hydrodesulphurization (HDS) and hydrodemetallization (HDM)⁴⁷. Aromatic nitrogen is typically found in petroleum in two forms, two thirds in pyrrolic (five membered rings) structures and the remainder in pyridinic (six membered rings) structures. Unlike catalytic direct desulfurization reactions that are common with thiophenes, aromatic nitrogen compounds require ring hydrogenation followed by C-N bond cleavage. Improvements in the commercial nitrogen removal methods are desirable in order to reduce reaction severity⁴⁸ and to reduce the consumption of large quantities of hydrogen⁴⁹.

It is well established that the effect of nitrogen-bearing compounds on catalyst performance during cracking reactions is complex. As was mentioned previously, nitrogen-bearing

compounds contribute to the reduction in gasoline yields due to the contamination of refinery catalysts⁵⁰; their effectiveness as poison varies depending upon the structure of the nitrogen-bearing compound. In particular, it has been found that the poisoning effect follows the trend: quinaldine > quinoline > pyrrole > piperidine > decylamine > aniline⁵¹. It is also known that some basic nitrogen compounds, such as aniline and pyridine, have very low poisoning strengths, similar to that of benzene⁵². Also, bigger molecules are considered to have a higher fouling and poisoning activity since they cannot enter the pores in a typical catalyst, thus deactivating only the external acid sites⁵³ and blocking the pores entrance. While some authors report that nitrogen content does not increase the coke formation⁵⁰, others report that nitrogen-bearing compounds can adsorb onto Lewis acid sites and form coke⁵². Notably, nitrogen-bearing compounds have been found to partially reduce the overall cracking rate of oils by adsorbing preferentially onto strong acid sites, and not onto medium strength acid sites. This preference seems to be somewhat general as, interestingly, nitrogen compounds do not affect the rate of acid catalyzed oligomerization reactions of light olefins when medium strength acid catalysts were employed⁵⁴.

The complexity of the adsorption of nitrogen-bearing compound increases on catalysts that have a mix of both Lewis and Brønsted acid sites. There are few reports on the interaction of pyrrolic compounds with these types of solids. For pyridinic nitrogen species, such as quinoline, studies show preferential adsorption onto Brønsted acid sites. A temporary coordination with Lewis acid sites can occur, however, before saturation of Brønsted acid sites⁵⁰. Strong adsorption on Brønsted acid sites does not only effectively poison the active site, but seems to reduce the acidic strength of neighboring acid sites as well⁵⁰. Notably, the catalytic activity of Lewis acid sites is only slightly affected by the presence of nitrogen-bearing compounds.

In recent studies, economical and abundant natural zeolites have been identified as viable petroleum cracking catalysts due to their properties as both a catalyst and an adsorbent. Natural zeolites have been used to catalytically crack raw oil sands into lighter products with reduced nitrogen and metal content; without having to add hydrogen gas to the reactor⁵⁵. In those studies, nitrogen removal up to 74% was reported using chabazite as catalyst⁴³. Chabazite is known to have a platy morphology allowing for a relatively large external surface area, 59 m²/g, and high acidity⁵⁶.

Given the chemical complexity of petroleum fractions, and especially heavy oils, it is extremely difficult to completely characterize chemical changes that occur during reactions. For this reason, defined model compounds are usually selected to probe specific chemical activity. In this study, model compounds are particularly relevant because the catalyst is known to already work with the complex system⁵⁶. For this study, indole was chosen as one of the model compounds. Indole is a widely used model compound used mainly for HDN studies and sometimes for cracking reactions^{52,53}, it gives a reasonably good representation of the two thirds of the nitrogen that is present in oil as five-member rings⁵⁷. While free indole is not usually reported to be present in heavy feeds, it has been found in several petroleum products^{45,58,59}. The presence of indole in biofuels is also important. Indole and methylindole are the main nitrogenated compounds found in biofuels^{60,61}. In addition, indole is considered a non-basic nitrogen compound; it is hard to remove through conventional HDN⁴⁶ due to the fact that the electrons are delocalized and unavailable for donation⁶².

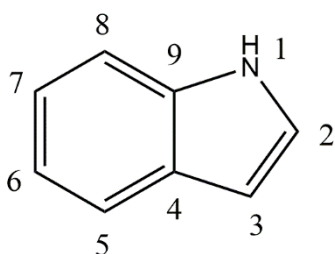


Figure 6. Numbering convention for indole

The chemistry of indole is an important area in heterocycle chemistry. Indole has many applications in different fields not only due to its presence in the oil products but also as an intermediate for pharmaceutical drugs, dyes and fine chemicals⁶³. The numbering convention for indole used in this paper can be found in *Figure 6*. The indole ring is considered aromatic and very active towards electrophilic substitution. Its 3-position is especially active toward protonation, halogenation, alkylation and acylation. Importantly, methyl groups attached to the indole ring can dramatically change the reactivity of the indole molecule. The general order of reactivity of substituted indoles is 1-methylindole > indole > 2-methylindole⁶⁴. Another indole reaction that has been studied is the oligomerization reaction. Polyindole has received special attention due to its conductive properties. Oligomerization of indole can occur in the presence of

acid catalysts or by electrochemistry. It has been found that the structure of the oligomer is dependent on the nature of the acid used as catalyst^{64,65}. Under cracking conditions, indole undergoes a very complex network of reactions leading to several different products that include aniline, phenol⁶⁶, indole oligomers⁶⁷, ammonia, cyanides⁶⁸ and ethylaniline⁶⁹ among others. Indole reaction paths have been proposed for HDN⁶², thermocracking⁶⁸ and hydrothermal liquefaction⁶⁰; however, the catalytic cracking of indole has not been widely studied.

Quinoline and carbazole are also typically chosen as a model compounds to represent the basic and non-basic heterocyclic nitrogen compounds, respectively, that are found in reaction products of petroleum⁴⁵. Quinoline-based compounds represent the second most abundant basic nitrogen compounds found in reaction products of petroleum fractions, after aniline⁵⁸. They are reportedly harder to crack than indole during HDN and their removal generally requires a catalyst with high hydrocracking activity⁷⁰. Both quinoline and indole have been reported to crack into aniline and ammonia during catalytic cracking⁷¹.

In industrial processes, most petroleum fractions are relatively dry and without free water. Raw oil sands, however, contains varying amounts of connate water (from 2.5 to 3.7% according to Hooshiar et. al.⁷²). This water content is important since the raw oil sands used in previous studies on the activity of natural zeolites as upgrading catalysts⁵⁵ are known to contain water. The presence of water is well known to affect the cracking of oil and oil products⁴¹. It also worthwhile to mention that biomass, that can also be converted into biofuels using natural zeolites, have significant amounts of water^{60,61}. Several studies have explored the effect of water in cracking using zeolites and sulfated zirconia catalysts. A complete understanding of the phenomena, however, is still far away. Most of the studies have found that the water does not convert Lewis acid sites to Brønsted acid sites³⁸ but rather changes the adsorption behavior of the molecules on the catalyst surface. Other studies suggest the possibility of water enhancing transport properties or promoting proton transfer reactions⁴².

There has been a lot of attention on the chemical composition of the petroleum fractions and their reaction products or on the effect of these components on the activity of the catalyst, and not much on the reactions themselves. Understanding the reactions that the oil components

undergo in the presence of the catalyst could help to improve the catalyst and the process itself. Also, the effects of water on catalysts have been investigated in two general themes: cracking of hydrocarbons, and adsorption of molecules. Given the chemical complexity of petroleum feed stocks and the relatively large abundance of elements other than carbon and hydrogen, studies including heteroatoms are needed and could prove useful in the optimization of existing processes or even in the creation of new processes capable of dealing with the high-nitrogen content feeds that are currently available. The scope of this study is to present an insight on the way the nitrogen-bearing compounds react and are removed from solution in the presence of chabazite without adding hydrogen, and to investigate the possibility that the water present in the raw oil sands contributes to the activity of the zeolite.

2.3 Experimental Section

2.3.1 Materials

The model compounds used were indole (99+%), 2, 3-dihydroindole (99%), quinoline (98%) and carbazole (99%). The solvent used was 1-methylnaphtalene (95%). Naphthalene (99%) was also used as solvent for selected reactions. All compounds were obtained from Aldrich and used as received. All of the model compounds were used as solution with a concentration equivalent to 0.2 % w/w of nitrogen, the abundance of nitrogen found in oil sands derived bitumen.

Proton and calcium forms of chabazite (from the deposits of Bowie, Arizona) were used. Clinoptilolite (from the deposits of St. Claude, New Mexico) and zeolite Y (from Engelhard Corporation) were also used in some reactions. A detailed description of the zeolites and some characterization data were previously published⁵⁵. In order to minimize the adsorbed water content of the zeolites, they were kept in a desiccator and taken out just before loading the reactor.

For the reactions with water addition, deionized water from a MilliQ water purification system by Millipore was used.

2.3.2 Reactions

The reactions were carried out in 12 ml stainless steel microreactors that were made in-house. The reactors and general procedure are described in detail elsewhere⁷³. For every experiment, the

reactor was loaded with 3.0 ml of nitrogen solution (indole, 2, 3-dihydroindole, carbazole or quinoline). The catalyst loading for all the reactions was 10% w/v with respect to the amount of solution. For selected reactions, 30.0 μ l distilled water was added.

After filling with the liquid reactants, the reactors were closed and tested for leaks at 20 MPag with nitrogen. Once the reactors were leak free, they were pressurized with nitrogen to 2 MPag and vented to the atmosphere three times in order to ensure an inert atmosphere. The reactors were then filled to 1.7 MPag at room temperature and sealed. This pressure was set to ensure that even the lowest boiling point reactants were in liquid phase at reaction conditions. The pressure during the reaction at 400 °C is estimated to be 3.9 MPag.

The reactions were carried out at 300 or 400 °C. These temperatures were achieved and maintained by submerging the reactors in a fluidized sand bath. Details on the stability and reproducibility of the sand bath conditions can be found elsewhere⁷³. In order to reduce the variability between the water added vs. no water added reactions, comparable experiments were conducted simultaneously in the same sand bath. During the reactions, the reactors were mechanically shaken to improve the mass and heat transfer. After the reaction, the reactors were cooled, initially with flowing air for 5 minutes and then by submerging in cold water. After the reaction and product recovery, the reactors were thoroughly cleaned and reused.

2.3.3 Product recovery and analysis

After each experiment, the reactor was cooled and the amount of gas was measured by water displacement. The amount of gas inside the pressurized reactors prior to experiments was quantified by venting a pressurized reactor, initially at 1.7 MPag, and measuring the volume of nitrogen released by water displacement. The difference between the initial and final volumes was taken as a measure of gas products formation.

The liquid and the solid products were separated by centrifugation at 5000 rpm for 5 minutes. The liquid products were analyzed by gas chromatography using a Varian 3800 GC fitted with an 8200 autosampler. The GC was equipped with an Alltech Heliflex AT-35 Column (30m x 0.53mm x 2.65 μ m). A Flame Ionization Detector (FID) and a Pulsed Flame Photometric Detector (PFPD) were used in parallel by fitting a splitter at the end of the column. The PFPD

can detect specific elements and was operated in nitrogen mode. Intermediate polarity column guards were used to connect the splitter to the detectors. The results were recorded and processed using Galaxy software, by Varian Inc. Total nitrogen content was determined in both the liquids and the solids by oxidative combustion and chemiluminescence detection using an ANTEK sulfur and nitrogen analyzer. Selected liquid samples were characterized by GC-MS in the Analytical and Instrumentation laboratory, Department of Chemistry at the University of Alberta. Additional chemical identification of the product residue was performed using ^1H nuclear magnetic resonance (NMR) spectroscopy and infrared (IR) spectroscopy, Department of Chemistry at the University of Alberta. Prior to NMR and IR spectroscopic analysis, liquid samples were concentrated using a rotavap.

To characterize the nitrogen species adsorbed on the catalysts, samples of the solids recovered after centrifugation were dried at room temperature overnight and analyzed by X-Ray photoelectron spectroscopy (XPS) at the Alberta Centre for Surface Engineering and Science (ACES) at the University of Alberta. The resulting XPS spectra were deconvoluted using the CasaXPS software. Powder X-ray diffraction (XRD) studies were performed at the Chemical and Materials Engineering Department of the University of Alberta.

2.3.4 Adsorption Studies

Adsorption on the chabazite was studied using 1% and 2% solutions of aniline in 1-methylnaphthalene. Approximately 1.5 ml of solution was mixed with 1.5 g of Ca-chabazite. To study the effect of the water, 1% water was added to some of the experiments. A similar study into adsorption of aniline from aqueous solution using activated carbon⁷⁴ shows that adsorption equilibrium can be achieved in two hours. The solution in this study was in contact with the catalyst for 8 h to ensure that the mixture reached equilibrium. During this time, the slurry was stirred twice using a PT 1300D disperser by Kinematica. Aniline concentration in the liquid products was determined by gas chromatography.

2.4 Results

2.4.1 Quantification of reaction products.

Indole solutions were analyzed after reaction at 400 °C using GC-FID/PFPD. The reduction in indole present in solution is shown in *Table 5*. Nitrogen contents in both liquid and solid (catalyst) products were analyzed. The results are also shown in *Table 5*. To verify that the observed conversions were due to the presence of the chabazite, control reactions without catalyst were conducted. No detectible conversion of the indole was observed in these reactions. Production of significant quantities of gaseous products was not detected in the catalyzed reactions at 400 °C and 1 hour. The nitrogen balance was calculated and found accurate within $95\% \pm 4.4\%$. Details on the nitrogen balance of one of the reactions can be found in *Table 6*.

Table 5. Indole and nitrogen removal from a 0.2% w/w nitrogen solution at 400 °C, 1 h reaction, 10 % chabazite catalyst loading.

	Indole removal [#]		Nitrogen removal ^{&}	
	No added water	1% water	No added water	1% water
Calcium	43.7%	41.2%	13.0%	17.7%
Proton	33.2%	30.5%	14.1%	15.8%

[#] Standard deviation of indole removal 2.2%

[&] Standard deviation of total nitrogen removal 3.5%

Table 6. Nitrogen balance of indole reaction over Ca-chabazite. Based on 7.5 mg of initial nitrogen. (0.2% w/w nitrogen solution at 400 °C, 1 h reaction, 10% ca-chabazite loading, no added water)

Phase	Percentage of total nitrogen
Gas	Non detected
Solid	10.3%
Liquid	85.3%
Total	95.6%

Three nitrogen-containing compounds not present in the initial solution were detected with the PFPD: two with shorter retention times and one with a longer retention time with respect to the indole peak. All samples presented chromatographic peaks with the same retention times, regardless of the form of chabazite and water addition. In an effort to determine the reaction path, reactions with 2,3-dihydroindole were made under the same conditions the indole reactions were made. The conversion of 2,3-dihydroindole was approximately 83% with indole as the main reaction product. In order to compare results between chabazite, clinoptilolite and zeolite Y, a set of reactions at various temperatures was done (from 300 to 425 °C). The conversion of 2,3-dihydroindole is show in *Figure 7*.

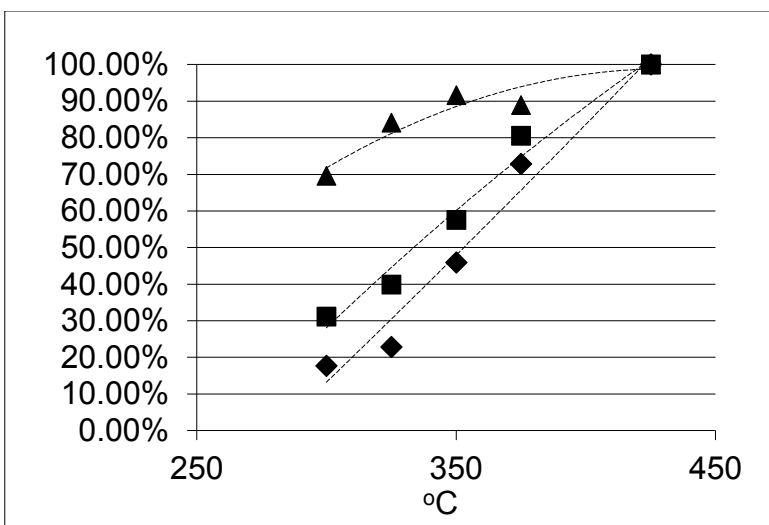


Figure 7. Conversion of 2, 3 dihydroindole using different types of zeolites. ◆ Clinoptilolite, ■ Chabazite, ▲ Zeolite Y. 1 h reaction, 10% catalyst loading.

In order to test the activity of the zeolite towards pyridinic nitrogen removal, reactions were also made with quinoline as the nitrogen-bearing compound. Conversions under different temperatures in the presence of clinoptilolite are found in *Table 7*. The liquid products were analyzed by GC-FID. Analysis of the chromatograms indicates the formation long retention time products.

Carbazole was reacted under the same conditions used for the indole reactions. The GC-MS analysis for the liquid phase shows the presence of methylcarbazole. No other nitrogen-bearing products were detected.

Table 7. Conversion of quinoline using clinoptilolite (0.2 % w/w nitrogen solution, 1 h reaction, 10% catalyst loading)

Temperature (° C)	Conversion (%)
400	7.4
410	10.2
425	12.2

2.4.2 Identification of products

In order to identify the nitrogen-bearing reaction products detected in the GC-FID/PFPD studies, IR and $^1\text{H-NMR}$ spectroscopies were performed using the procedure noted above. The main peaks found and their assignments are presented in *Table 8*. It is important to note that the peaks corresponding to primary amines (aniline) were strong and well defined in contrast with the rest of the signals in both IR and $^1\text{H-NMR}$ spectra.

Table 8. Results for $^1\text{H-NMR}$ and IR spectroscopies for non-volatile products after reaction

Groups	IR Spectroscopy (cm^{-1})	$^1\text{H-NMR}$ spectroscopy (ppm)
Primary amines (aniline)	3424.3	3.523
Vinyl groups	3051.2-2880.1	5.316
Methyl and methylene	1500	-
Substituted benzenes	790 – 747	2 - 3

In order to further characterize the nitrogen products, GC-MS studies were performed. The presence of aniline was detected in the GC-MS and confirmed by injection of aniline samples into the GC-FID/PFPD. Different toluidine isomers were also detected in the GC-MS studies as the second short-retention time nitrogen-bearing compound. The third nitrogen-bearing compound was not identified due to poor separation between non-nitrogen and nitrogen bearing high molecular weight products. The molecular weight of this product is estimated around 241 u. GC-MS studies also revealed the presence of methylindole in the product mixture.

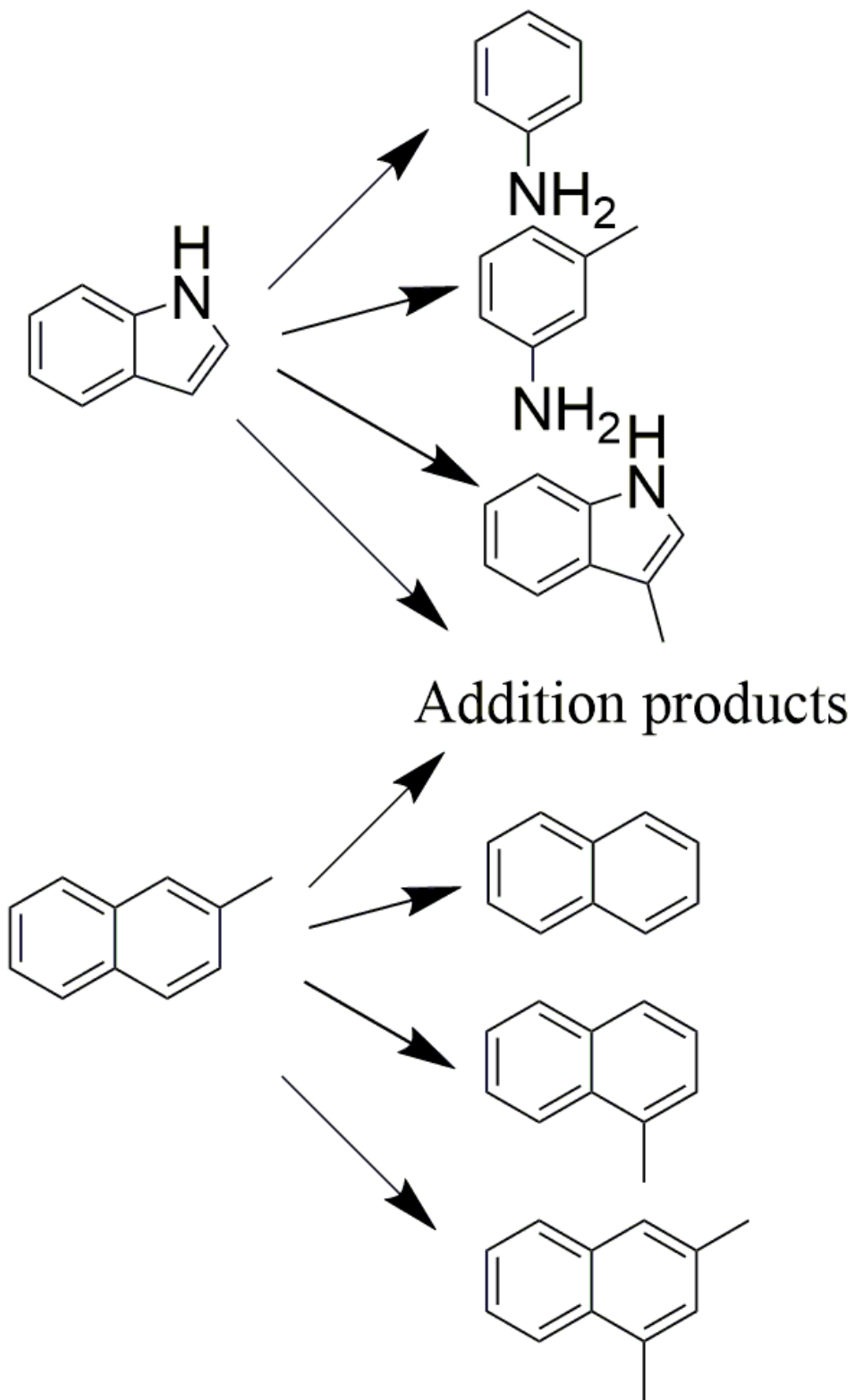


Figure 8. Major reaction products for indole and 1-methylnaphthalene reactions

In addition to the nitrogen bearing products, naphthalene, 2-methylnaphthalene, dimethylnaphthalene and other high-molecular weight products not containing nitrogen were detected. The products detected are summarized in *Figure 8*. All of the peak information for the pure compounds was taken from the Spectral Database for Organic Compounds of the National Institute of Advanced Industrial Science and Technology⁷⁵.

To reduce the presence of methyl groups that could be promoting transalkylation reactions, experiments were conducted using naphthalene instead of 1-methylnaphthalene as solvent. Aniline, methylindole and addition products were detected using GC-MS. Traces of toluidine were also detected.

2.4.3 Spent Catalyst Characterization

The spent catalyst was analyzed by XPS. The nitrogen 1s region shows the presence of a signal that is a single peak centered at 399.2 eV with a Full Width at Half Maximum (FWHM) around 1.5 with a maximum residual of 0.98 and can be assigned to adsorbed aniline⁷⁶. The four samples (proton and calcium chabazite, with and without added water) present highly similar XPS results (See *Table 9*). An illustrative XPS spectra (N 1s region) is shown in *Figure 9*.

Table 9. XPS results after 1 h reaction at 400 °C, 0.2 % w/w nitrogen (added as indole), 10% chabazite catalyst loading

	Position (eV)		FWMH		Residual	
	No added water	1% water	No added water	1% water	No added water	1% water
Calcium	399.3	399.3	1.5	1.7	0.833	0.822
Proton	399.2	399.2	1.4	1.3	0.987	0.956

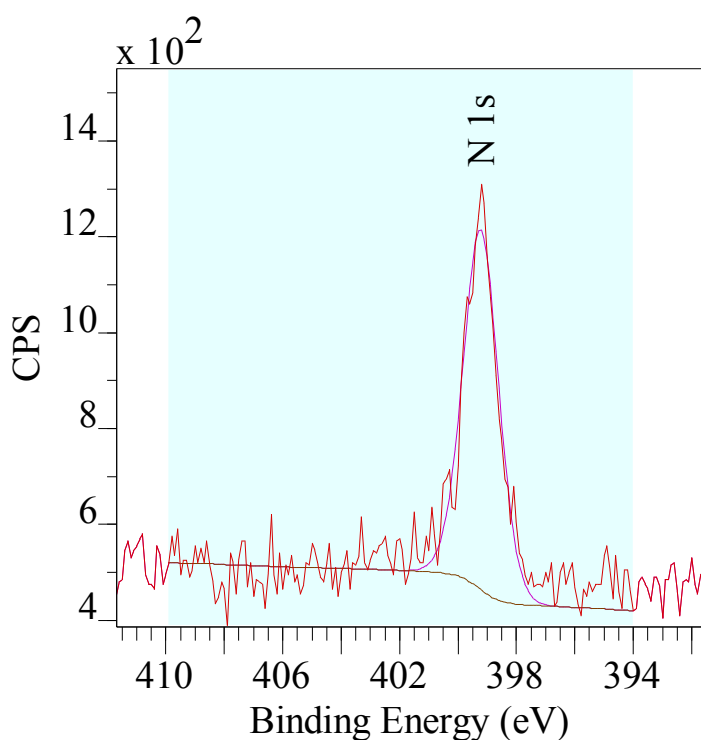


Figure 9. Typical XPS results N 1s region after 1 h reaction at 400 °C. (10% Ca-chabazite loading, 0.2% nitrogen solution added as indole)

XRD studies were conducted on fresh catalyst as well as on spent catalyst. Fresh catalyst was heated at 400 °C for 1 h with and without added water, in absence of reacting mixture, in order to determine any structural changes that may occur in the zeolite due to the temperature and presence of water. These temperature-exposed fresh catalysts and the spent catalyst samples present the same XRD peaks; the major XRD peaks found in all of the samples are assigned to the crystalline structure of chabazite. No significant difference could be found between the samples.

2.4.4 Chemical resistance tests

In order to test the resistance of the chabazite to higher nitrogen concentrations, reactions with indole solutions 10 times more concentrated than that found in oil sands bitumen (2.0% nitrogen w/w) were carried out. GC-FID/PFPD study shows no evidence of other nitrogen-bearing products being formed than those already reported in this work. The quantification of indole and nitrogen removal for these reactions is shown in *Table 10*.

Table 10. Indole removal from a 2.0% w/w nitrogen solution at 400 °C, 1 h reaction, 10 % catalyst loading.

	Indole removal		Nitrogen removal	
	No added water	1% water	No added water	1% water
Calcium	41.6%	38.9%	5.1%	6.6%
Proton	44.5%	48.4%	5.3%	4.0%

Also, the catalyst was tested by using a 10% nitrogen solution of 2,3-dihydroindole at 425 °C and clinoptilolite as catalyst. After the reaction, the catalyst was recovered, washed with pentane, dried and reused. The results show complete removal of the 2,3-dihydroindole after four successive experiments.

2.4.5 Aniline adsorption

Aniline adsorption experiments shows that the amount adsorbed is affected by the presence of water. Starting from a 2.0% concentration of aniline, the amount adsorbed was 2.2×10^{-5} g nitrogen/m² external surface area. That amount decreases to 1.2×10^{-5} g nitrogen/m² external surface area when 1% water is added to the system.

2.5 Discussion

2.5.1 Reaction Path

Reactions of indole over a natural zeolite catalyst demonstrate a clear method to remove pyrrolic nitrogen compounds without needing to hydrogenate the aromatic ring structure prior to cracking the C-N bonds. In order to further understand this combination of catalyst and model compound, it is necessary to identify all of the reaction products. Three main types of nitrogen containing products were identified: aromatic amines (primarily aniline and toluidine), methylindole and high molecular weight addition products. The presence of aniline and toluidine are in agreement with the IR and ¹H NMR spectroscopies, specifically, the bands at 3424.3 cm⁻¹ (primary amines) and the bands between 790 and 747 cm⁻¹ (substituted benzenes) for IR spectroscopy and the peaks in the region of 2-3 ppm (substituted benzenes) and 3.523 ppm

(aniline) for ^1H NMR spectroscopy. The production of aniline is consistent with the previous literature. Aniline has been reported to be in the products from both FCC and hydrogenation processes of petroleum fractions^{77,78}.

Elucidation of the mechanism by which the natural zeolites tested in this study cleaved the indole heterocyclic ring without the addition of hydrogen is extremely difficult. Conventionally, supported transition metal sulphides are used for hydrodenitrogenation reactions. At the reaction conditions used in this study, acidic natural zeolites were used at elevated temperatures under an inert atmosphere. These conditions present the possibility of two parallel reaction manifolds, one thermal and the other catalytic, which can interact to lead to ring cleavage. The presence of both Lewis and Brønsted–Lowry type acidity on the catalyst surface further complicate this analysis.

The indole molecule is a relatively stable aromatic species that is not usually reported to crack directly over an acidic catalyst. As mentioned previously, methylation of indole is known to greatly increase its reactivity. The mechanism of production of toluidine in this study, however, is not readily apparent. The presence of small quantities of the different toluidine isomers is potentially the result of trans-methylation reactions with the solvent, 1-methylnaphthalene, providing a source of methyl groups. The presence of naphthalene in the products supports this possibility. Furthermore, zeolites in general are known as strong transmethylation catalysts. A strong indication of the ability of the chabazite for transmethylation is the presence of a variety of methylated species in the reaction products from the conversion of indole, including: toluidine isomers, methylindole, 2-methylnaphthalene and dimethylnaphthalene. Importantly, the solvent is not the only sources of methyl groups. When naphthalene instead of 1-methylnaphthalene is used as solvent, the same types of reaction products are present, including toluidine.

In addition to toluidine, reactions of indole over chabazite resulted in the formation of a class of nitrogen bearing products having molar masses higher than indole. While this product was not accurately identified the molecular weight obtained from the MS studies is close to that of the addition product of two indole molecules (234.30 u) or one indole molecule plus one 1-methylnaphthalene molecule (259.35 u). The formation of indole polymers during HDN of

indole has been reported previously⁶⁷. *Figure 10* presents a sketch of one possible formation path of an indole dimer and trimer.

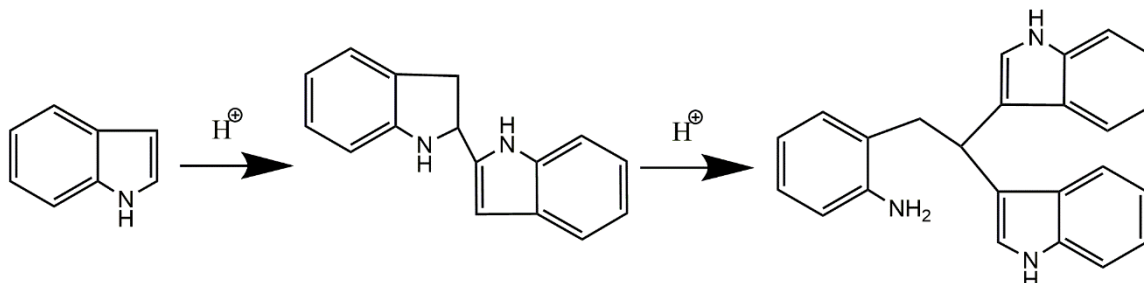


*Figure 10. Indole reactions to form a dimer and trimer*⁶⁴

Polyindole has been widely investigated for being conductive polymers. Different structures for this polymers have been elucidated and it is suggested that the structure of the polymer is highly dependent on the method used for the synthesis^{65,79,80}. It is important to note in *Figure 10* the loss of aromaticity in the heterocycle ring in the dimer and the opening of the ring structure in the trimer. Since these indole oligomers have been reported undergo decomposition starting at 410 °C⁷⁹, it is highly probable that the temperature used in this study would lead to the thermal decomposition of the oligomers, thus reducing the amount of high molecular weight products at the end of the reaction, and lead to the formation of aniline and toluidine (thermal manifold). Different cracking paths can be suggested for both dimer and trimer. One possible thermal decomposition path of an indole trimer is presented in *Figure 11*. In this scheme, formation of both aniline and toluidine are shown. The resulting dimers would continue to further thermally decompose into indole or substituted indoles. This step could account for the methylindole presence in the product mixture as well as the presence of methyl groups when the reaction is conducted using naphthalene as solvent. Also, methylindole is more reactive than indole. The formation of this species could promote the indole conversion.

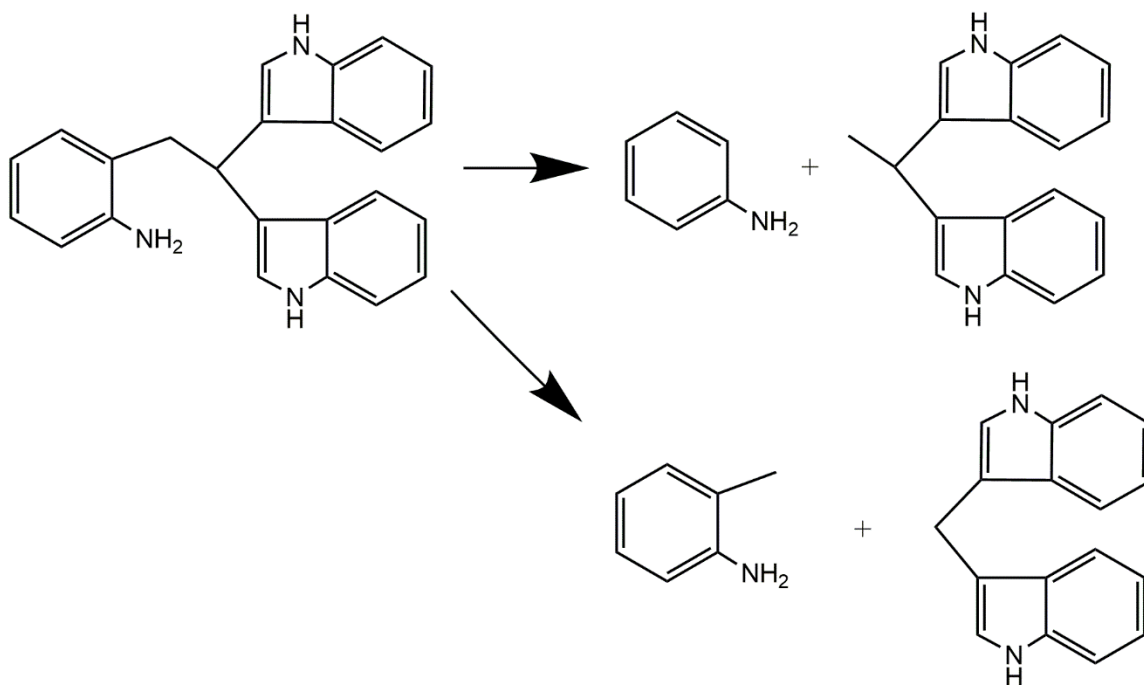


Figure 11. Trimer cracking for direct aniline/toluidine formation

To test the hypothesis of indole polymers formation, reactions were conducted at lower temperatures to reduce polymer decomposition. Carbon disulfide was added at the end of the reaction to dissolve heavy products that might be deposited on the surface of the catalyst. The products of this reaction were identified by GC-MS and include aniline, toluidine, methylindole, an indole dimer, a possible indole trimer, anthracenes and phenanthrenes. It is important to mention that, while in the 400 °C reactions, combination products were detected but not identified due to the low concentration. In this low temperature reactions, the concentration of indole dimer was high enough to make a positive identification. Unfortunately, not enough information was collected to enable the elucidation of the structure of the indole polymer. Due to the presence of Lewis and Brønsted acid sites, it is possible that different structural isomers of the polymer are being formed. Different cracking paths can be suggested for both dimer and trimer. In this work, only one was presented for clarity. *Figure 11* alone, however, is not sufficient to describe the entire reaction that is observed in this work since the observed indole conversion were very high.

Elucidation of reaction pathways occurring on heterogeneous catalysts is very challenging. In this study, the generation of four different nitrogen containing compounds from indole can be explained via at least two different reaction pathways:

- Formation of the indole (or indole—1-methylnaphthalene) oligomers followed by decomposition to generate aniline and toluidine. (reactions in series) as shown in *Figure 11* or
- Catalytic cracking of the indole to form aniline followed by methylation to form toluidine. Concomitant reaction of indole to form oligomers (reaction in parallel).

A reaction similar to the series pathway has been proposed for thiophene cracking over zeolites by B. Li *et al.*⁸¹ and it consist in two main steps. 1) protonation of the thiophene followed by an electrophilic substitution on a second thiophene together with the regeneration of the acidic site and 2) protonation of the sulphur with a simultaneous dissociation of the C-S bond. Even though the chemistry of sulfur heterocycles is very different from the chemistry of nitrogen heterocycles, there is some evidence that this mechanism could be applied to the system described in this study. The oligomer could be formed either with two or more indole molecules or by one indole molecule plus one methylnaphthalene molecule. A concerted reaction scheme for indole, incorporating both the thermal and catalytic manifolds, is presented in *Figure 12*.

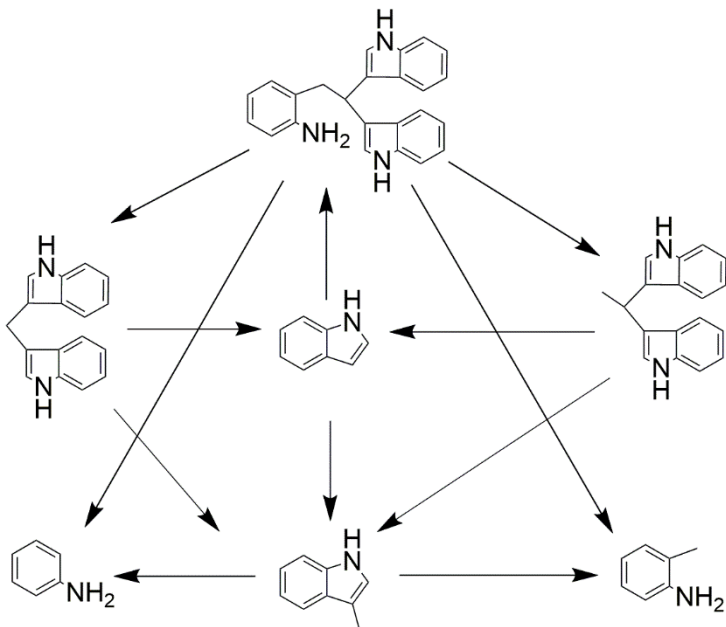


Figure 12. Possible reaction network for indole cracking in presence of chabazite.

Reactions of indole over chabazite likely follow a combination of oligomerization and direct cracking reactions. This parallel pathway could start by adsorption of indole at the C2-C3 position onto the active sites on the zeolite catalyst. The C2-C3 position has been reported as one of the preferred positions for indole adsorption over zeolite Y⁸². Bond scission at both the C3-C4 and the C2-N1 positions would yield adsorbed aniline. The aniline fragment could then be desorbed leaving an ethylene group over the surface of the zeolite. This ethylene fragment could then react to form coke or other aromatics⁸³. Another possibility for the parallel reaction path is that the indole is first methylated. Methylation of the indole could increase the reactivity of the molecule making the direct cracking easier in a mechanism similar to Hofmann elimination directed towards C3 position instead of towards the nitrogen atom. Discrimination of the two proposed pathways is, unfortunately, not possible using the data collected in this study. For both pathways, the production of naphthalene was detected suggesting the possibility of trans-methylation of the aniline to form different toluidine isomers. The presence of aniline in the low temperature reactions suggests that both reaction paths could be present in this reacting system. The lack of cracking products for the carbazole reaction suggests that access to C2 and C3 is necessary in order to open the pyrrolic ring.

The formation of 2,3-dihydroindole as a reaction intermediate prior to the cracking of the indole has been suggested for hydrodenitrogenation reactions⁸⁴; however, it was discarded for this system since the reactions with 2,3-dihydroindole solutions gave indole as the main product and the presence of 2,3-dihydroindole in the indole reactions was not detected. This result is to be expected since no hydrogen was added to the reactor. Conversion of 2,3-dihydroindole occurs at temperatures as low as 300 °C in presence of both natural and synthetic zeolites. (*Figure 7*).

The surface of the zeolites is highly heterogeneous, including not only different types of acid sites but also the strength of the acid sites is variable thorough the zeolite. Due to the heterogeneity of the surface and the possibility of interactions between the Lewis and Brønsted-Lowry acid sites, a very complex reaction network is to be expected. This complexity makes nearly impossible to achieve a more profound understanding of the basic science behind this reactions. Additionally, quantitative data on the products is hard to obtain due to the significant amount of adsorbed species on the surface of the catalyst. However, knowledge of the general reaction paths can greatly increase the potential applicability of the chabazite into very complex mixtures such as the ones found in the oil upgrading industry.

Quinoline has been reported to form the same products as indole during cracking and it could be suggested that the reaction path is similar to that of the indole; however, no aniline was detected after quinoline reaction in presence of the natural zeolite clinoptilolite. This result could suggest that the proton-donating ability of the clinoptilolite is not high enough to catalyze quinoline cracking reactions. Formation of high molecular weight products is in agreement with the proposed reaction paths discussed previously for indole. The absence of low molecular weight products could indicate a slow cracking step either in the parallel or series pathway.

2.5.2 Nitrogen Removal

Analysis of the reaction products of indole over chabazite showed both indole conversion and a reduction of the total nitrogen from solution. XPS spectra of the spent catalyst on the N 1s region show only one peak that can be assigned to aniline. These results suggest that the majority of the nitrogen on the catalyst surface is in form of aniline or aniline derivatives. Aniline can be considered basic in contrast with the indole, which is considered a non-basic nitrogen compound.

As a base, aniline is more likely to remain adsorbed into the zeolite's acid sites. In the XPS spectrum of the used catalyst, a FWHM of 1.5 could indicate the presence of small peaks around the aniline peak. Those small peaks can be assigned to aromatic nitrogen, organic ammonium salts or different aniline-like compounds⁷⁶; however, deconvolution of those peaks could lead to subjective results as the binding energies are close together. Aniline adsorption studies show lower nitrogen removal from solution than is observed with the reaction products, suggesting that aniline adsorption is equilibrium-limited, thus reversible. Comparing the data of the aniline adsorption against the nitrogen removal, only 20% of the removal can be accounted by straight adsorption. It is clear that the reaction creates additional pathways for the nitrogen removal. Additional pathways could include trapping of nitrogen compounds through coke formation and adsorption of basic compounds other than aniline. Curiously, ammonia is not observed in either the gas or liquid phase reaction products. XPS analysis also did not clearly show adsorbed ammonia on the chabazite. This result is contrary to the reported formation of ammonia during cracking of indole solutions using zeolite Y⁷⁷.

2.5.3 Effect of Surface Acidity and Water Addition

While water enhances the rate of bitumen conversion over natural zeolites⁵⁶, it has little to no effect on overall kinetics of indole conversion (*Table 5*). There is, however, a pronounced effect of the water on nitrogen removal from the liquid phase, especially for the Ca-chabazite (*Table 5*). These results highlight the possibility that water does not affect the adsorption and subsequent reaction of indole, but instead affects the adsorption or displacement of the reaction products from the active sites. These observations are similar to those reported by Loveless *et al.*³⁷ in which they detected no change in acidity caused by water addition but they found that water displaces adsorbed molecules. Water may be displacing weakly adsorbed molecules thus making room for more basic species as the aniline causing an increment in nitrogen removed by aniline adsorption. Since the reactions were made in pairs (no water added vs. 1.0% water), the error between the different surface acidities is higher and the difference among them can be considered non-significant for this study. The reaction path seems unaltered by the surface acidity or the addition of water since the same products were detected in the GC-FID/PFPD studies for all the reactions. XPS results also show no difference in the chemical identity of the

adsorbed products for all the reactions. Also, XRD data shows that there was no significant change in the structure of the catalyst due to the temperature or water addition.

It is important to mention that no efforts were made to ensure a completely dry catalyst. Studies show that chabazite easily picks up water from the ambient atmosphere. Chabazite can reach an equilibrium state of hydration in 20 minutes. Depending on the ambient conditions, the water content in the zeolite at equilibrium accounts for 15 to 22 %wt.^{85,86}. Due to the water content present in the zeolite, dehydration of the solvent was considered unnecessary and the solvents were used as received.

The nature of the zeolite (calcium vs proton exchanged) did not show a significant effect either on the reaction or the adsorption. It could be expected a higher removal from proton chabazite due to higher acidity; however, the adsorption depends also on the strength of the acid sites. As mention in the introduction, nitrogen compounds seems to adsorb preferentially on the stronger Brønsted-Lowry acid sites leaving the medium and low acidity sites untouched, as well as the Lewis acid sites⁵⁴. It is possible that only medium and low strength acid sites are created during the calcium to proton exchange.

The nature of the zeolite did not affect the reaction rate either. Reactions made with different concentration (0.2% and 2.0%) suggest that the indole removal is linearly dependent on the concentration. This result could indicate that the reaction is mass-transfer controlled. In this case, as it was observed, changes on the nature of the zeolite would have limited effect on the conversion.

2.5.4 Chemical Resistance

Comparison of the results of the reactions made with initial nitrogen concentrations of 0.2 and 2.0% indicate that the indole removal is directly proportional to concentration. Nitrogen removal results also show that the amount removed is dependent on other factors that includes the ratio of nitrogen / surface area, aniline concentration, indole concentration and others. The maximum amount of nitrogen adsorbed in the catalyst observed in these experiments is 1×10^{-4} g / m² external surface area. The saturation point of the chabazite with nitrogen is expected to be higher

than that since the conditions used in this study were not optimized for maximum nitrogen removal.

During the aniline adsorption studies, a maximum removal of 2.2×10^{-5} g nitrogen / m² external surface area was observed when no water was added. The decrease of the amount of nitrogen adsorbed when 1% water is added might be caused by changes in the dispersion or partial coverage of the surface with the water. The discrepancy between the nitrogen removal by reaction and the adsorption suggest that the reaction provides an additional path for nitrogen removal probably by chemical adsorption or by entrapment in heavier products (coke). This observation is in agreement with the XPS results showing the possible presence of nitrogen compounds other than aniline on the surface of the catalyst.

2.5.5 Industrial Applications

The results presented in this study support another pathway for nitrogen removal from oil that does not require large amounts of added hydrogen. Chabazite, an abundant and cheap natural zeolite, could be used to reduce nitrogen content in the petroleum feeds, including heavy oils, and to convert non-basic nitrogen compounds into basic nitrogen compounds that are easier to remove during HDN. While the capabilities of this zeolite are still not well known, several processes could be envisioned. Natural chabazite could be used in a step previous to catalytic cracking to reduce the poisoning of the catalyst used thus increasing the life of such catalyst. Also, it could be used as a pretreatment for hydrotreating reducing the consumption of hydrogen and the rate of poisoning of the catalyst. Another possible application is to use the chabazite as an additive for cracking or hydrotreating catalyst. The presence of the natural zeolite could reduce the poisoning of the catalyst and increase the nitrogen removal. The low cost of the natural chabazite might make these processes economically feasible.

2.6 Conclusions

The nitrogen removal capability of the natural zeolite chabazite has been proved. Removal of nitrogen up to 17.7% (starting from 0.2% nitrogen) was observed at 400 °C, after 1 h of reaction using 10% chabazite loading but the maximum removal could be higher. According with the results presented in this work, the nitrogen removal from oil sands using natural chabazite

reported by J. Bian *et al*⁴³ may be the result of transformation of non-basic nitrogen into basic nitrogen and posterior adsorption. In addition to the removal, chabazite converts hard to remove nitrogen species into species that are easier to remove with HDN and require less hydrogen consumption. Also, aromatic amines have significantly less poisoning activity towards acidic catalyst. With the evidence presented, two reactions path are proposed. These reactions generate aniline. After formation, the aniline is adsorbed onto the surface of the zeolite. Reactions with quinoline suggest that the proton-donating strength of the natural zeolites is not as high as those of zeolite Y but yet, at temperatures around 400 °C, the activity of the natural zeolites is comparable to that of the zeolite Y. In general, the activity of the natural zeolites for pyridinic nitrogen removal is lower than the activity for pyrrolic nitrogen removal.

The nature of the acid sites does not seem to affect the reaction path or the adsorption. The addition of water does not seem to affect the reaction path but has a significant influence in the adsorption especially in the case of Ca-chabazite.

The understanding of this mechanism of nitrogen removal could open the possibility of a new, improved process of oil upgrading using a cheap, abundant material.

3 Ni and V Removal from Oil and Model Compounds without Hydrogenation: Natural Chabazite as Solid Acid

3.1 Preface

In the previous chapter, quantification and reaction path for nitrogen removal using indole as model compound was presented. It was found that the nitrogen is removed from solution through a combination of reactions catalyzed by the zeolite and adsorption. The next chapter will focus on nickel and vanadium removal. Those metals are responsible for deactivation of catalysts, corrosion of the equipment and pollution when they are present in the final fuel products. Previous work with raw oil sands shows vanadium removal up to 67.5% but no information about how the vanadium is removed was presented. For this part of the study, Ni and vanadyl octaethylprophyrin were chosen as model compounds. The scope of this part of the study was not only to quantify the metals removal and propose a mode of action, but also to look for similarities between the activity of the zeolite towards indole and porphyrin.

3.2 Introduction

Demand for light oil products has increased sharply in the last 30 years⁸⁷ while the reserves of conventional light oil has decreased. The world's petroleum reserves are largely comprised of heavy oil, with an estimated 50 to 70% of the world's oil reserves being categorized as heavy, with an °API of less than 22.3. These heavy oils are normally associated with high levels of impurities such as sulphur, nitrogen and metals. As the reserves of light oil diminishes it is imperative that environmentally friendly processes be developed that are able to transform heavy crude oils into refinery products with high yields⁸⁸.

A recent study shows that chabazite, a cheap and abundant natural zeolite, can catalyze reactions in whole oil sands that lead to a residue conversion of up to 81% after reaction at 350 °C for 1 h³⁵. At the same conditions, in the presence of added water (3 % wt on a feed basis), this reaction produces liquid yields up to 96% with a low residue content (<29%). After reaction, liquid products contained around 5% wt. of asphaltenes. Reductions of 75% in average molecular weight (AMW) were also obtained. It has also been reported that, in similar

conditions, reactions in the presence of chabazite result in lower residue and gas oil liquid products as well as higher distillate, kerosene and naphtha fractions when compared to reactions conducted without catalyst (thermal), with zeolite Y or with clinoptilolite. Also, when water is added to the chabazite – oil reaction, an increase in the C2+ fraction and paraffins content is observed, and a decrease in vacuum residue fraction and in aliphatic hydrogen is obtained³⁵.

Efforts to gain a better understanding of the modes of action of the chabazite in oil sands upgrading are underway. In previous papers, using model compounds, it has been reported that chabazite is able to remove pyrrolic nitrogen from an indole solution without hydrogen addition. Nitrogen removal of 17 % was reported. In that study, it was also found that chabazite is able to convert 47% of hard to remove pyrrolic nitrogen into nitrogen species that are easier to remove in a later catalytic hydrodenitrogenation (HDN) step with less hydrogen consumption (see Chapter 2). Using n-hexadecane and cumene, it was reported that chabazite is able to catalyze cracking and transalkylation reactions and that the water increases the conversion for both compounds³⁵.

Heavy crude oil usually contains variable amounts of heteroatoms that need to be removed due to their harmful effects either during processing of the oil or during the use of the oil-derived products. Metals, usually nickel and vanadium, can be present in oil in concentrations ranging from 10 to 2000 ppm⁸⁹. In spite of the relatively low concentration, the effects of the nickel and vanadium on oil processing are significant and lead to decreased yields⁹⁰, corrosion⁹¹ and lower quality of products⁹²⁻⁹⁵ and ultimately to catalyst deactivation^{94,96,97}.

The presence of nickel and vanadium in oil has been studied by several researchers. It is generally agreed that most of the vanadium is contained in highly polar and highly aromatic fractions of the heavy oil. It is also reported for a number of crude oils, that the vanadium is mainly contained in the high boiling fractions. Another study found that both nickel and vanadium can be found in the acid, neutral and basic fractions of the Wilmington and Maya crude oil⁹⁸. With that information, it can be safely assumed that most of the nickel and vanadium in the oil are associated with large, aromatic molecules. Recent studies show that all the metals in the oil are present in porphyrin and porphyrin-like structures⁸⁹. X-ray studies also showed that all the

vanadium in oil is in the form of vanadyl porphyrins. The most common structures found in oil for vanadyl porphyrins are the vanadyl etioporphyrin and the vanadyl deoxophylloerythroetioporphyrin⁹⁹. (see Figure 13) Octaethylporphyrin (OEP) is widely used as model compound^{27,100-102} since its structure and properties resemble those of the aforementioned porphyrins.

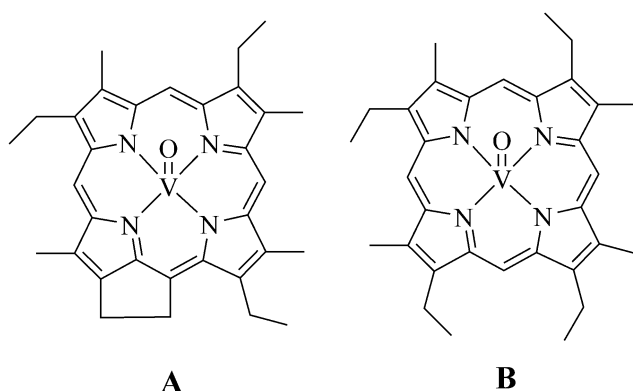


Figure 13. Structures of (A) vanadyl deoxophylloerythroetioporphyrin and (B) vanadyl etioporphyrin

As previously mentioned, the metals present in crude oil must be removed in order to minimize their effects on subsequent operations. Several methods have been reported for the demetallization of crude oils and related products. Since the porphyrins are demetallated by acids, a variety of liquid phase acids were used in industrial scale for metals removal since 1908; however, they promoted undesirable side reactions and product contamination²⁶ and are no longer used commercially. Several methods for metals removal have been published, but they have not been applied at industrial level. Those methods include extraction with a variety of solvents^{98,103}, adsorption¹⁰⁴, a variety of chemical methods^{105,106}, and combinations of reaction and adsorption or extraction⁹⁸. Also, in an effort to minimize the effect of the metals in the catalyst, the use of metal passivators have been proposed^{26,107}.

The processes currently used for metals removal at industrial level are not specifically designed for deep metals removal. These methods include deasphalting, coking and hydroconversion. The disadvantages of these processes include a reduction in product yield, high

metals content in the coke preventing it from being used as fuel, catalyst deactivation⁹⁹ and consumption of relatively large amounts of hydrogen. A recent trend is the use of additives and disposable catalyst for coking operations in order to improve the quality of coker products including lowering the metal content^{108,109}. These proposed processes require the use of inexpensive catalysts in order to be economically feasible. Natural zeolites, like the chabazite, are good candidates due to their price, abundance, and physical and chemical properties. While the cost of synthetic zeolites as zeolite Y can reach 1.00 USD/lb, natural zeolites can be as cheap as 0.01 USD/lb. Also, chabazite has been proven to have comparable meso and macropore surface area (59 m²/g compared to 78 of zeolite Y) and meso and macropore volume (0.1461 cm³/g compared to 0.1667 of zeolite Y), higher BET surface area (437 m²/g compared to 268 of zeolite Y), higher Si/Al ratio (3.55 over 2.41 of zeolite Y), higher acid site densities (0.25-0.65 or 2.44-3.66 meq/g depending on raw/exchange forms and the method of measurement compared to the 0.21-0.23 meq/g of zeolite Y) and higher acid strength measured by the heat of ammonia adsorption (56.4-60.2 kJ/mol depending on the raw/exchange type over 50.4 of the zeolite Y)³⁶. Chabazite has been found to be attractive for commercial processes including selective catalytic reduction (SCR) of nitrogen oxides¹¹⁰⁻¹¹² and heavy metals and ammonia removal from waste water¹¹³⁻¹¹⁶. It is important to mention that the focus of this study it is not to find a replacement for the zeolite Y commercially used as cracking catalyst but to develop a new process based on the physical and chemical properties of natural chabazite.

In order to develop low cost chabazite-based catalysts for partial upgrading, deeper knowledge of the reactions involved is needed. In this paper, quantification of nickel and vanadium removal using chabazite is reported; also, an insight into the way the metals are removed and side reactions take place is presented. Understanding the properties of the chabazite will allow to propose and optimize novel and existing processes for heavy oil upgrading that can simultaneously decrease viscosity, molecular weight, density, and nitrogen and metals content.

3.3 Experimental

3.3.1 Materials

For oil sands reactions, samples were obtained from the Syncrude Facility (Mildred Lake) near Fort McMurray, Alberta, Canada. The samples were determined to be a medium–high grade

ore. Some characterization data is shown in Table 11. Complete analysis of the sample can be found elsewhere⁵⁶. Model compounds were used to represent the naturally occurring nickel and vanadium porphyrins. Specifically, the compounds used were 2,3,7,8,12,13,17,18-Octaethyl-21H,23H-porphine nickel(II) (OEP-Ni) (97% assay) and 2,3,7,8,12,13,17,18-Octaethyl-21H,23H-porphine vanadium(IV) oxide (OEP-VO) (95% assay) due to its similarity with the porphyrins commonly found in oil. The structures of both molecules are presented in Figure 14. The solvent used for all reactions was 1-methylnaphthalene (97% assay). All the substances were obtained from Sigma-Adrich and used as received. Solutions of the porphyrins were prepared with a concentration of 66 ppm nickel or 140 ppm vanadium in 1-methylnaphthalene. This concentration is close to that reported for vacuum residue of Arabian heavy crude¹¹⁷.

Table 11. Composition of untreated oil sands and extracted bitumen

Fraction	Amount
<hr/>	
Dean Stark analysis on feed oil sands	% wt.
Solids	86.9
Bitumen	12.1
Water	1
<hr/>	
Boiling point distribution of toluene-extracted bitumen by SIMDIST and mass balance	% wt.
<hr/>	
Naphtha (>191 °C)	0
Kerosene (191–277 °C)	2
Distillate oil (277–343 °C)	9.2
Gas oil (343–566 °C)	46.8
Residuum (566 °C+)	42
<hr/>	
Heteroatoms and metals contents of toluene-extracted bitumen	
<hr/>	
Nitrogen	0.65 % wt.
Sulfur	5.18 %wt.
Vanadium	228 ppm
<hr/>	

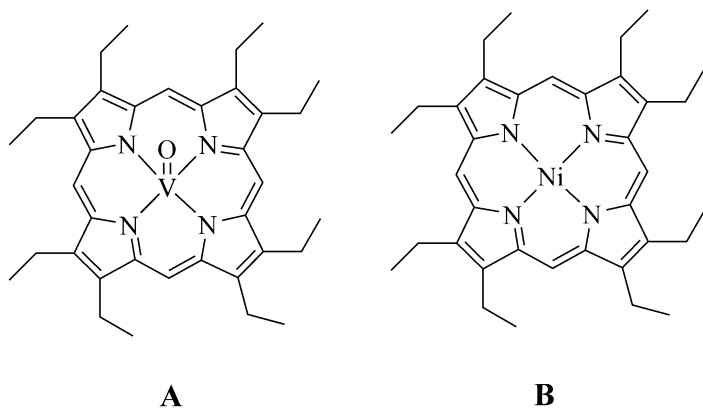


Figure 14. Structures of (A) 2,3,7,8,12,13,17,18-Octaethyl-21H,23H-porphine vanadium(IV) oxide and (B) 2,3,7,8,12,13,17,18-Octaethyl-21H,23H-porphine nickel(II)

Proton exchanged (H-Chabazite) and raw forms of natural calcium-rich chabazite (Ca-chabazite) were used. This particular natural zeolite was obtained from the Bowie deposits in Arizona. A detailed description of this zeolite is found elsewhere³⁶. The zeolites were kept in a desiccator until they were used in order to minimize the water content. Deionized water from a MilliQ water purification system by Millipore was also used for selected reactions.

3.3.2 Reactions

For the oil sands reactions, a stainless steel Par autoclave was used. This autoclave is custom-designed and has an approximate capacity of 1000 cm³ and uses a helical impeller specifically designed for oil sands handling. Details on the design of the reaction, schemes and detailed procedure can be found elsewhere⁵⁶. Reactions were conducted for 1 h at 350 °C using 500 g of oil sands. The catalyst (Ca-chabazite) loading was 5 % wt with 3 % wt of water addition based on the oil sands weight. After the reaction, the degasified and light fraction-stripped mixture was extracted with toluene to separate the oil products from the sand and spent catalyst. The solvent was then separated by distillation and the products analyzed. Raw oil sand samples were also toluene-extracted in a similar manner to provide benchmark samples.

For the model compounds, a 12 mL batch stainless steel microreactor was loaded with 3 mL of either nickel or vanadium solution and 0.3 g of proton or calcium chabazite (¹H-chabazite or Ca-chabazite). For selected reactions, 0.03 mL of deionized water was added. Detailed

descriptions of the reactor used and the general reaction procedure were documented previously⁷³. After loading the reactors, they were closed and pressurized to 20 MPaG to test for leaks. Once the reactors were leak free, nitrogen was added and vented three times to reduce the oxygen content. Prior to heating, the reactor pressure was adjusted to 1.7 MPaG, ensuring the reactions were in the liquid phase at reaction temperature. The reactors were submerged in a fluidized sand bath and heated to 400 °C for reaction times between 15 and 90 minutes. Reactions with and without added water were performed simultaneously in the same sand bath in order to reduce experimental variability. The reactors were mechanically shaken to minimize the effects of heat and mass transfer. The shaken was performed by an up-down movement with a frequency of 6.5 Hz and an amplitude of 2.6 cm. The pressure during the reactions is estimated to be 3.9 MPaG at reaction temperature. After the reaction times, the reactors were initially cooled with air for 15 minutes and then submerged into cold water immediately. The products were recovered and the solids were separated from the liquids by centrifugation (3 minutes at 5000 rpm). The reactors were thoroughly cleaned after each reaction and reused several times.

3.3.3 Product analysis

Vanadium quantification for the oil sands reactions was done by Instrumental Neutron Activation Analysis (INAA) at the Nuclear Reactor Facility of the University of Alberta. This facility uses a SLOWPOKE-II reactor for such analysis. Nickel was not quantified on the oil sands reactions.

For the model compounds, vanadium in both liquid and solid phases was quantified by electron paramagnetic resonance (EPR) spectroscopy. This technique is described in details elsewhere¹¹⁸. UV-visible spectroscopy is a common technique to quantify porphyrins; however, byproducts from reactions involving the solvent caused interference in the region where the Soret bands are located, thus preventing this technique from being useful for this study. EPR spectra were recorded at the Electron Paramagnetic Resonance Facility of the Department of Biochemistry at the University of Alberta.

Also for the model compounds, nickel removal was quantified by GC-PFPD (Pulsed Flame Photometric Detector) by using a Varian 3800 GC equipped with a 15 m x 0.32 mm x 0.1 µm

MXT-Biodiesel TG column. The injector was set up for on-column injections. The temperature program for the injector was maintained at an initial temperature of 70 °C for 0.74 min and then increased to 427 °C at 27 °C/min. The final temperature was maintained for 5 minutes. The oven temperature started at 53 °C and immediately ramped at a rate of 27 °C/min until it reached 430 °C. The final temperature was maintained for 5 minutes. Helium was used as a carrier gas at a rate of 6.1 mL/min. The detector temperature was set at 300 °C. This method was based on that used by Taegon, K. *et. al.*¹¹⁹ and Zeng, Y and Uden, P.C.¹²⁰ To optimize the signal of the PFPD, a solution of aniline and OEP-Ni in 1-methylnaphthalene was used. The emission spectra was surveyed from 0.5 to 7.0 ms gate delay using a 0.5 ms gate width. The parameters that gave the best nickel signal with a minimum response towards nitrogen and carbon were a gate delay of 4.5 ms with a gate opening of 0.5 ms. A R5070 photomultiplier was used in combination with a GG495 filter. The tube voltage was set at 580 V and the trigger level to 400 mV.

The spent catalyst for the model compounds reactions was analyzed by X-ray photoelectron spectroscopy (XPS) at the Alberta Centre for Surface Engineering and Science (ACES) at the University of Alberta. The resulting XPS spectra were deconvoluted using the CasaXPS software. Reference samples were prepared by wetting chabazite in the initial solution and letting it dry at ambient conditions.

For the model compounds reactions, nitrogen quantification was performed by oxidative combustion and chemiluminescence detection using a Multitek nitrogen and sulfur analyzer.

3.4 Results

Natural zeolite catalyzed upgrading of whole oil sands using Ca-chabazite was conducted to determine metals removal from complex mixtures. These experiments resulted in significant amounts of metals removal from the toluene-extracted liquid products (Table 12). INAA analysis showed a ~67.5% reduction of vanadium concentration in the toluene-extracted liquid products (from 228 ppm in the raw bitumen extracted from unreacted oil sands to 74 ppm in the Ca-chabazite catalyzed liquid products after 1 h reaction time at 350 °C). INAA analysis of the solids fractions showed that the vanadium removed from the liquid products is concentrated on the waste sand-spent catalyst mixture (vanadium concentration increased to 22.8 ppm in the

waste solids from the catalyzed reaction from 3.3 ppm left on the unreacted raw oil sands waste solids). With the corresponding masses of the solid and liquid fractions, vanadium mass balances on the unreacted and reacted samples showed that this translates to ~78.1% removal of the actual vanadium content by mass from the liquid product by the catalyzed upgrading reaction. The vanadium balance closure was within 6% of the total initial vanadium content.

Table 12. Vanadium concentration (ppm) for whole oil sands for both starting oil sands and after reaction at 350 °C for 1 hr, 10% catalyst loading.

		Toluene-Extracted Liquid Products	Waste Solids Fraction (including sand)
Raw Sands	Unreacted Oil	228±4	3.3±0.4
Ca Reacted Oil Sands	Chabazite-Catalyzed	74.1±1.4	22.8±1

For the vanadium model compounds, both the catalyst and the OEP-VO solution after reaction at 400 °C were analyzed by EPR spectroscopy. The obtained spectra for the solution is shown in Figure 15 and agrees with previously reported studies on OEP-VO¹²¹. For the spent catalysts, the same bands present in the liquid solutions can be identified; however, the spectra are distorted by the presence of a broad, isotropic band (Figure 16). The quantification of the vanadium was not adversely affected by the distortion of the spectra.

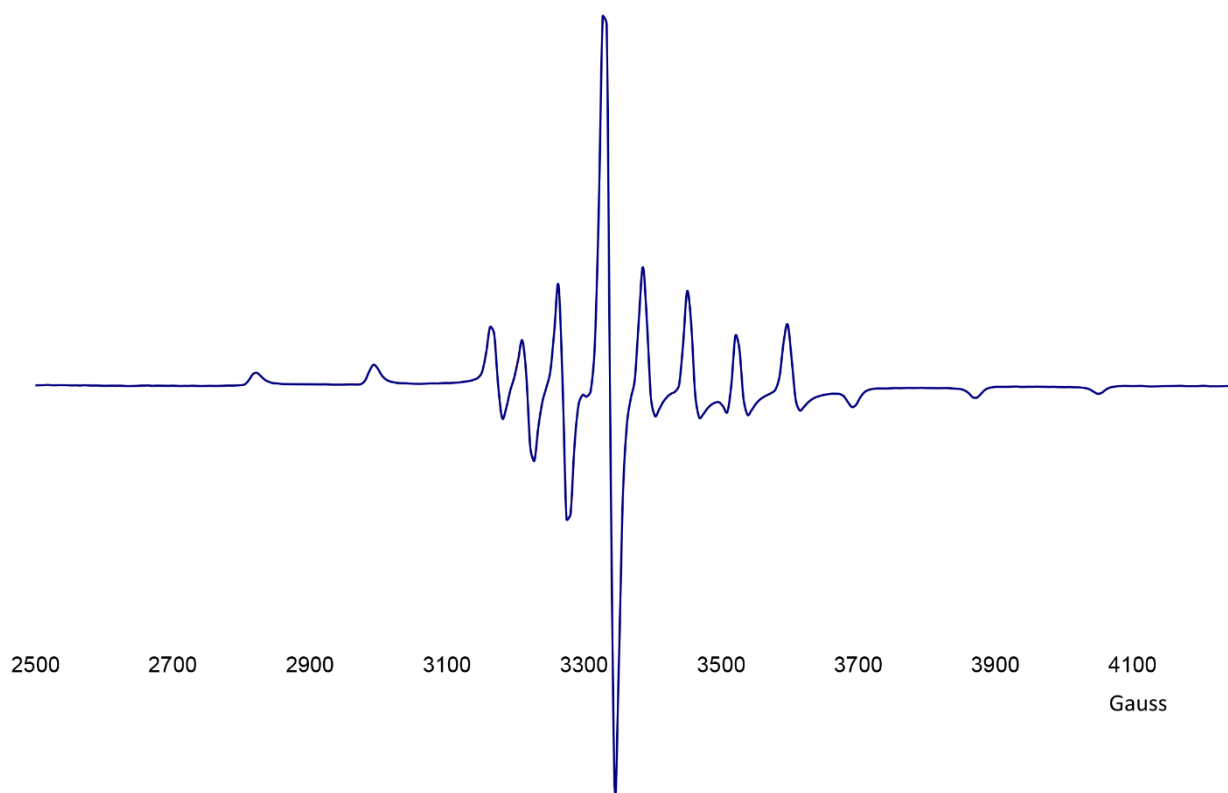


Figure 15. EPR spectra for OEP-VO in 1-methylnaphthalene solution after 1 hr reaction at 400 °C with 10% loading of Ca-chabazite. Initial concentration of vanadium was 140 ppm.

The concentration of vanadium in the OEP-VO solution was calculated using the intensity of the EPR signal as described by Stöcker *et al.*¹¹⁸ Vanadium removal from OEP-VO solution is presented in Table 13. The concentration of vanadium in the spent catalyst for the same reactions was also determined using the same method; the vanadium balance was found accurate within 4% variation from closure. Vanadium concentration in the spent catalyst are presented in Table 14. Nitrogen concentration for the model compound reactions was determined using a Multitek nitrogen and sulfur analyzer. Nitrogen removal results can be found in Table 13. Due to the difficulties of quantifying nickel in solids, the nickel balance was not performed.

Table 13. Vanadium and nitrogen removal (percentage from initial concentration) from OEP-VO solutions after 1 hr at 400 °C, 10% catalyst loading, 140 ppm initial vanadium concentration, 154.0 ppm initial nitrogen concentration.

	Vanadium Removal (%)		Nitrogen Removal (%)	
	¹ H-Chabazite	Ca-Chabazite	¹ H-Chabazite	Ca-Chabazite
1% added water	34.7	24.2	28.4	25.2
No-added water	47.9	35.0	41.0	32.0

Standard deviation 0.2% (vanadium) and 8.0% (nitrogen).

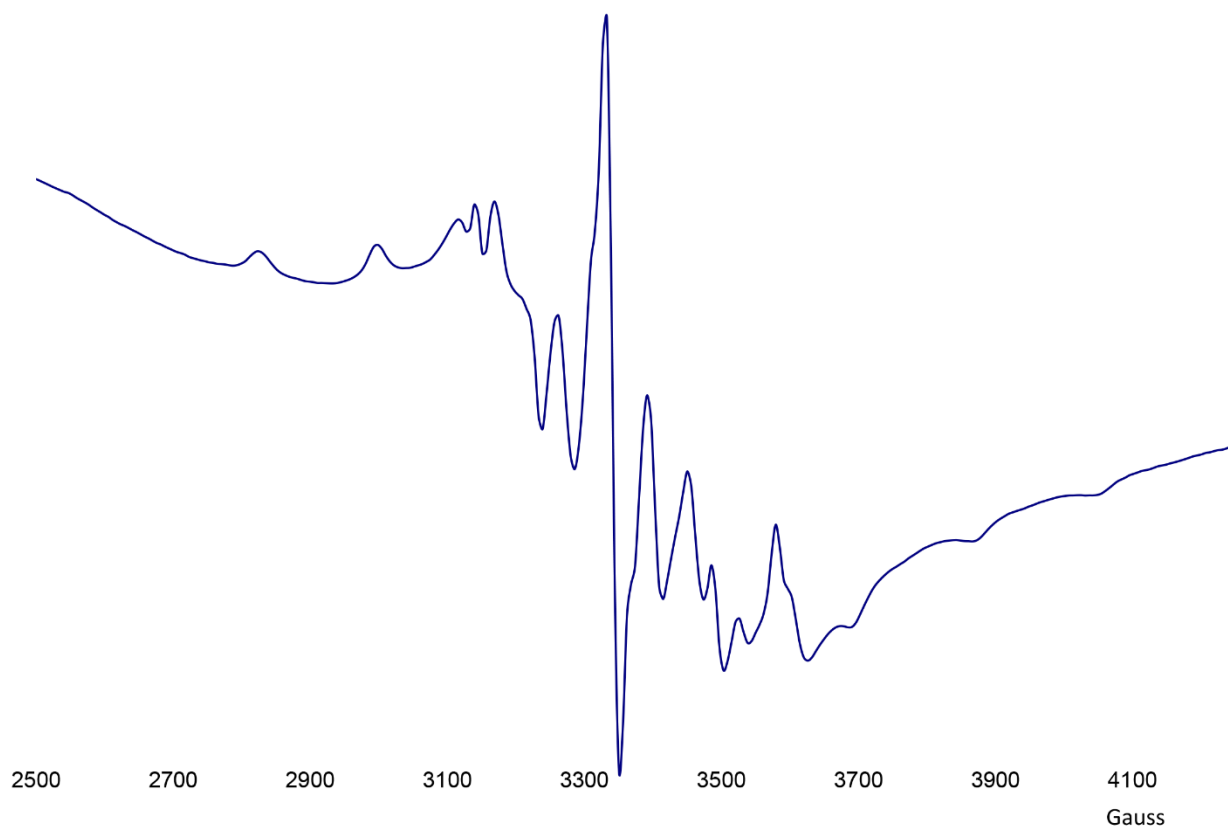


Figure 16. EPR spectra for spent Ca-chabazite after 1 hr reaction with a solution of OEP-VO in 1-methylnaphthalene at 400 °C. Initial concentration of vanadium in the solution was 140 ppm.

Table 14. Vanadium concentration in spent catalyst after 1 hr at 400 °C, 10% catalyst loading, 140 ppm initial vanadium concentration using OEP-VO.

	Vanadium in solid (ppm)		Vanadium in solid (% of initial vanadium)	
	¹ H-Chabazite	Ca-Chabazite	¹ H-Chabazite	Ca-Chabazite
1% added water	512.4	338.8	36.6	24.2
No-added water	614.6	509.6	43.9	36.4

Standard deviation 0.2% (vanadium)

Spent catalyst after reaction with OEP-Ni was also analyzed by XPS. Results are summarized in Table 15, Table 16, Table 17 and Table 18. For both nickel and vanadium, the XPS signal in the correspondent regions for the metals was not strong enough to be deconvoluted satisfactorily. Nickel removal for OEP-Ni reactions was quantified by GC-PFPD. After 1 h at 375 °C, 3.4% of the initial nickel remained in solution. Samples of the same nickel solution were left in contact with the catalyst at room temperature until equilibrium was achieved. In these samples, GC-PFPD analysis showed 90.0% removal of nickel after 7 days. No significant differences were found between samples generated from reaction conducted with and without added water. The OEP-Ni showed a retention time of 15.75 min while, after one hour reaction, three overlapping peaks were detected at 14.25, 15.00 and 15.75 min as well as a small peak at 8.40 min. The samples that were allowed to reach equilibrium showed two nickel signals at 9.9 and 10.3 min.

Table 15. C 1s XPS bands for spent catalyst of OEP-VO solution after 1 hr at 400 °C, 10% catalyst loading, 140 ppm initial vanadium concentration. Position in eV

C 1s									
¹ H-Chabazite				Ca-Chabazite				Reference Sample	
No added water		1% added water		No added water		1% added water			
Position	FWHM	Position	FWHM	Position	FWHM	Position	FWHM	Position	FWHM
282.4	1.36	282.4	1.38	282.3	1.42	282.4	1.41	282.7	1.36
283.8	2.29	283.7	2.43	283.9	2.19	283.8	2.34	284.3	1.48
286.8	1.49	286.8	1.62	286.7	1.49	286.8	1.29	286.5	2.48

Table 16. N 1s XPS bands for spent catalyst for OEP-Ni solution after 1 hr at 400 °C, 10% catalyst loading, 140 ppm initial vanadium concentration. Position in eV

N 1s									
¹ H-Chabazite				Ca-Chabazite				Reference Sample	
No added water		1% added water		No added water		1% added water			
Position	FWHM	Position	FWHM	Position	FWHM	Position	FWHM	Position	FWHM
396.3	1.36	396.1	1.01	396	0.95	396.2	1.16		
397.9	1.21	397.2	1.46	396.8	0.42	397.1	0.48		
398.6	2.55	398.2	1.47	397.8	1.83	397.9	1.33	398.2	2.48
400.4	1.74	400.3	2.11	400	1.82	400.1	2.2	400.8	1.78

3.5 Discussion

Metals removal processes that avoid the use of expensive reagents (such as hydrogen) and minimize the waste byproducts are desired in order to reduce the environmental impact and the cost of upgrading heavy oils. At the conditions used in the present study, 67.5% of the vanadium

present in oil sands was removed proving that low cost natural zeolites can be effective in lowering the metals concentration from Athabasca oil sands. Since previous reports^{35,56} also showed that the natural zeolites are able to remove nitrogen and metals from a heterogeneous and chemically complex systems (see Chapter 2), the use of model compounds is an attractive alternative to investigate how natural zeolites remove both Ni and V from the heavy oil. By using EPR spectroscopy, vanadium removals from OEP-VO solution up to 47.9% were observed after one hour of reaction. Nickel porphyrins are considered one of the most stable of the metal porphyrins¹²². Since EPR spectroscopy cannot detect Ni (II) species, nickel removal from OEP-NI solution in this case was quantified by GC-PFPD and shown to be 3.4% after one hour of reaction. The higher removal of vanadium after reaction when compared with nickel is consistent with the higher inherent stability of the nickel porphyrins. A direct comparison of the nickel and vanadium concentrations by GC-PFPD was not possible due to the difficulty in separating the vanadium emissions with those from carbon and nitrogen. In order to test how much nickel could be removed using chabazite, OEP-Ni solution samples were left in contact with the catalyst at room temperature until equilibrium was reached. It was found that nickel removal up to 90.0% is possible, but very long contact times are needed. The vanadium removal from OEP-VO solutions is comparable to that of the Athabasca oil sands reactions.

Table 17. C 1s XPS bands for spent catalyst of OEP-Ni solution after 1 hr at 400 °C, 10% catalyst loading, 66 ppm initial nickel concentration. Position in eV.

C 1s

								Reference Sample	
¹ H-Chabazite				Ca-Chabazite					
No added water		1% added water		No added water		1% added water			
Position	FWHM	Position	FWHM	Position	FWHM	Position	FWHM	Position	FWHM
282.4	1.4	282.4	1.37	282.3	1.42	282.4	1.43	282.7	1.42
283.7	2.37	283.7	2.39	283.7	2.32	283.9	2.11	284.1	1.36
286.9	2.16	286.8	1.58	286.8	1.44	286.8	1.34	286.7	2.28

While most of the oil processed industrially has a very low water content, whole oil sands contains water up to 3.7 % wt. in the pore structure in the formation⁷². This connate water content is important since it has been shown that water can have a deleterious impact on the performance of zeolites and other catalysts at high temperatures. In the present study, in an effort to understand the effect of water on the metals removal from whole oil sands, water was added to some of the model compound reactions. For OEP-VO reactions, water consistently reduces the amount of metal removed from solution. While the specific nature of interaction between the porphyrin and the natural zeolite surface is unknown, they are thought to interact through a donor-acceptor interaction with either Lewis or Brønsted-Lowry acid sites¹²³. It has also been shown that water can displace adsorbed nitrogen species from the surfaces with Lewis acidity³⁷. Therefore it is probable that, in this study, the added water and metal porphyrins competitively adsorbed on the zeolite surface. Previous XRD studies showed that, under the conditions used in this paper, there is no significant change in the crystallinity of the chabazite in the presence of water (see Chapter 2).

Table 18. N 1s XPS bands for spent catalyst of OEP-Ni solution after 1 hr at 400 °C, 10% catalyst loading, 66 ppm initial nickel concentration. Position in eV.

N 1s									
¹ H-Chabazite				Ca-Chabazite				Reference Sample	
No added water		1% added water		No added water		1% added water			
Position	FWHM	Position	FWHM	Position	FWHM	Position	FWHM	Position	FWHM
396.7	1.46	396.5	0.91	396.2	1.08	396.3	1.2		
-	-	397.2	0.46	397.6	1.63	397.5	1.1		
398.2	1.46	398	1.99	398.7	0.34	398.5	1.62	398.5	2.8
400.4	2.12	400.5	1.95	400	2.23	400.3	2.96	400.7	1.8

Several methods were used to determine the vanadium and nickel species present in both liquid and solid phases after the reactions. It is expected that both nickel and vanadyl porphyrins react similarly in the presence of the chabazite. EPR spectroscopy on the OEP-VO liquid products show no differences with the initial solution except the concentration, suggesting that all the metal in solution is still bonded to porphyrin rings. However, GC-PFPD studies on the OEP-Ni showed different nickel containing compounds with lower retention times than the parent porphyrin. Previous studies showed that chabazite is able to catalyze trans-alkylation reactions (see Chapter 2). It is possible that the chabazite is removing the side chains of the OEP producing a variety of dealkylated products without opening the porphyrin ring structure. Such reactions are able to produce several different species of porphyrins with different retention times when analyzed by GC-PFPD. Six different peaks were detected at 15.75, 15.00, 14.25, 10.3, 9.9 and 8.40 min. Since all the peaks have shorter retention times than those of the original porphyrin, it is safe to assume that all the products have a lower molecular weight than the starting material. Accounting for the symmetry of the OEP, removing one ethyl group would result in two different peaks showing on the GC-PFPD. Removing two ethyl groups would produce five different products. Since six porphyrin peaks were detected (including the parent compound), it can be assumed that five different molecules were produced. One of the products can be expected to be a heptaethyl porphyrin while the other four might be hexaethyl porphyrins. The other two hexaethyl porphyrins may well not be thermodynamically or kinetically favorable to form in enough quantity to be detected.

Further evidence of the integrity of the porphyrin ring structure can be obtained from XPS data. The C 1s region of the chabazite impregnated with the initial OEP solutions (reference sample) shows a peak that can be deconvoluted into three components which are consistent with those reported previously¹²⁴. The bands at 282.7 eV (OEP-VO) and 282.7 eV (OEP-Ni) can be assigned to ethylenic and methinic carbons respectively. The bands at 284.3 eV (OEP-VO) and 284.1 eV (OEP-Ni) correspond to aliphatic carbons (C-N) and the bands at 286.5 eV (OEP-VO) and 286.7 eV (OEP-Ni) are shake up or satellite bands caused by the presence of the aromatic ring. Results for the spent catalyst from the OEP reactions at the C 1s region show small changes after the reaction. The satellite bands shift to a higher binding energy while the two other bands

shift to a lower binding energy. The peaks found for the spent catalyst are consistent with those reported in the literature for free base (demetallated) OEP¹²⁵. These results suggest that at the reaction conditions under investigation, the porphyrin ring is not being opened; however, the shifts in binding energy suggest that dealkylation reactions may be occurring in the system.

The mechanism of metals removal is difficult to determine from experiments using whole oil sands. Using the model compounds, it was possible to determine if the metals removal was through molecular adsorption of porphyrin molecules or if the porphyrin molecules were demetallated. The difference in metals removal for OEP-VO reactions is determined through the use of EPR spectroscopy of the spent catalyst. The spectra showed differences from the reference samples, primarily the presence of a broad isotropic band. This band is caused by the vanadium being in a different electronic environment. For XPS in the N 1s region, the reference sample shows two peaks (398.2 eV and 400.8 eV for OEP-VO and 398.5 eV and 400.7 eV for OEP-Ni). These two peaks have been assigned to the sp³ and sp² hybridization of the nitrogen in the porphyrin¹²⁶. In addition to those peaks found in the reference sample, two additional peaks were detected in the spent catalyst for the model compound reactions. These peaks were shifted to lower binding energies by more than 2.0 eV. Figure 17 shows selected spectra in the N 1s region. Lower binding energies on this region for porphyrins are usually associated with low-electronegativity ligands or free base porphyrins¹²⁷. This trend is observed in all the samples regardless of the metal, the ion on the chabazite or water addition. This result suggests that the porphyrin is being either demetalated or bonded to the calcium ions present on the zeolite. Since calcium porphyrins are among the least stable porphyrins and demetalate in the presence of water¹²⁸, demetalation is the most probable reaction. The two peaks associated with the reference sample indicate that not all of the porphyrin is being demetalated. Demetalation of porphyrins in the presence of an acid is well known¹²⁹. Furthermore, porphyrins can be classified by their resistance to demetalation under different acids, including acetic, hydrochloric and sulfuric acids. Demetalation by solid acids (acidic clays) has been also reported previously¹³⁰. The ESR spectroscopy is consistent with reports that shows that removed metal ions could be present in the spent catalyst as several different compounds¹³¹.

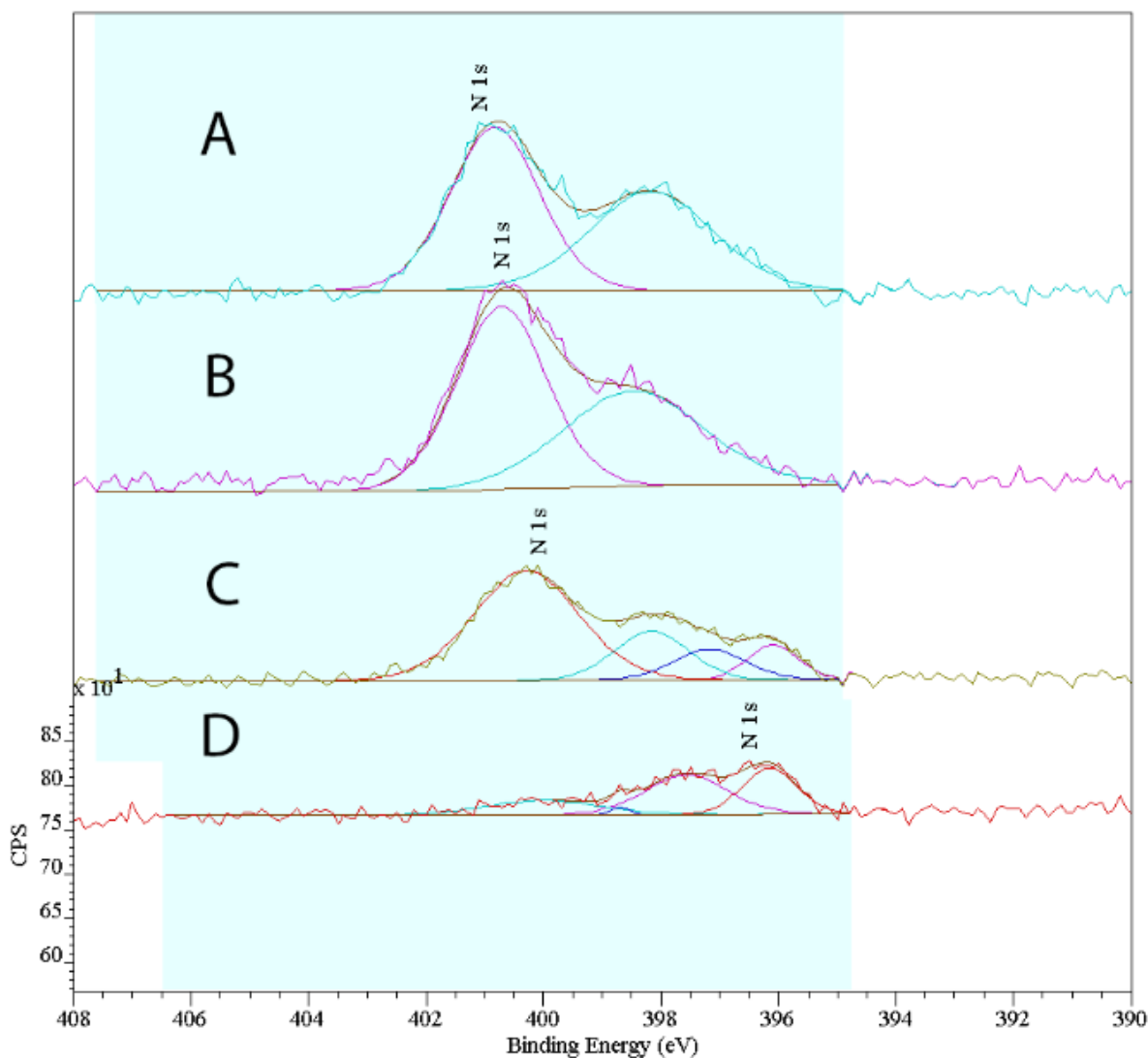


Figure 17. XPS spectra, N 1s region. A) Ca-chabazite impregnated with OEP-VO solution (reference sample); B) Ca-chabazite impregnated with OEP-Ni solution (reference sample); C) 1H-chabazite after reaction with OEP-V, 400 °C, 1 hr, 1% water added; D) Ca-chabazite after reaction with OEP-Ni, 400°C, 1 hr, no water added.

Since each porphyrin molecule contains four nitrogen atoms and there is no other source of nitrogen in the model compound solutions, total nitrogen analysis can be used as a tool to track the porphyrins in solution. From Table 13, it can be seen that the nitrogen removal is consistently lower than the vanadium removal. As it was mentioned before, the vanadium left in solution is in

the form of vanadyl porphyrin according to ESR studies. This evidence suggests that some non-metal-bonded nitrogen is present in solution after the reaction. It is possible that the porphyrin is being demetalated and then desorbed from the chabazite surface. Demetalation of the porphyrin ring was also observed in the XPS studies. The maximum desorption of free base porphyrin is observed for ¹H-chabazite with no water addition (47.9 vanadium removal vs 41.0 nitrogen removal). The minimum was observed using Ca-chabazite and adding 1% water. Unfortunately, in this last case, the amount of free base porphyrin desorbed is within the experimental error and cannot be quantified accurately. The maximum desorption observed is 6.9% of the initial nitrogen concentration. Dividing this quantity by the amount of vanadium removed (47.9%), it can be found that the desorbed non-metal-bonded nitrogen corresponds to 14.4% of the total porphyrin associated with the removed vanadium. When adding 1% water to this system, the absolute desorption of free base porphyrin is 6.3% of the initial nitrogen; however, this represents 18.2% of the total porphyrins associated with the removed vanadium. Since porphyrin demetalation depends on acidic strength, these results indicate that the ¹H-chabazite has higher acidic strength than the Ca-chabazite and thus is more active towards demetalation of the porphyrin. This acidic strength is increased by the addition of water, though the water may be competitively adsorbing into the surface, thus increasing the amount of free base porphyrin desorption and reducing the amount of vanadium removed from solution.

Summarizing the results, there are four main phenomena occurring in this system: porphyrin adsorption onto the surface, demetalation, desorption of free base porphyrins and dealkylation of the porphyrin ring structure. Only part of the demetalated porphyrin is desorbed as free base porphyrin. There is no evidence of a relation between the dealkylation and the adsorption/demetalation processes. Figure 18 shows the possible reaction network for the OEP in presence of chabazite. For brevity, only one hexaethylporphyrin is shown.

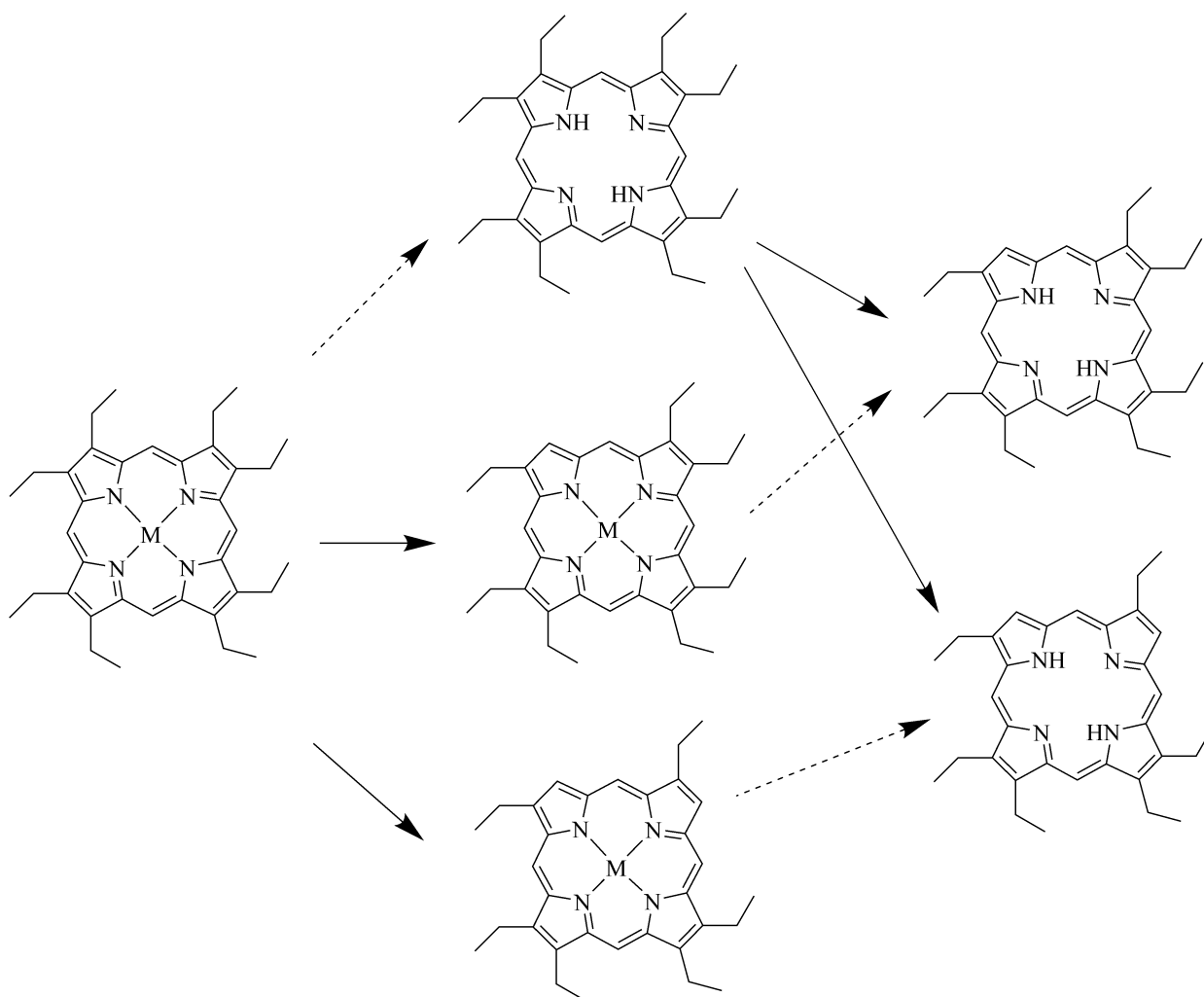


Figure 18. Possible reaction network for OEP in presence of chabazite. Dashed lines indicate demetalation and full lines indicate dealkylation.

The effect of the metals on poisoning cracking catalysts has been widely investigated; however, the mechanism in which the metals deposit in the catalyst is not well understood. In this paper, by using model compounds, an insight of how the natural zeolites could remove metals from oil is presented. A better understanding of the path for this removal could open the door for new processes that reduce the metal content in oil without sacrificing product yield. The results presented here can help to develop new processes that reduce the metals content in petroleum without using hydrogen or producing large quantities of waste. Together with the nitrogen removal properties of this material (see Chapter 2), new primary upgrading processes

for heavy oils can be envisioned. The chabazite, being a natural, abundant and inexpensive material, can make the new processes even more economically attractive. *In situ* processes could provide long contact times required for nickel reduction while FCC like processes using chabazite could prove to be beneficial for heavy oils with high metals and nitrogen content. Used in combination with subsequent hydrodenitrogenation (HDN) and hydrodemetallization (HDM) processes, reductions on hydrogen consumption required for deep nitrogen and metals removal could be achieved. This material could also be used as an additive to current processes to increase the lifetime of the catalyst by reducing the poisoning due to metals.

3.6 Conclusions

The metals removal ability of the natural chabazite was demonstrated using both oil sands and model compounds. Removal up to 67.5% of vanadium from oil sands and up to 47.9% using OEP-VO as model compound were achieved. Nickel removal at the same conditions was considerably lower at 3.4% (starting from 66 ppm) but increased to 90.0% when the solution was allowed to reach equilibrium at room temperature.

Evidence of demetalation of both nickel and vanadium porphyrin rings was found through nitrogen quantification, EPR spectroscopy and XPS studies. It is possible that demetalated porphyrins are able to desorb from the catalyst. Addition of water reduces the amount of metal removed from the solution by approximately 28% for vanadium and 31% for nickel; however, the water increases the relative amount of nitrogen desorbed from the surface. GC-PFPD studies showed that the chabazite is not only active towards demetalation but also has some cracking ability (side chain removal).

By understanding the way the chabazite removes the metals from solution, new and improved processes that decrease the metals content from organic liquids can be envisioned. Using no hydrogen, this low cost catalyst seems to be a good opportunity for the heavy oil industry.

4 Cracking and Transalkylation of Oil and Model Compounds: Natural Chabazite as Solid Acid

4.1 Preface

In the previous chapters, nitrogen and metals removal were quantified and reaction paths were suggested. Chabazite shows a dual action as solid acid and adsorbent that allows the removal of metals from solution; Also, evidence suggest that chabazite is active towards transalkylation even in the presence of metals. In the next chapter, reactions with alkanes (using n-hexadecane as model compound) and aromatics (cumene as model compound) will be discussed. Both n-hexadecane and cumene are commonly used as model compounds for cracking reactions. Previous work showed that chabazite is able to reduce the presence of asphaltenes for up to 26.2%¹³². Also, it can reduce the residue by 15% and increase the pentane soluble liquids by 15%³⁶ as well as reduce the molecular weight from 1409 u to 360 u⁵⁶. The scope of this part of the study is to determine the cracking activity of the chabazite and to get an insight into the main reactions that could be leading to the changes observed while processing raw oil sands with natural zeolites.

In this study, both cumene and n-hexadecane are used to determine the catalytic cracking ability of the chabazite. Both types of model compounds are needed due to the very complex and varied composition of the bitumen. It is know that cumene reacts through different paths in presence of Brønsted-Lowry and Lewis acid sites giving different sets of products. Since chabazite has both types of acid sites, a wide range of products is expected and, by using nitrogen compounds as poisoning agents, it is possible to determine the role of the different acid sites.

It is important to mention that transalkylation reactions have been observed in both indole and octaethylporphyrin reactions. These reactions, together with the cracking ability of the zeolites, can results in a complex net of reactions capable to drastically change the properties of oil through molecular rearrangements. By alkylating highly aromatic molecules present in the oil, it

is possible to change their solubility in alkanes and by changing the solubility of asphaltenes, reduction in viscosity is also to be expected.

4.2 Introduction

The demand for gasoline, jet fuel, heating oil and diesel sharply increased from 1980 to 2006. Since these products are derived from the light and middle distillates from crude oil, the need for deep conversion of heavy ends to lighter fractions has increased⁸⁷. In order to achieve this conversion, heavy crudes and bitumen must be upgraded before being processed in a conventional refinery. Currently, the upgrading process can be divided into two steps: primary upgrading and secondary upgrading. In addition to these steps, separation processes (such as deasphalting) can be used.

The primary upgrading operation has the main objective of reducing the molecular weight of the feed¹³³. Secondary upgrading is used to prepare the oil for processing in conventional refineries by increasing the H/C ratio and reducing the heteroatoms concentration. The differences between primary and secondary upgrading can be summarized in two points: severity and selectivity. Primary upgrading uses high severity processes that have low selectivity while secondary upgrading uses low severity processes that achieve a high selectivity¹³³. Thermal cracking is the main option for primary upgrading while hydroconversion, catalytic cracking and hydrocracking are the main options for secondary upgrading. Catalytic cracking possesses some advantages over the thermal cracking and hydrocracking including: having C3 to C5 as major products, using lower temperatures compared to thermal cracking and avoiding the use of relatively expensive hydrogen¹³⁴; however, cracking catalyst are known to be poisoned by basic nitrogen and inhibited by non-basic nitrogen and polynuclear aromatics¹³⁵ and it is not as selective as the hydrogen addition processes.

Recently, studies have shown that natural zeolites, specifically chabazite, can catalyze reactions that reduce the viscosity of raw oil sands and its average molecular weight and remove heteroatoms at temperatures close to those used for catalytic cracking. It is reported that calcium chabazite (Ca-chabazite) can convert 80% of the vacuum residue when used at temperatures above 350 °C for 1 h Compared to zeolite Y under the same conditions, Ca-chabazite reactions

give less residue and gas oil and more distillate, kerosene and naphtha and vanadium is reduced from 228 ppm to 74 ppm⁵⁶. Other studies show that water interacts with the chabazite increasing the C₂+ gas fraction, the paraffin fraction and causes an increase in protons bonded to carbons in alpha positions. At the same time, water addition decreases the vacuum residue fraction and the aliphatic protons³⁵.

Zeolites are known by its highly regular structure; however, they are also considered a very complex catalyst since it contains both Lewis and Brønsted-Lowry acid sites of different strength and capable of synergism¹³⁶. This complexity together with the intricacy of the mixture of molecules that comprise the oil makes the oil-zeolite reacting system extremely hard to characterize. Cracking process in presence of zeolites involves a network of reactions occurring both in parallel and in series. Figure 19 shows some of the reactions involved in the cracking processes. Petroleum is not strictly a hydrocarbon but also contains heteroatoms and metals. In addition to the hydrocarbon reactions, other phenomena occurs during catalytic cracking including reactions of molecules containing heteroatoms, adsorption in both catalyst and coke, changes in solubility and trapping of chemical species inside the coke. It is important to mention that the word cracking is applied to both the overall process and to the specific reaction that yields C-C bond scission. Throughout this paper, “cracking process” will refer to the general network of reactions while “cracking” will be used for the specific C-C bond scission step.

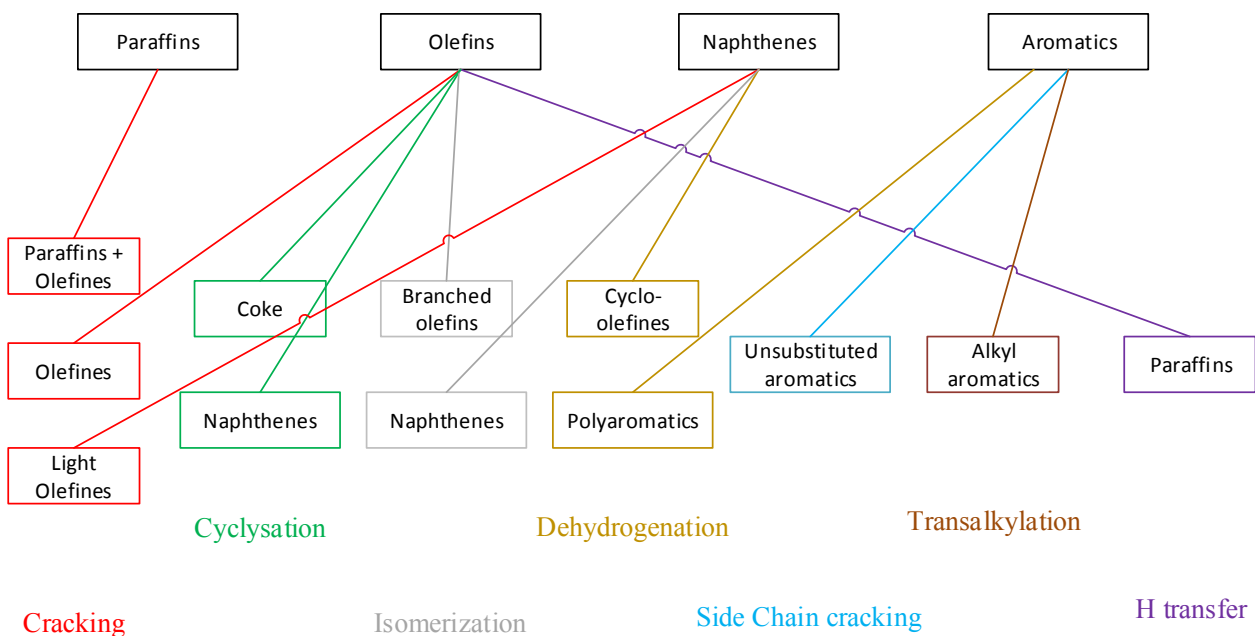


Figure 19. Main reactions network for cracking process of hydrocarbon molecules¹³⁷.

Due to the complexity of the catalytic cracking reaction systems, model compounds are routinely used in an effort to understand and improve the zeolite-based processes. The cumene cracking process is often used as a test reaction for catalytic cracking and as a model compound to determine the strength and nature of the acid sites in solid catalyst¹³⁸. The reactions of cumene in presence of an acid catalyst were initially thought to be very simple and to have only benzene and propylene as products; however, in 1965 some discrepancies on the stoichiometry of the products lead to the discovery of additional species as ethylbenzene, cymene, diisopropylbenzene, ethyltoluene and others¹³⁸. Instead of discouraging the use of cumene due to the complex network of reactions, the gas phase reaction of cumene was proposed as a model for identifying Lewis and Brønsted-Lowry acid sites on catalysts¹³⁹. Some authors suggest that the major reactions are dealkylation over Brønsted-Lowry acid sites to give benzene, propene and ethylbenzene and dehydrogenation over Lewis acid sites to give α -methylstyrene¹³⁹. Since the product distribution is highly dependent on the catalyst's time on stream, this data should be carefully examined. It is known that longer times on stream decreases the alkylation products and increases the dehydrogenation products¹³⁹. Corma and Wojciechowski proposed a list of the main reaction products (Table 19).

Table 19. Summary of the main cumene acid catalysed reaction products¹³⁸.

Product	Primary or secondary product	Stability	Type of acid site
Benzene	Primary	Stable	Brønsted-Lowry
Propylene	Primary	Stable	Brønsted-Lowry
Diisopropylbenzene	Primary	Unstable	Brønsted-Lowry
n-propylbenzene	Primary + secondary	Stable	Lewis
Cymene	Primary	Stable	Lewis
Ethyltoluene	Primary	Unstable	Lewis
Ethylbenzene	Primary + secondary	Stable	Lewis
1-, n- Butene	Primary + secondary	Stable	Lewis + Brønsted Lowry

Due to this complexity of the acid-catalyzed cumene reaction, several groups have contributed to the understanding of this reaction but a full characterization is still out of reach. From the different contributions to the study of the cumene reactions over zeolites, it is known that the dealkylation of cumene to propylene can be considered to be the first step¹⁴⁰. Part of the propylene seems to oligomerize. This propylene oligomer can then undergo fragmentation¹⁴¹ to yield smaller products or undergo condensation to ultimately form coke¹⁴². Lewis acid sites accelerate the oligomerization reaction, as well as the subsequent cracking and hydride transfer reactions¹⁴¹. Weak acid sites also favour oligomerization and, since more active acid sites decay faster than the less active¹⁴³, the product distribution tends to change with increasing time-on-stream¹³⁹. Figure 20 shows a possible reaction network proposed by Corma and Wojciechowski¹³⁸. It is important to note that the formation of several primary products in this reaction network involves not only dealkylation reactions but also transalkylation reactions.

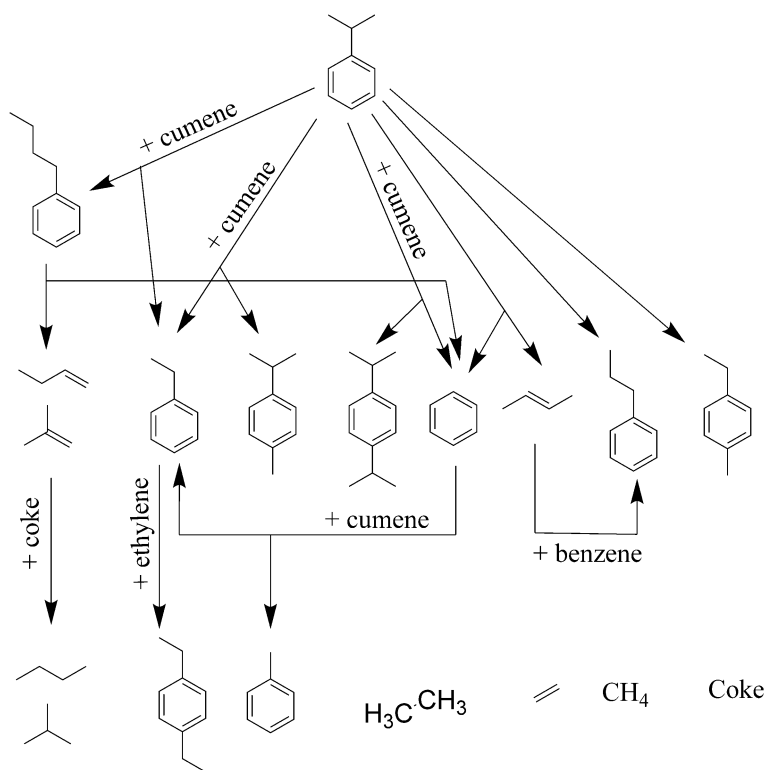


Figure 20: Possible reaction path of cumene over zeolites¹³⁸

n-Hexadecane is also a commonly used model compound for acid catalyzed reactions, specifically at cracking conditions. There is generally a better understanding of alkane cracking than for cumene and several review papers have been published on this matter^{19,144}; however, alkane acid-catalyzed reactions are more complex than those of the cumene especially when both Lewis and Brønsted-Lowry acid sites are present. Three mechanisms for cracking have been proposed: a monomolecular mechanism, a bimolecular mechanism and an oligomeric mechanism¹⁴⁵. The monomolecular path is favoured by high temperatures and low olefin concentration and is catalysed by Brønsted-Lowry acid sites. The bimolecular path is favoured by low temperatures and high olefin concentration. Both mechanisms combined can present an auto-catalytic behaviour where olefins are produced via the monomolecular path until the concentration is high enough to make the bimolecular path significant. The oligomeric mechanism might be the main path for propylene production from ethylene, but not much information is available¹⁴⁶. Overall, n-alkane cracking requires higher acidity than dealkylation¹⁴⁷.

As mentioned previously, alkane cracking process is a very complex system and is influenced by a variety of parameters. One parameter is the phase on which the reaction takes place. Liquid phase reactions will produce an equimolar mixture of n-alkanes and 1-alkenes at low conversion while at high conversion, more alkanes than alkenes will be produced¹⁴⁸. The hydrogen needed for the saturation of the products is supplied by hydride transfer¹⁴⁹ forming hydrogen deficient species (coke)¹⁵⁰. Also, liquid phase cracking will produce more addition compounds and less gas products than gas phase reactions.

Zeolites have become widely used as refining catalyst at industrial level. The zeolite's frameworks are not neutral and require cations to balance the charge. In an effort to improve the properties of the zeolitic catalyst, several groups have modified the activity of the zeolites by exchanging the cations. It is reported that replacing sodium cations by calcium increases the activity of the zeolite as well as the production of branched hydrocarbons¹⁵¹. For ferrierite, exchanging sodium by calcium cations does not change the selectivity, but suppresses coke formation. This reduction might be caused not by a change in the acidic strength, but by narrowing of the pore entrance and thus reducing hydride transfer reactions¹⁴⁹. A different study reports that calcium increases the olefin to paraffin ratio and decreases conversion¹⁵². Gallium and chromium¹⁵³ exchanged zeolites have been also studied. Gallium exchanged zeolites are reported to have more Lewis acid sites¹⁵⁴ which can activate the paraffins by hydride abstraction¹⁵⁵; more specifically, they can catalyze heterolytic dissociation over Lewis acid sites. In that study, it was found that the zeolite can promote cyclization and aromatization reactions¹⁵⁴.

The search for a better understanding of the catalytic cracking mechanism is ongoing with the goal to create new and improved processes for oil upgrading. Recent studies (see Chapter 2) showed that chabazite is able to remove pyrrolic nitrogen from model compounds solutions and to transform the pyrrolic nitrogen compounds into species that are easier to remove through conventional methods. Also, the ability of the chabazite to demetallize nickel and vanadyl porphyrins has been reported with up to 48% removal of metals from solution. Those studies also suggest the reaction paths in which the chabazite may be reacting with the model compounds. The objective of the present study is to investigate the activity of the natural zeolite chabazite and the effect of water addition on the cracking process. This work is part of an effort to improve

existing upgrading processes and to design new processes able to upgrade heavy oils and bitumens with high nitrogen and heavy metals concentrations using natural, abundant and inexpensive materials.

4.3 Experimental Section

4.3.1 Materials

Cumene (98%) and n-hexadecane ($\geq 99\%$) were used as model compounds. Indole (99+%) was used in poisoning experiments. In selected artificial oil sands reaction, 2,2,4-trimethylpentane (TMP) ($>99\%$) was used. These substances were obtained from Sigma-Aldrich and were used as received. Carbon disulfide (CS_2) (99.9% spectroscopy grade) was obtained from ACROS Organics. Athabasca vacuum tower bottoms from Cold Lake, Alberta (courtesy of Syncrude) was used as vacuum residue (VR). Sand was obtained from QUIKRETE (premium play sand no. 1113). Deionised water from a MilliQ water system was used for selected reactions. Natural chabazite from the Bowie deposits in Arizona was used in both calcium and proton forms. The zeolites were stored in a desiccator prior to use. A detailed description of the zeolite can be found elsewhere⁵⁵. Zeolite Y was also used for selected reactions and was obtained from standard commercial fluidized catalytic cracking microspheres from Engelhard Corporation

4.3.2 Artificial Oil Sands

In order to have a controlled system compared to the raw oil sands, artificial oil sands were prepared using sand and VR. The sand was washed thoroughly using tap water first and then, deionized water until it was free of fine particles. The sand then was dried in an oven for 2 days. Vacuum residue was diluted using CS_2 (2:1 ratio) and mixed with the sand to achieve a concentration of 12% VR with respect to the sand. The VR / CS_2 / sand mixture was left in a fumehood at room temperature until more than 98% of the CS_2 evaporated according to weight. A comparison between the simulated distillation of the VR and the extracted oil from the artificial oil sands indicates that the evaporation did not change the composition of the VR.

4.3.3 Reactions

The reactions were conducted in 15 ml microreactors fabricated at the Department of Chemical and Materials Engineering machine shop at the University of Alberta. The reactors and

a description of their operation are described in detail elsewhere⁷³. For the reactions with VR, 3 g of artificial oil sands was added to the reactor. For some reactions, some or all of the following substances were added: Ca-chabazite (0.3g), deionized water (0.03 ml) and TMP (0.3 g). For each reaction with model compounds, 3 ml of liquid and 0.3 g of zeolite were added to the reactor. The liquids used were n-hexadecane or cumene or a solution of indole in cumene. For some reactions, 0.03 ml of deionized water was also added.

Once the reactor was loaded, it was closed and tested for leaks at pressures up to 2.0 MPag. To displace the oxygen, the reactor was then pressurized to 1.7 MPag and vented 3 times with nitrogen. After purging, the reactor was filled with nitrogen at 1.7 MPag. The reactor was then submerged in a fluidised sand bath at temperatures between 300 and 420 °C. To ensure a good mixing, the reactor was shaken in a vertical motion with an amplitude of 2.6 cm and a frequency of 6.5 Hz. Selected reactions were shaken with an amplitude of 3 cm and a frequency of 3 Hz to investigate the effect of mixing. The reaction times were 1 or 4 hours. Once the reaction time was over, the reactors were taken out of the bath and cooled, initially with air for 5 minutes and then submerged in water at room temperature. The cooled reactors were vented and the products collected. For selected reactions, the total volume of the gas inside the reactor was measured. This volume was compared with the volume of nitrogen contained in the reactor at the beginning of the experiment to determine the amount of gas produced. For the oil sands reactions, CS₂ was added after the reaction to facilitate the collection of the sample and to achieve the concentration necessary for SimDist analysis (0.8 % wt). In average, 33.5 ml of CS₂ were added to each sample. Prior to injection in the GC, samples were filtered using Durapore membrane filters with 0,22µm GV. For model compounds, the liquid and solid products were separated by centrifugation at 5000 RPM for 5 minutes. After each reaction, the reactors were thoroughly cleaned and reused 3 to 10 times

4.3.4 Analysis

The products from the oil sands reactions were analyzed by SimDist using a Varian 450 GC equipped with a Agilent MXT©-1HT Sim Dist 5 m x 0.53 µm x 0.9 µm column and following the ASTM 7169 standard. For the reactions in which TMP was added, the TMP peak was identified and excluded from the integration. The model compounds liquid products were

analysed by GC-FID and GC-MS. For GC-FID, an Agilent Technologies 7820A GC was used. This GC was fitted with a split / splitless injector and a J&W DB-5ms 30m x 250 μm x 0.25 μm column. Helium was used as carrier gas. For GC-MS studies, an Agilent Technologies 7820A GC connected to a 5977e MSD mass spectrometer was used. This GC was fitted with an HP-5ms 30m x 250 μm x 0.25 μm column with helium as carrier gas. The parameters for the analysis can be found in Table 20. Products from the n-hexadecane reactions were also analysed by $^1\text{H-NMR}$ spectroscopy at the Nuclear Magnetic Resonance Laboratory at the University of Alberta. The spent catalyst from hexadecane reactions was analysed by thermogravimetry using a Mettler Toledo TGA DSC 1 STAR^e system.

Table 20. Parameters for GC analysis of cumene and n-hexadecane reaction products.

Parameter	Cumene	n-hexadecane
Injector temperature	325 °C	300 °C
Carrier gas flow	1 ml / min	1 ml / min
Split	100 : 1	100 : 1
Initial oven temperature	50 °C	100 °C
Initial hold time	0.5 min	0.5 min
Ramp rate	3 °C / min	16 °C / min
Final temperature	315 °C	300 °C
Final hold time	-	14 min
Detector temperature	325 °C	310 °C

4.4 Results

Oil sands reactions with 10% catalyst loading and with 10% catalyst loading, water and TMP were analyzed by SimDist. A thermal reaction in absence of catalyst was also performed. Both reactions were conducted at 380 °C for 1 h. Results for those experiments are shown in Figure 21. Unreacted VR from the artificial oil sands was extracted using the same procedure used to collect reaction products. All of the samples were analyzed using SimDist. Results were included in Figure 21 as reference. Liquid recovery was quantified and an average of 101.9% of the initial liquid was recovered as products (6.7 % std deviation) and the solids recovery was 96.6% of the initial solids (2.9% std deviation.)

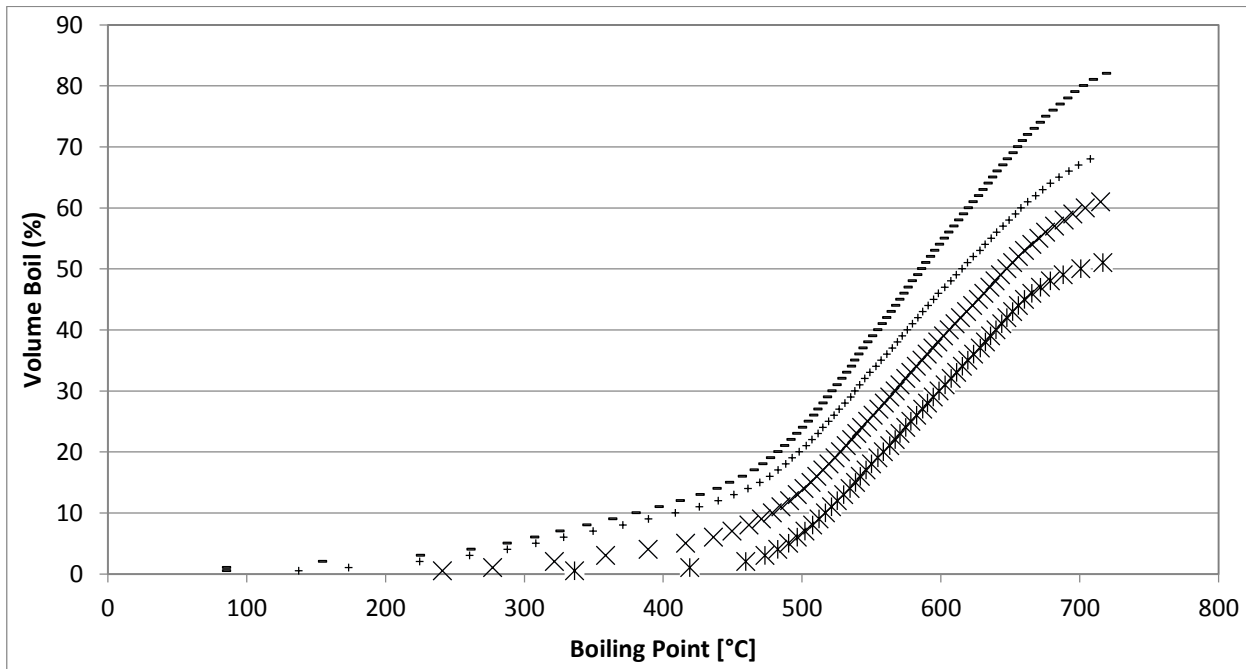


Figure 21. SimDist results for oil sands reactions: *Unreacted oil sands (reference), ^xthermal reaction, ⁺Ca-chabazite 10% loading, ⁻Ca-Chabazite 10% loading plus 0.03g water plus 0.3g TMP. All reactions performed at 380 °C for 1 h.

Hexadecane reactions were conducted at 400 °C for 1 hour using the high speed mixing. The average conversion was 8.9% with a standard deviation of 0.9%. No significant differences were

found with water addition. $^1\text{H-NMR}$ spectroscopy studies were also performed on these samples. Also, no significant differences were found with water addition.

Coke content was measured in the spent catalyst by TGA. After reaction at 400 °C for 1 hour and using 10% Ca-Chabazite loading, the non-water-added reaction produced 0.19 g of coke (8.2% standard deviation); while for the 1% water-added reaction, the coke production was reduced to 0.14 g (1.7% standard deviation).

To investigate the effect of mixing, hexadecane reactions were conducted at 400 °C for 1 hour and low shaking speed. Hexadecane conversion was quantified by GC-FID. Results are presented in Figure 22. The products from hexadecane reactions were also analysed by $^1\text{H-NMR}$ spectroscopy. The spectra was integrated according to the ranges in Table 21.

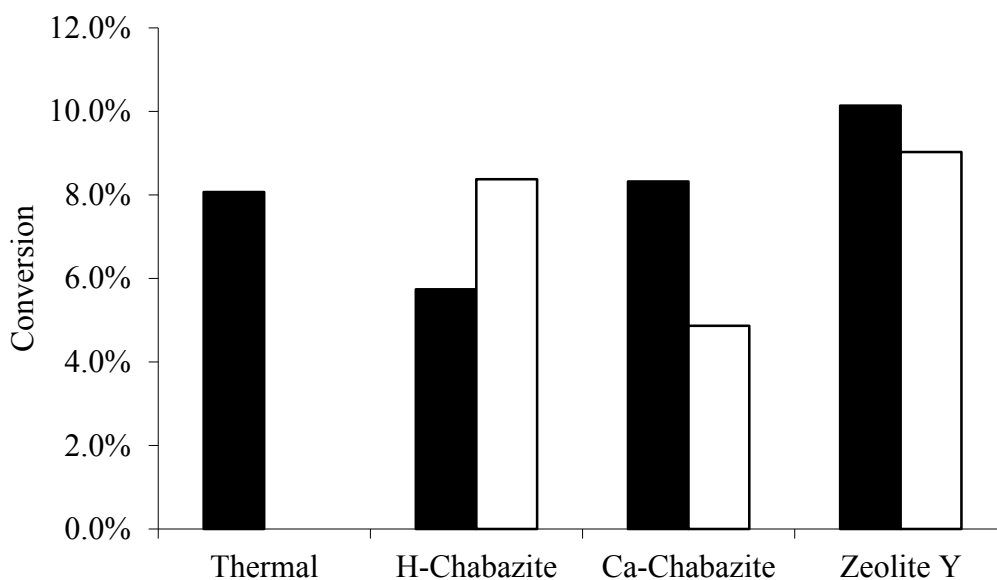


Figure 22. Hexadecane conversion after reaction at 400 °C, 1 hour, 10% catalyst loading. No-added water in black, 0.1% water added in white. Average standard deviation: 3.9% standard deviation. Thermocracking with 0.1% water was not determined.

Table 21. Integration ranges for ¹H-NMR spectroscopy of hexadecane reaction products.

Type of proton	Range (ppm)
Aromatic	6.0 – 9.0
Olefinic alpha	4.6 – 5.0
Olefinic beta +	5.0 – 6.0
Aliphatic	0.5 - 4.5

The integration results were used to estimate the ratio of produced olefins / produced paraffin and the ratio of internal olefins / terminal olefins. The amount of terminal olefins was estimated by dividing the amount of olefinic alpha protons by 2. The amount of internal olefins was estimated using Equation 1

$$Int\ Olefins = 1/4 \left(H_{Ole\ \beta+} - \frac{H_{Ole\ \alpha}}{2} \right) \quad (1)$$

Where *Int Olefins* is the amount of internal olefins produced, $H_{Ole\ \beta}$ is the percentage of protons bonded to an olefinic carbon in β position and $H_{Ole\ \alpha}$ is the percentage of protons bonded to an olefinic carbon in α position. The ratio of produced olefins / produced paraffin was estimated using Equation 2

$$\frac{Olefins}{Paraffins} = \frac{Int\ Olefins + Terminal\ Olefins}{X} \quad (2)$$

Where *Olefins / Paraffins* is the ratio of produced olefins over produced paraffins. *Int Olefins* is the amount of internal olefins calculated by equation (1), *Terminal Olefins* is the amount of produced terminal olefins and *X* is the hexadecane conversion. Results can be found in Figure 23 and Figure 24

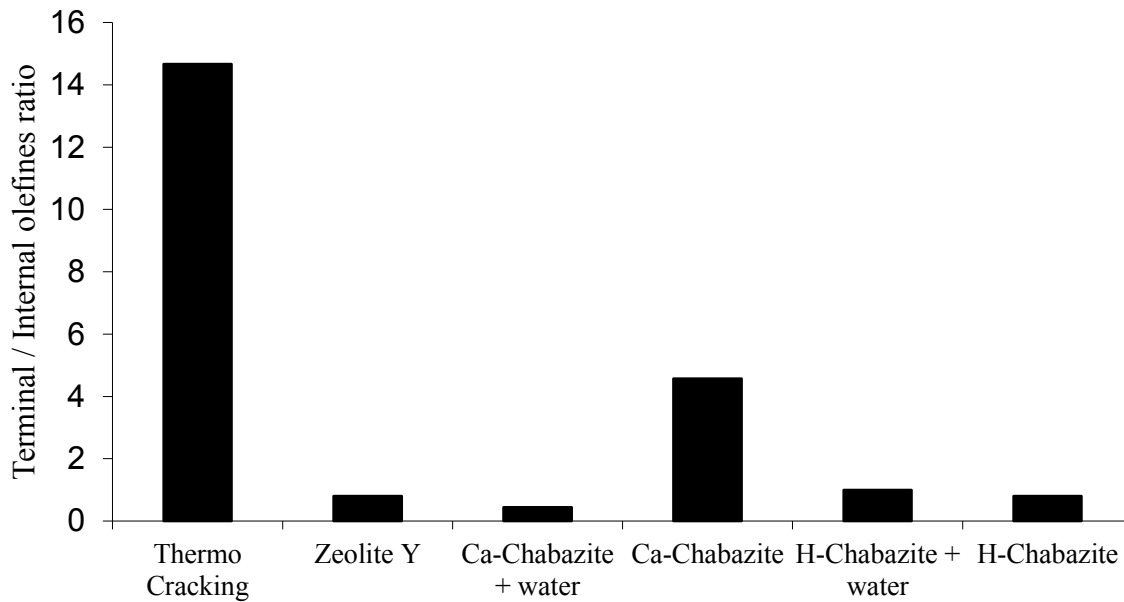


Figure 23. Terminal / Internal olefin ratio in hexadecane after reaction at 400 °C, 1 hour, 10% catalyst loading.

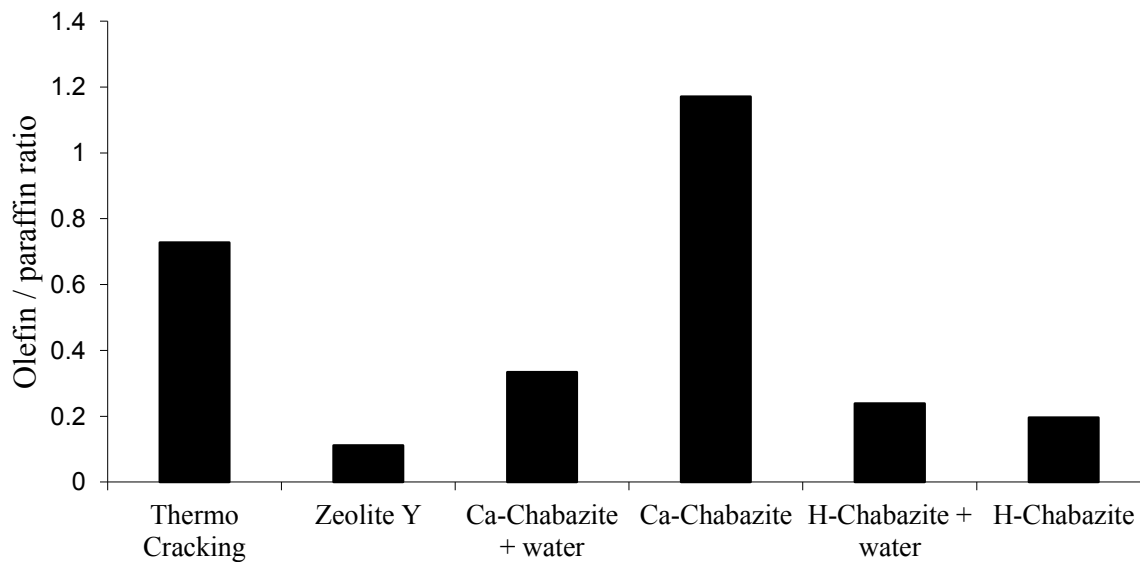


Figure 24. Produced olefin / produced paraffin ratio in hexadecane after reaction at 400 °C, 1 hour, 10% catalyst loading.

Cumene reactions were conducted at 300 °C and quantified by GC-FID. Conversion of cumene in presence of different zeolites is presented in Figure 25. Most of the reaction products were identified using GC-MS. The identified products can be found in Table 22. Due to the low concentration of some of the products and bad separation, quantification was deemed unreliable and it is not reported; however, relative strength of the peaks is reported with strong peaks being the major products.

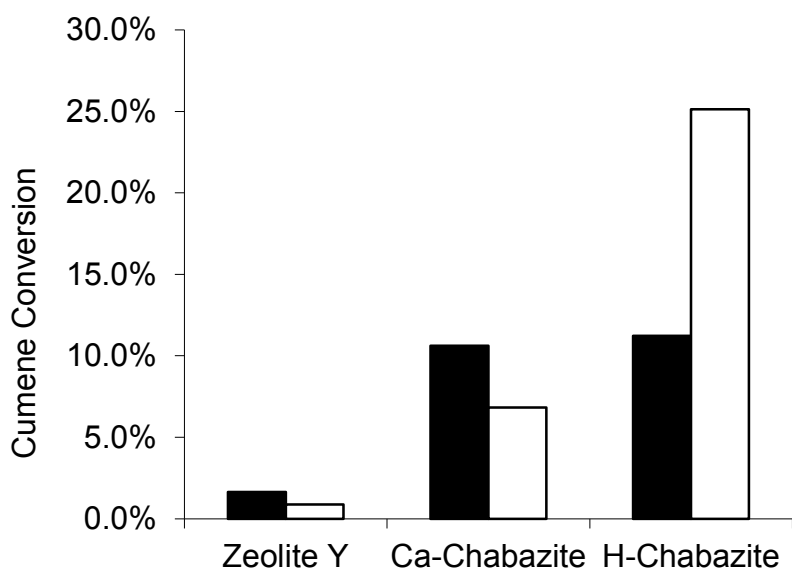


Figure 25. Cumene conversion after reaction at 300 °C, 4 hours, 10% catalyst loading. No-added water in black, 0.1% water added in white. 6.7% standard deviation.

Table 22. Liquid reaction products for chabazite and zeolite Y catalysed cracking of cumene.

Compound	Chabazite	Zeolite Y
Benzene	S	-
Toluene	M	-
n-Propylbenzene	W	-
α -Methylstyrene	W	S
sec-Butylbenzene	M	-
Cymene	S	-
Diisopropylbenzene	S	S
2,5-Dibenzyl-3-hexene	W	W
4,4-Diisopropylbiphenyl	W	W
Other conjugated products	-	W ⁺

Relative height of the peak: S: strong peaks; M: Medium peaks; W: Weak peaks. Products are reported in order of elution.

Reaction conditions: 300 °C, 4 hours, 10% catalyst loading.

⁺Individually the conjugated product peaks are weak but in total there is a significant yield of these products.

In order to determine the role of the different acid sites and the effect of the water on them, reactions were carried out. A temperature of 420 °C was used to increase the conversion and the time was reduced to 1 hour to decrease the formation of secondary products. Indole was added to the mixture to poison the acid sites. Cumene conversion as a function of initial indole concentration is plotted in Figure 26. Gas production was measured by water displacement. Results can be found in Figure 27. In order to follow the activity of Lewis and Brønsted-Lowry

acid sites, selectivity towards benzene and cymene was calculated for reactions with an initial concentration of 2.5% w/w of indole. Results can be found in Figure 28

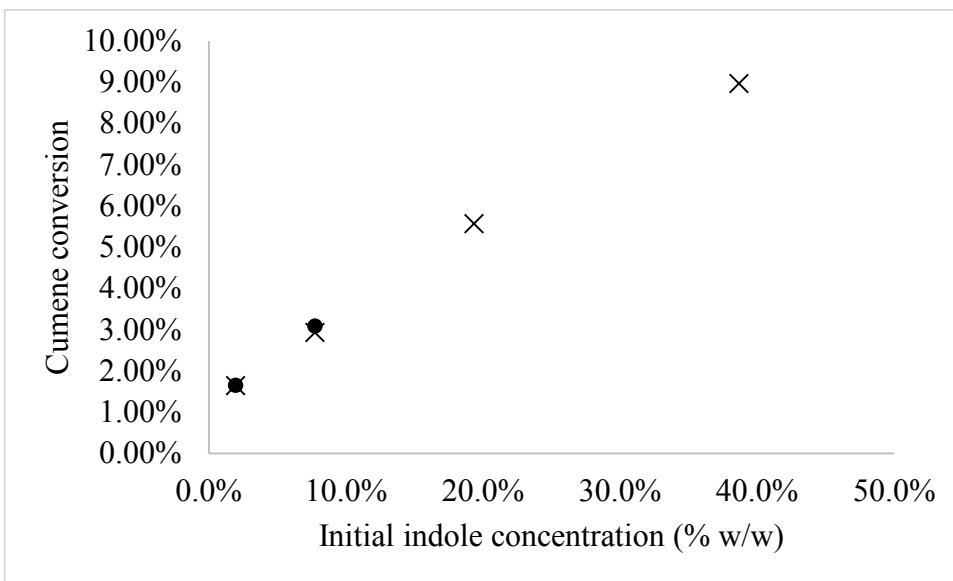


Figure 26. Cumene conversion in the presence of indole. x no water added, • 1% water added. 420 °C, 1h, 10% Ca-chabazite loading.

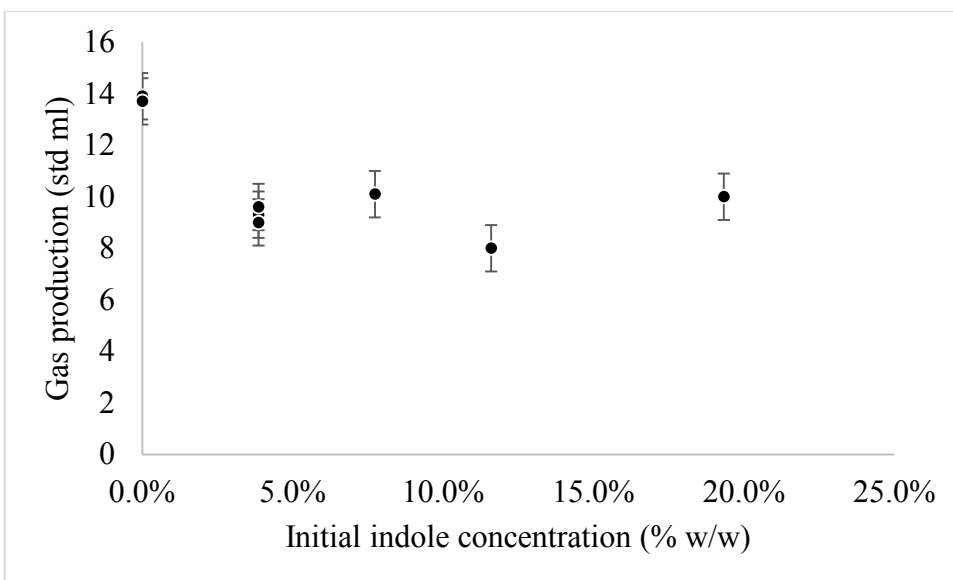


Figure 27. Gas production for cumene cracking reactions as a function of initial indole concentration. 10% Ca-chabazite as catalyst, 420 °C, 1 hour, no water added.

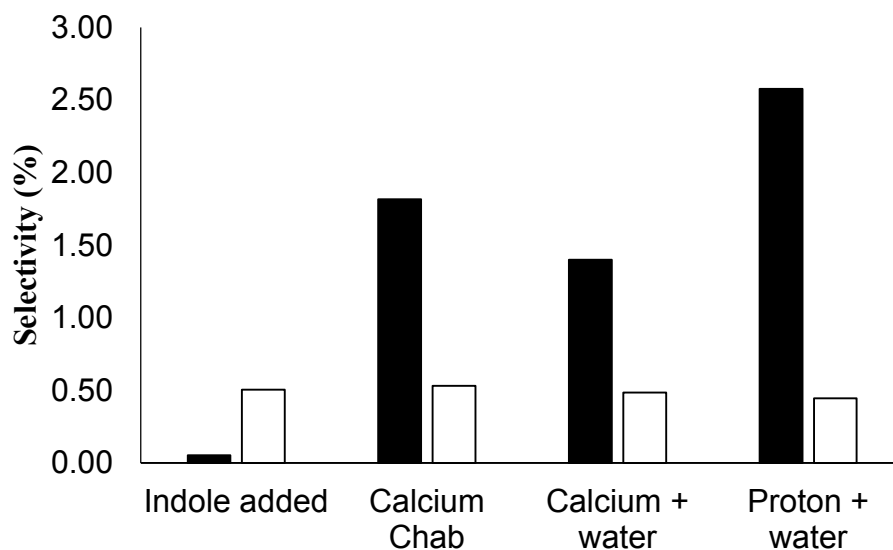


Figure 28. Selectivity (percentage) towards benzene (black) and cymene (white). 10% catalyst loading (calcium chabazite unless otherwise noted), 420 °C, 1 hour reaction. 2.5% w/w initial concentration of indole.

Thermal reaction of cumene in the presence of 2.5% w/w indole was carried out as a control. The conditions for this reaction was 420 °C and 1 hour. No catalyst or water was added during this reaction. Products were analysed by GC-MS. Cumene conversion was calculated at 28.8%. The main products were propylbenzene (10.3% selectivity) and styrene (24.8% selectivity). Other products include alkyl and alkenyl substituted benzenes and dimers (cumene and cumene-indole).

4.5 Discussion

Cracking process reacting mixtures are very complex and the use of controlled feeds can help to gain understanding of the phenomena involved. Using artificial oil sands, thermal and Ca-chabazite catalyzed reactions were performed. Compared to the initial oil sands, thermal reactions increase the amount of middle distillate (177 to 343 °C boiling range) from 0.5 % to 3% and the amount of gas oil (343 to 524 °C) from 11.5% to 16% by volume. Ca-chabazite catalyzed reactions increased the amount of naphtha (<177 °C) to 1%, the middle distillate to 6% and the gas oil to 19%. These results prove that the Ca-chabazite can promote reactions that increase the amount of distillable fractions on the VR. Since the liquid and solid recovery are close to 100%, it is estimated that the coke formation is below experimental error and considered negligible thus the increase in the recovered fraction is considered to be produced by the reaction and not an increase in concentration due to carbon rejection.

Hexadecane and cumene were used as model compounds to gain an insight on the reactions that the chabazite was promoting within the oil sands. Using the low speed shaker for n-hexadecane reactions, the zeolite Y has the highest conversion and the H-chabazite the lowest. The presence of water increases the conversion on the reactions with H-chabazite. Interestingly, adding water decreases the conversion when using zeolite Y and Ca-chabazite. The conversion while using H-chabazite and adding water is comparable to that of the Ca-chabazite with no water added.

In order to further investigate the role of the water, ¹H-NMR spectroscopy was performed over the n-hexadecane reaction products and the ratio of olefin / paraffin and terminal / internal paraffin was calculated. As expected, thermal cracking reactions produce a high amount of

terminal olefins and the ratio olefin / paraffin is close to 1. Ca-chabazite delivered similar results to those of the thermal cracking with an olefin / paraffin ratio over 1 and relatively high amounts of terminal olefins. Water added to the Ca-chabazite reactions lowered both olefin / paraffin and terminal / internal olefin ratio to a level comparable to those of the H-chabazite. This result indicates that proton availability of the Ca-chabazite is low and the water increases such availability. Reactions with a higher shaking speed showed no significant difference due to the water addition. It is possible that the water addition is facilitating the dispersion of the catalyst thus increasing the mass transfer and the proton availability. This effect becomes negligible as the mixing increases

Water also affects the coke formation in n-hexadecane reactions. 0.1% water addition reduces the coke formation by 25%. Reduction of coke formation is consistent with the reported findings that water displaces weakly adsorbed species³⁷ (see Chapter 2) Water could be displacing coke precursors from the surface, thus avoiding coke formation.

Both calcium and proton chabazite are active for hexadecane and cumene cracking. In order to do a better comparison, the ratio hexadecane / cumene conversion is proposed. The cumene reactions at 300 °C were chosen to calculate this ratio in order to avoid the effects of supercritical conditions (cumene's critical temperature is 358 °C). The values for this ratio can be found in Table 23. Using this ratio, it is clear that zeolite Y is more active towards hexadecane cracking than towards cumene cracking and H-chabazite is more active towards cumene cracking than towards hexadecane cracking.

Table 23. Hexadecane / cumene conversion ratio. 10% catalyst loading. For hexadecane, 400 °C, 1 hour reaction. For cumene, 300 °C, 4 hours reaction

	Zeolite Y	Ca-Chabazite	H-Chabazite
No-added water	6.22	0.78	0.51
Added water	10.23	0.71	0.33

Despite its complexity, several authors suggest the use of cumene cracking process as a model reaction, especially for systems possessing both Lewis and Brønsted-Lowry acid sites. The difference in conversion while using Ca- vs H-chabazite is non-significant when no water is added. Adding water increases the conversion when H-chabazite is used and decreases the conversion when Ca-chabazite is used. For zeolite Y at 300 °C and 4 hours reaction, mainly heavy liquid products were detected. The lack of light products could be caused by the low temperatures and long reaction times used. Reactions conducted in the presence of chabazite produce less variety of conjugated cumene products. In general, the products obtained when using chabazite as catalyst suggest that the natural zeolite has both Brønsted-Lowry and Lewis acid sites that are active for cumene cracking process at temperatures of 300 °C and higher. Gas products were not analysed due to the low concentration caused by a combination of a relatively large headspace in the reactor and the nitrogen pressure used to keep the reaction occurring in liquid phase. It is important to mention that analysis of the products from chabazite reactions indicates that more transalkylation reactions are occurring compared to the reactions in presence of zeolite Y. These transalkylation products include cymene, benzene and toluene. This ability of the chabazite to catalyze transalkylation reactions has been observed previously for 1-methylnaphthalene - indole (see Chapter 2) and 1-methylnaphthalene – octaethylporphyrin (See Chapter 3) systems.

In order to test the hypothesis that the chabazite's Lewis and Brønsted-Lowry acid sites are active for cumene cracking, indole was added to the reacting mixture in concentrations up to 40% w/w. Since nitrogen compounds seem to adsorb preferentially on Brønsted-Lowry acid sites⁵⁰, adding nitrogen compounds could selectively poison those acid sites but leaving the Lewis sites untouched. The gas production shown in Figure 27 indicates that indole reduces the production of light molecules. Figure 28 shows a great reduction in benzene production when 2.5 % w/w of indole is added. The formation of cymene is not significantly affected by the presence of indole. According to Corma *et al*¹³⁸, both benzene and cymene are primary, stable products generated on Brønsted-Lowry and Lewis acid sites respectively and the production of benzene is tied up to the production of either diisopropylbenzene or propylene. A decrease in gas and benzene production indicates that the Brønsted-Lowry acid sites are being deactivated by the

indole while the unchanged cymene production shows that the Lewis acid sites are not being affected by the presence of pyrrolic nitrogen. Interestingly, indole addition causes an increase in cumene conversion. GC-MS studies show the formation of indole – cumene conjugated products. Production of indole – aromatics oligomers have been reported previously⁸¹ (see Chapter 2) and might indicate that the indole adsorbed on Brønsted-Lowry acid sites is not inert but can further react especially with aromatics to form conjugated products.

Oil sands are known to contain up to 3.4% of connate water. Adding 1% water to the cumene reactions has an effect in the conversion that depends on the type of chabazite used. When using Ca-chabazite, water addition reduces the cumene conversion. When H-chabazite is used, the conversion increases with water addition. When indole is added to the reaction, water addition does not have a significant impact. Data also shows that water addition does not affect the cymene selectivity but it does affect the benzene selectivity. This result suggests that water interacts mainly with the Brønsted-Lowry acid sites; however, the role of the water is still not clear at this point. This trend is also observed on the hexadecane reactions with low shaking speed.

Significant transalkylation has been observed in several model compound studies (see chapters 2 and 3). Even the 1-methynaphthalene solvent used in those studies was subjected to transalkylation. Assuming that transalkylation follows a stochastic path, the result of this reaction in bitumen would be a redistribution of alkyl groups among the aromatic species. **Error! eference source not found.** shows solubility parameters of several alkyl-substituted aromatics. In **Error! Reference source not found.**, data from **Error! Reference source not found.** is plotted showing a general trend of lower solubility parameter as the amount of aliphatic carbons in an aromatic species increases. In the case of transalkylated bitumen, this decrease in solubility parameter by alkylation of aromatics will make the reaction products more soluble in light n-alkanes.

Table 24. Solubility parameters of selected aromatic molecules. *n*-Heptane solubility included as reference¹⁵⁶

	Solubility Parameter (Mpa ^{1/2})		
	Hansen	Hildebrand	Aliphatic carbons
n-Heptane	15.3	15.1	7
p-Diisopropylbenzene		16.9	6
Propylbenzene		17.6	3
Cumene		17.3	3
o-Xylene	18		2
m-Xylene		18	2
Ethylbenzene		18	2
2,7-Dimethylnaphthalene		18.3	2
2-Ethyl-naphthalene		19.4	2
Toluene	18.2	18.2	1
1-methylnaphthalene		20.3	1
Benzene	18.5	18.8	0
Naphthalene		20.3	0

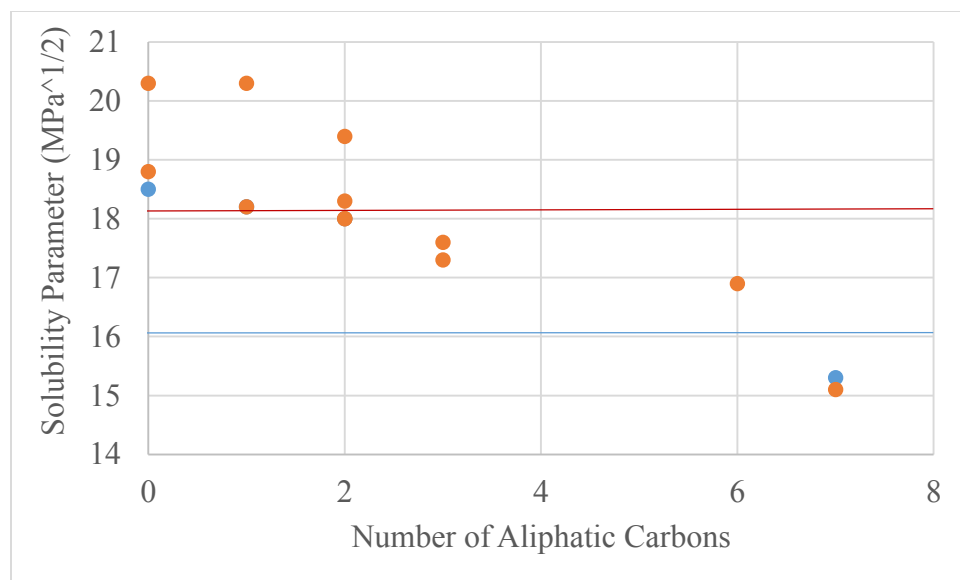


Figure 29. Solubility parameter of various substituted aromatics vs number of aliphatic carbons. *n*-Heptane shown as reference. Blue line indicates the value for *n*-heptane. The red line indicates the value for toluene. Orange dots for Hildebrand parameter, Blue dots for Hansen parameter.

Since the results indicate that the chabazite promotes mainly transalkylation reactions, it is possible that the results obtained with the raw oil sands⁵⁶ and artificial oil sands are obtained by a combination of cracking and transalkylation reactions. In order to test this hypothesis, TMP was added to artificial oil sands as a source of methyl groups available for transalkylation. SimDist results show that the addition of TMP increased the naphtha fraction to 2%, the middle distillate to 6% and the gas oil to 23%, proving that the presence of TMP increases the VR conversion (See Figure 3). This results are consistent with those published by Junaid, *et al*⁵⁶. In that work, raw oil sands that included 46% gasoil were used. This gasoil fraction could be the source of alkyl groups needed to promote transalkylation reactions. Furthermore, low gas formation was reported in that work. This is consistent with the theory that the small alkyl groups are being incorporated into higher boiling point species instead of being released as gas products.

The results presented here demonstrate that the natural zeolite chabazite is more active than the commercially used zeolite Y towards cracking process of substituted aromatics and that the presence of alkyl-donating species further increases this activity. With this information, new and

improved processes for upgrading of highly aromatic crude oil fractions can be proposed. Together with the nitrogen and heavy metals removal abilities of this natural zeolites^{35,56} (see Chapter 2 and 3), a primary upgrading process focused on highly aromatic fractions and without the use of expensive hydrogen is possible. The use of an abundant and cheap material as the chabazite could make this processes more economically attractive.

4.6 Conclusions

Natural chabazite is able to promote reactions that convert VR into distillable fractions. The natural zeolite chabazite is also able to catalyse cracking process type reactions of both n-hexadecane and cumene. Compared to the zeolite Y, chabazite is more active towards cumene cracking process but less active towards n-hexadecane cracking process.

Natural chabazite possess both Brønsted-Lowry and Lewis acid sites that are active towards cumene cracking process giving different products. Adding indole to the reacting mixture effectively poisons the Brønsted-Lowry acid sites without affecting the Lewis acid sites. Also, indole is able to react with cumene producing different condensation products.

Adding 1% water to the reaction has different effects. For hexadecane reactions, water appears to increase the dispersion of the catalyst in the reacting mixture and reduces the coke formation by 25%. For cumene, results show that the water affects the Brønsted-Lowry acid sites, but not the Lewis acid sites; however, it was not possible to clarify the role of the water in this reactions.

Adding alkyl-donating species to the reaction mixture further increases the VR conversion in artificial oil sands reactions. The results obtained in this study suggest that the natural chabazite could be used for highly aromatic oil fractions upgrading. Together with the chabazite's ability to remove nitrogen and heavy metals, new processes that reduce the use of expensive hydrogen can be proposed.

5 General Conclusion

The current world economic situation for the oil and fuels market requires new and improved processes for oil upgrading and refining. Current processes can be improved by reduction of the waste produced (coke and asphaltenes) or by decreasing the use of expensive chemicals (catalysts and hydrogen). Natural zeolites, specifically chabazite, has been proven to be a good option for oil sands bitumen upgrading as they can catalyze reactions that increase the bitumen's solubility in heptane and can remove nitrogen and metals from heavy oil. Additionally, natural chabazite is cheap and abundant thus reducing the needs of expensive synthetic catalyst.

In order to explain the results observed when raw oil sands are treated with chabazite, cumene, hexadecane, indole and OEP were used as model compounds to study the reactions of aromatic and saturated fractions as well as the nitrogen and metals removal properties. By knowing the predominant reactions of these compounds, it is possible to suggest reaction paths that lead to the changes observed on raw oil sands reactions.

In the present study, removals up to 17.7 % nitrogen, 67.5% vanadium and 90.0% nickel were obtained. These values are the maximum observed in this study but no attempts were made to optimize the process. Nitrogen was removed by transformation of non-basic nitrogen to basic nitrogen and adsorption. Metals were removed by porphyrin demetallation and adsorption. Chabazite showed to be more active than zeolite Y for cumene conversion while it was less active towards hexadecane cracking. Cumene reactions also showed that both Brønsted-Lowry and Lewis acid sites are active and indole poisons Brønsted-Lowry acid sites selectively. The role of the water in the reactions is not clear. In some cases, the presence of water does not seem to have a chemical role but a physical role improving the dispersion of the catalyst and adsorbing competitively thus keeping some species from adsorbing. Cumene reactions indicate that water affects Brønsted-Lowry acid sites but not Lewis acid sites.

Transalkylation was identified as one of the main reactions promoted by chabazite. Indole, OEP, 1-methylnaphthalene and cumene studies showed the presence of transalkylation products. As it was shown in Figure 29, transalkylation of aromatic molecules could increase their

solubility on light n-alkanes. Raw oil sands contains light gas oil that could be providing the alkyl groups needed for the transalkylation reactions. Increasing the concentration of light alkyl-donating molecules increases the transalkylation activity as it was proven by adding TMP.

In addition to transalkylation activity, chabazite has been proved that can act as a solid acid. This property of the chabazite promotes demetalation of porphyrins and adsorption of basic nitrogen compounds leading to nitrogen and metals removal from bitumen. Brønsted-Lowry acid sites are easily poisoned by indole, but Lewis acid sites are not significantly affected by indole and are able to promote the transalkylation reactions. It is also worth mentioning that indole (a non-basic form of nitrogen) is converted mainly into aniline (basic nitrogen) that is not only easier to adsorb into a solid acid, but it is also easier to eliminate through conventional refinery processes.

The role of the water was also studied; however, the way the water participates in the reacting mixture is not clear. Water seems to have a minimal effect on the surface reaction in this study when compared to previous reports. One major difference in this study was the use of a superior agitation unit during reactions and in this case the addition of water may have yielded in better catalyst dispersion. Conversely, water seems to have a pronounced effect in the adsorption and desorption of both the reactants and products on the surface of the natural zeolite. By affecting the interaction of the reaction components with the catalyst surface, nitrogen and metals removal are modified and the coke formation was decreased.

Based on the results presented in this thesis, a new oil upgrading process using transalkylation (molecular rearrangement) and catalytic cracking (molecular weight reduction) is proposed. By using TMP as a alkyl donating molecule, the conversion of VR is increased. Together with the nitrogen and metals removal capability of the chabazite, the new process is attractive for the partial upgrading of bitumen and heavy oils. The low cost and abundance of the natural chabazite increases the desirability of the process.

6 Recommendations

In this study, it was demonstrated that natural chabazite is able to catalyze reactions that could be used for oil upgrading including transalkylation and cracking. Additionally, chabazite is able to adsorb nitrogen compounds and to remove metals from porphyrin rings.

It is suggested to continue studying the properties of the chabazite in order to propose a novel oil upgrading process that is economically attractive and environmentally friendly. Optimization of the reaction parameters (temperature, pressure, reaction time, catalyst loading) is highly recommended. Studies on the life cycle of the catalyst are needed including deactivation, regeneration and disposal options. These data, together with kinetics information, will allow to suggest what kind of reactor should be used and to design reactors for this process.

Transalkylation reactions was proven to be one of the main pathways for upgrading using chabazite. In order to continue this study, several alkyl donating molecules should be considered. Methanol, ethanol and alkylated aromatics are suggested.

This process also has the potential to be applied to different feedstocks. Since previous studies showed that the solubility of bitumen in heptane is increased, this process might be suitable for asphaltenes processing in an effort to reduce waste byproducts of deasphalting plants. This process could also be applied to vacuum residue and heavy gasoil.

References

1. Anonymous Oil. In *World Energy Resources 2013 Survey* World Energy Council: 2013; pp 2.1-2.56.
2. Czarnecki, J.; Radoev, B.; Schramm, L. L.; Slavchev, R. On the nature of Athabasca Oil Sands. *Adv. Colloid Interface Sci.* **2005**, *114–115*, 53-60.
3. Strausz, O. P.; Lown, E. M. *The chemistry of Alberta oil sands, bitumens and heavy oils*; Calgary, Alta. : Alberta Energy Research Institute, c2003: 2003; .
4. Gray, M. R. *Extraction and upgrading of oilsands bitumen : Intensive short course*; University of Alberta: Edmonton, Canada, 1988; .
5. Yui, S. Producing quality synthetic crude oil from Canadian oil sands bitumen. *J. Jpn. Pet. Inst* **2008**, *51*, 1-13.
6. Doan, D. H.; Delage, P.; Nauroy, J. F.; Tang, A. M.; Youssef, S. Microstructural characterization of a Canadian oil sand. *Can. Geotech. J.* **2012**, *49*, 1212-1220.
7. Selucky, M. L.; Chu, Y.; Ruo, T.; Strausz, O. P. Chemical Composition of Athabasca Bitumen. *Fuel* **1977**, *56*, 369-381.
8. Selucky, M. L.; Chu, Y.; Ruo, T. C. S.; Strausz, O. P. Chemical Composition of Cold Lake Bitumen. *Fuel* **1978**, *57*, 9-16.
9. Payzant, J. D.; Hogg, A. M.; Montgomery, D. S.; Strausz, O. P. A field ionization mass spectrometric study of the maltene fraction of Athabasca bitumen. Part II - The aromatics. **1985**, *1*, 183-202.

10. Speight, J. G. Asphaltene Constituents. In *The Chemistry and Technology of Petroleum* CRC Press: 2014; pp 315-344.
11. Payzant, J. D.; Hogg, A. M.; Montgomery, D. S.; Strausz, O. P. A field ionization mass spectrometric study of the maltene fraction of Athabasca bitumen. Part III - The Polars. **1985**, *1*, 203-210.
12. Durand, E.; Clemancey, M.; Lancelin, J.; Verstraete, J.; Espinat, D.; Quoineaud, A. Effect of Chemical Composition on Asphaltenes Aggregation. *Energy Fuels* **2010**, *24*, 1051-1062.
13. Mullins, O. C.; Sabbah, H.; Eyssautier, J.; Pomerantz, A. E.; Barre, L.; Andrews, A. B.; Ruiz-Morales, Y.; Mostowfi, F.; McFarlane, R.; Goual, L.; Lepkowicz, R.; Cooper, T.; Orbulescu, J.; Leblanc, R. M.; Edwards, J.; Zare, R. N. Advances in Asphaltene Science and the Yen-Mullins Model. *Energy Fuels* **2012**, *26*, 3986-4003.
14. Majumdar, R. D.; Gerken, M.; Mikula, R.; Hazendonk, P. Validation of the Yen-Mullins Model of Athabasca Oil-Sands Asphaltenes using Solution-State H-1 NMR Relaxation and 2D HSQC Spectroscopy. *Energy Fuels* **2013**, *27*, 6528-6537.
15. Speight, J. G. *Petroleum chemistry and refining*; Washington, DC : Taylor & Francis, c1998: 1998; .
16. Castañeda, L. C.; Muñoz, J. A. D.; Ancheyta, J. Combined process schemes for upgrading of heavy petroleum. *Fuel* **2012**, *100*, 110-127.
17. Nelson, W. L. *Petroleum refinery engineering*; New York : McGraw-Hill, 1958; 4th ed: 1958; .
18. Axens IFP Group technologies Solvahl. <http://www.axens.net/product/technology-licensing/10094/solvahl.html> (accessed 04/02, 2015).
19. Corma, A.; Wojciechowski, B. The Chemistry of Catalytic Cracking. *Catal. Rev.* **1985**, *27*, 29-150.

20. Humphries, A.; Harris, D. H.; O'connor, P. Chapter 2 The Nature of Active Sites in Zeolites: Influence on Catalyst Performance. *Studies in Surface Science and Catalysis* **1993**, *76*, 41-82.
21. Gray, M. R.; Masliyah, J. H. *Extraction and upgrading of oilsands bitumen : Intensive short course. Instructors: Murray R. Gray and Jacob H. Masliyah*; Edmonton, Alta. : University of Alberta, 1998: 1998; .
22. Mochida, I.; Choi, K. An overview of hydrodesulfurization and hydrodenitrogenation. *J. Jpn. Pet. Inst* **2004**, *47*, 145-163.
23. Sapre, A.; Broderick, D.; Fraenkel, D.; Gates, B.; Nag, N. Hydrodesulfurization of Benzo[b]naphtho[2,3-D]thiophene Catalyzed by Sulfided Coo-Moo3-Gamma-Al2o3 - the Reaction Network. *AICHE J.* **1980**, *26*, 690-694.
24. Jokuty, P.; Gray, M. Nitrogen Bases Resistant to Hydrodenitrogenation - Evidence Against using Quinoline as a Model-Compound. *Ind Eng Chem Res* **1992**, *31*, 1445-1449.
25. Furimsky, E. Chemistry of Catalytic Hydrodeoxygenation. *Catal. Rev. -Sci. Eng.* **1983**, *25*, 421-458.
26. Ali, M. F.; Abbas, S. A review of methods for the demetallization of residual fuel oils. *Fuel Process. Technol.* **2006**, *87*, 573-584.
27. Hubaut, R.; Dejonghe, S.; Grimblot, J.; Bonnelle, J. Hdm of the Vanadyl Octaethylporphyrin on Mos2-Based Catalysts - Nature and Repartition of the Vanadium Deposit. *React. Kinet. Catal. Lett.* **1993**, *51*, 9-17.
28. Chen, H.; Massoth, F. Hydrodemetalation of Vanadium and Nickel Porphyrins Over Sulfided Como/al2o3 Catalyst. *Ind Eng Chem Res* **1988**, *27*, 1629-1639.
29. Scherzer, J. Octane-Enhancing, Zeolitic Fcc Catalysts - Scientific and Technical Aspects. *Catalysis Reviews-Science and Engineering* **1989**, *31*, 215-354.

30. Leyva, C.; Rana, M. S.; Trejo, F.; Ancheyta, J. On the use of acid-base-supported catalysts for hydroprocessing of heavy petroleum. *Ind Eng Chem Res* **2007**, *46*, 7448-7466.
31. Breck, D. W. *Zeolite molecular sieves: structure, chemistry, and use*; New York, Wiley c1974.]: 1974; .
32. KH. M. Minachev; YA. I. Isakov. Catalytic Properties of Zeolites-A General Review. In *Molecular Sieves*; Meier, W. M., Uytterhoeven, J. B., Eds.; AMERICAN CHEMICAL SOCIETY: 1973; Vol. 121, pp 451-460.
33. Lee, S.; Park, S. A review on solid adsorbents for carbon dioxide capture. *Journal of Industrial and Engineering Chemistry* **2015**, *23*, 1-11.
34. Zorpas, A. A.; Inglezakis, V. J. *Handbook of Natural Zeolites*; Bentham Science: Oak Park, Ill], 2012; .
35. Junaid, A. S. M.; Rahman, M. M.; Rocha, G.; Wang, W.; Kuznicki, T.; McCaffrey, W. C.; Kuznicki, S. M. On the Role of Water in Natural-Zeolite-Catalyzed Cracking of Athabasca Oilsands Bitumen. *Energy Fuels* **2014**, *28*, 3367-3376.
36. Junaid, A. S. M.; Rahman, M.; Yin, H.; McCaffrey, W. C.; Kuznicki, S. M. Natural zeolites for oilsands bitumen cracking: Structure and acidity. *Micropor. Mesopor. Mat.* **2011**, *144*, 148-157.
37. Loveless, B. T.; Gyanani, A.; Muggli, D. S. Discrepancy between TPD- and FTIR-based measurements of Bronsted and Lewis acidity for sulfated zirconia. *Appl. Catal. B-Environ.* **2008**, *84*, 591-597.
38. Corma, A.; Marie, O.; Ortega, F. Interaction of water with the surface of a zeolite catalyst during catalytic cracking: a spectroscopy and kinetic study. *J. Catal.* **2004**, *222*, 338-347.
39. Keogh, R. A.; Srinivasan, R.; Davis, B. H. Pt-SO₂-4-ZrO₂ Catalysts: The Impact of Water on Their Activity for Hydrocarbon Conversion. *J. Catal.* **1995**, *151*, 292-299.

40. Morterra, C.; Cerrato, G.; Pinna, F.; Signoretto, M.; Strukul, G. On the Acid-Catalyzed Isomerization of Light Paraffins over a ZrO₂/SO₄ System: The Effect of Hydration. *J. Catal.* **1994**, *149*, 181-188.
41. Matsushi, K.; Emmett, P. Influence of Added-Back Water Vapor on Chemisorption and on Rate of Catalytic Cracking of Paraffins on a Silica-Alumina Catalyst. *J. Catal.* **1969**, *13*, 128-&.
42. Alberti, A.; Martucci, A. Proton Transfer Mediated by Water: Experimental Evidence by Neutron Diffraction. *J. Phys. Chem. C* **2010**, *114*, 7767-7773.
43. Bian, J.; Kuznicki, S. M.; McCaffrey, W. C.; Koenig, A.; Lin, C. C. H. Chabazite-Clay Composite for Bitumen Upgrading. *Chinese J. Catal.* **2008**, *29*, 1084-1088.
44. Caeiro, G.; Costa, A. F.; Cerqueira, H. S.; Magnoux, P.; Lopes, J. M.; Matias, P.; Ribeiro, F. R. Nitrogen poisoning effect on the catalytic cracking of gasoil. *Appl. Catal. A-Gen.* **2007**, *320*, 8-15.
45. Cheng, X.; Zhao, T.; Fu, X.; Hu, Z. Identification of nitrogen compounds in RFCC diesel oil by mass spectrometry. *Fuel Process. Technol.* **2004**, *85*, 1463-1472.
46. Bej, S.; Dalai, A.; Adjaye, J. Comparison of hydrodenitrogenation of basic and nonbasic nitrogen compounds present in oil sands derived heavy gas oil. *Energ. Fuel* **2001**, *15*, 377-383.
47. Koriakin, A.; Ponvel, K. M.; Lee, C. Denitrogenation of raw diesel fuel by lithium-modified mesoporous silica. *Chem. Eng. J.* **2010**, *162*, 649-655.
48. Kim, S.; Massoth, F. Hydrodenitrogenation activities of methyl-substituted indoles. *J. Catal.* **2000**, *189*, 70-78.
49. Angelici, R. An overview of modeling studies in HDS, HDN and HDO catalysis. *Polyhedron* **1997**, *16*, 3073-3088.

50. Caeiro, G.; Lopes, J. M.; Magnoux, P.; Ayrault, P.; Ribeiro, F. R. A FT-IR study of deactivation phenomena during methylcyclohexane transformation on H-USY zeolites: Nitrogen poisoning, coke formation, and acidity-activity correlations. *J. Catal.* **2007**, *249*, 234-243.
51. Mills, G.; Boedeker, E.; Oblad, A. Chemical Characterization of Catalysts .1. Poisoning of Cracking Catalysts Nitrogen Compounds and Potassium Ion. *J. Am. Chem. Soc.* **1950**, *72*, 1554-1560.
52. Fu, C.; Schaffer, A. Effect of Nitrogen-Compounds on Cracking Catalysts. *Ind. Eng. Chem. Prod. R. D.* **1985**, *24*, 68-75.
53. Caeiro, G.; Magnoux, P.; Ayrault, P.; Lopes, J. M.; Ribeiro, F. R. Deactivating effect of coke and basic nitrogen compounds during the methylcyclohexane transformation over H-MFI zeolite. *Chem. Eng. J.* **2006**, *120*, 43-54.
54. Van Grieken, R.; Escola, J. M.; Moreno, J.; Rodriguez, R. Nitrogen and sulphur poisoning in alkene oligomerization over mesostructured aluminosilicates (Al-MTS, Al-MCM-41) and nanocrystalline n-HZM-5. *Appl. Catal. A-Gen.* **2008**, *337*, 173-183.
55. Kuznicki, S. M.; McCaffrey, W. C.; Bian, J.; Wangen, E.; Koenig, A.; Lin, C. C. H. Natural zeolite bitumen cracking and upgrading. *Microporous Mesoporous Mater.* **2007**, *105*, 268-272.
56. Junaid, A. S. M.; Street, C.; Wang, W.; Rahman, M. M.; An, W.; McCaffrey, W. C.; Kuznicki, S. M. Integrated extraction and low severity upgrading of oilsands bitumen by activated natural zeolite catalysts. *Fuel* **2012**, *94*, 457-464.
57. Bunch, A.; Zhang, L.; Karakas, G.; Ozkan, U. Reaction network of indole hydrodenitrogenation over NiMoS/gamma-Al₂O₃ catalysts. *Appl. Catal. A-Gen.* **2000**, *190*, 51-60.

58. Shi, Q.; Xu, C.; Zhao, S.; Chung, K. H. Characterization of Heteroatoms in Residue Fluid Catalytic Cracking (RFCC) Diesel by Gas Chromatography and Mass Spectrometry. *Energy Fuels* **2009**, *23*, 6062-6069.
59. Zeuthen, P.; Knudsen, K.; Whitehurst, D. Organic nitrogen compounds in gas oil blends, their hydrotreated products and the importance to hydrotreatment. *Catal. Today* **2001**, *65*, 307-314.
60. Brown, T. M.; Duan, P.; Savage, P. E. Hydrothermal Liquefaction and Gasification of *Nannochloropsis* sp. *Energ. Fuel*. **2010**, *24*, 3639-3646.
61. Guan, Q.; Savage, P. E.; Wei, C. Gasification of alga *Nannochloropsis* sp in supercritical water. *J. Supercrit. Fluids* **2012**, *61*, 139-145.
62. Girgis, M.; Gates, B. Reactivities, Reaction Networks, and Kinetics in High-Pressure Catalytic Hydroprocessing. *Ind. Eng. Chem. Res.* **1991**, *30*, 2021-2058.
63. Gopal, D.; Srinivas, B.; Durgakumari, V.; Subrahmanyam, M. Vapor-phase alkylation of indole with methanol over zeolites. *Appl. Catal. A-Gen.* **2002**, *224*, 121-128.
64. Sundberg, R. J. . In *Heterocyclic Scaffolds II*; Gribble, G. W., Ed.; Springer: 2010; pp 47-115.
65. Quartarone, G.; Ronchin, L.; Tortato, C.; Vavasori, A. Thermodynamics and Kinetics of Indole Oligomerization: Preliminary Results in Aqueous Sulfuric Acid. *Int J Chem Kinet* **2009**, *41*, 107-112.
66. Katritzky, A.; Luxem, F.; Murugan, R.; Greenhill, J.; Siskin, M. Aqueous High-Temperature Chemistry of Carbocycles and Heterocycles .19. Pyrroles and Indoles. *Energ. Fuel*. **1992**, *6*, 450-455.
67. Massoth, F.; Kim, S. Polymer formation during the HDN of indole. *Catal. Lett.* **1999**, *57*, 129-134.

68. Laskin, A.; Lifshitz, A. Isomerization and decomposition of indole. Experimental results and kinetic modeling. *J Phys Chem A* **1997**, *101*, 7787-7801.
69. Sayag, C.; Benkhald, M.; Suppan, S.; Trawczynski, J.; Djega-Mariadassou, G. Comparative kinetic study of the hydrodenitrogenation of indole over activated carbon black composites (CBC) supported molybdenum carbides. *Appl. Catal. A-Gen.* **2004**, *275*, 15-24.
70. Aboulgheit, A. Comparison of the Hydrodenitrogenation of the Petroleum Model Nitrogen-Compounds Quinoline and Indole. *Appl. Catal.* **1985**, *16*, 39-47.
71. Yu, D.; Que, G.; Xu, H.; Wang, Z. In *In Co-cracking of indole and quinoline in catalytic cracking*; The 226th ACS National Meeting; 2003; .
72. Hooshar, A.; Uhlik, P.; Liu, Q.; Etsell, T. H.; Ivey, D. G. Clay minerals in nonaqueous extraction of bitumen from Alberta oil sands Part 1. Nonaqueous extraction procedure. *Fuel Process. Technol.* **2012**, *94*, 80-85.
73. Gupta, V. Cracking and heteroatom removal from hydrocarbons using natural zeolites, University of Alberta, Edmonton, 2008.
74. Vijan, L.; Neagu, M. Adsorption Isotherms of Phenol and Aniline on Activated Carbon. *Rev. Roum. Chim.* **2012**, *57*, 85-93.
75. Yamaji, T.; Saito, T.; Hayamizu, K.; Yanagisawa, M.; Yamamoto, O. Spectral Database for Organic Compounds SDBS. http://riodb01.ibase.aist.go.jp/sdbs/cgi-bin/cre_index.cgi?lang=eng (accessed December/14, 2011).
76. Benoit, R. LaSurface. <http://lasurface.com/database/elementxps.php> (accessed December/2, 2011).
77. Yu, D.; Xu, H.; Que, G.; Wang, Z. Study on conversion of non-basic nitrogen compound indole in FCC. *Acta Petrol. Sin.* **2004**, *20*, 22-28.

78. Hartung, G. K.; Jewel, D. M.; Larson, O. A.; Flinn, R. A. Catalytic Hydrogenation of Indole in Furnace Oil. *J. Chem. Eng. Data.* **1961**, *6*, 477.
79. Xu, J.; Nie, G.; Zhang, S.; Han, X.; Hou, J.; Pu, S. Electrosyntheses of freestanding polyindole films in boron trifluoride diethyl etherate. *J. Polym. Sci. A Polym. Chem.* **2005**, *43*, 1444-1453.
80. Katritzky, A.; Barcock, R.; Siskin, M.; Olmstead, W. Aqueous High-Temperature Chemistry of Carbocycles and Heterocycles .23. Reactions of Pyridine Analogs and Benzopyrroles in Supercritical Water at 460-Degrees-C. *Energ. Fuel.* **1994**, *8*, 990-1001.
81. Li, B.; Guo, W.; Yuan, S.; Hu, J.; Wang, J.; Jiao, H. A theoretical investigation into the thiophene-cracking mechanism over pure Brønsted acidic zeolites. *J. Catal.* **2008**, *253*, 212-220.
82. Liu, D.; Gui, J.; Sun, Z. Adsorption structures of heterocyclic nitrogen compounds over Cu(I)Y zeolite: A first principle study on mechanism of the denitrogenation and the effect of nitrogen compounds on adsorptive desulfurization. *J. Mol. Catal. A Chem.* **2008**, *291*, 17-21.
83. Langner, B. Reactions of Olefins on Zeolites - the Change of the Product Distribution with Time on Stream in the Reaction of Butene-1 on Calcined Nanh4-Y. *J. Catal.* **1980**, *65*, 416-427.
84. Li, S.; Lee, J.; Hyeon, T.; Suslick, K. Catalytic hydrodenitrogenation of indole over molybdenum nitride and carbides with different structures. *Appl. Catal. A-Gen.* **1999**, *184*, 1-9.
85. Shim, S.; Navrotsky, A.; Gaffney, T.; MacDougall, J. Chabazite: Energetics of hydration, enthalpy of formation, and effect of cations on stability. *Am. Mineral.* **1999**, *84*, 1870-1882.

86. Anonymous GSA Resources. <http://www.gsaresources.com/chabazit.htm> (accessed February/28, 2013).
87. Quignard, A. Part IV. Upgrading. In *Heavy Crude Oils - From Geology to Upgrading, an Overview*; Huc, A., Ed.; Editions Technip: 2010; .
88. Caniaz, R. O.; Erkey, C. Process intensification for heavy oil upgrading using supercritical water. *Chem. Eng. Res. Design* **2014**, *92*, 1845-1863.
89. Miller, J.; Fisher, R.; van der Eerden, A.; Koningsberger, D. Structural determination by XAFS spectroscopy of non-porphyrin nickel and vanadium in maya residuum, hydrocracked residuum, and toluene-insoluble solid. *Energy Fuels* **1999**, *13*, 719-727.
90. Sorokina, T. P.; Buluchevskaya, L. A.; Potapenko, O. V.; Doronin, V. P. Conversion of Nickel and Vanadium Porphyrins under Catalytic Cracking Conditions. *Petrol. Chem+* **2010**, *50*, 51-55.
91. Wormsbecher, R.; Cheng, W.; Kim, G.; Harding, R. Vanadium mobility in fluid catalytic cracking. In *Deactivation And Testing Of Hydrocarbon-Processing Catalysts*; OConnor, P Takatsuka, T Woolery, GL, Ed.; Amer Chemical Soc: Washington DC, 1996; Vol. 634, pp 283-295.
92. Caero, L.; Ordonez, L.; Ramirez, J.; Pedraza, F. Traps for simultaneous removal of SO_x and vanadium in FCC process. *Catal. Today* **2005**, *107-08*, 657-662.
93. Yumoto, M.; Kukes, S.; Klein, M.; Gates, B. Catalytic hydroprocessing of aromatic compounds: Effects of nickel and vanadium sulfide deposits on reactivities and reaction networks. *Ind. Eng. Chem. Res.* **1996**, *35*, 3203-3209.
94. Park, S.; Jeon, H.; Jung, K.; Woo, S. Regeneration of spent resid fluidized catalytic cracking catalyst by removing metal poisons such as V, Ni, and Fe. *Ind Eng Chem Res* **2003**, *42*, 736-742.

95. Roth, S.; Iton, L.; Fleisch, T.; Meyers, B.; Marshall, C.; Delgass, W. Metals Contamination of Aluminosilicate Cracking Catalysts by Ni-Tetraphenylporphin and Vo-Tetraphenylporphin. *J. Catal.* **1987**, *108*, 214-232.
96. Isaza, M. N.; Pachon, Z.; Kafarov, V.; Resasco, D. E. Deactivation of Ni-Mo/Al₂O₃ catalysts aged in a commercial reactor during the hydrotreating of deasphalted vacuum residuum. *Appl. Catal. A-Gen.* **2000**, *199*, 263-273.
97. Cho, S.; Jung, K.; Woo, S. Regeneration of spent RFCC catalyst irreversibly deactivated by Ni, Fe, and V contained in heavy oil. *Appl. Catal. B-Environ.* **2001**, *33*, 249-261.
98. Dechaine, G. P.; Gray, M. R. Chemistry and Association of Vanadium Compounds in Heavy Oil and Bitumen, and Implications for Their Selective Removal. *Energy Fuels* **2010**, *24*, 2795-2808.
99. Dechaine, G. P. Solubility and Diffusion of Vanadium Compounds and Asphaltene Aggregates, University of Alberta, Edmonton, Alberta, Canada, 2010.
100. Chen, A.; Chen, S.; Hua, D.; Zhou, Z.; Wang, Z.; Wu, J.; Zhang, J. Diffusion of heavy oil in well-defined and uniform pore-structure catalyst under hydrodemetallization reaction conditions. *Chem. Eng. J.* **2013**, *231*, 420-426.
101. Dechaine, G. P.; Maham, Y.; Tan, X.; Gray, M. R. Regular Solution Theories Are Not Appropriate for Model Compounds for Petroleum Asphaltenes. *Energy Fuels* **2011**, *25*, 737-746.
102. Dailey, K.; Rauchfuss, T. pi-complexes of metalloporphyrins as model intermediates in hydrodemetallation (HDM) catalysis. *Polyhedron* **1997**, *16*, 3129-3138.
103. Mandal, P. C.; Wahyudiono; Sasaki, M.; Goto, M. Non-catalytic vanadium removal from vanadyl etioporphyrin (VO-EP) using a mixed solvent of supercritical water and toluene: A kinetic study. *Fuel* **2012**, *92*, 288-294.

104. Wang, S.; Yang, J.; Xu, X. Effect of the cationic starch on removal of Ni and V from crude oils under microwave irradiation. *Fuel* **2011**, *90*, 987-991.
105. Welter, K.; Salazar, E.; Balladores, Y.; Marquez, O. P.; Marquez, J.; Martinez, Y. Electrochemical removal of metals from crude oil samples. *Fuel Process. Technol.* **2009**, *90*, 212-221.
106. Kunkely, H.; Vogler, A. Photodemetalation of silver(II) tetraphenylporphyrin. *Inorg. Chem. Commun.* **2007**, *10*, 479-481.
107. Tangstad, E.; Myrstad, T.; Myhrvold, E. M.; Dahl, I. M.; Stocker, M.; Andersen, A. Passivation of vanadium in an equilibrium FCC catalyst at short contact-times. *Appl. Catal. A-Gen.* **2006**, *313*, 35-40.
108. Etter, R. G.; Quinones, A. US 8361310 B2, 2013.
109. Etter, R. G. US 8372264 B2, 2013.
110. Metkar, P. S.; Harold, M. P.; Balakotaiah, V. Experimental and kinetic modeling study of NH₃-SCR of NO_x on Fe-ZSM-5, Cu-chabazite and combined Fe- and Cu-zeolite monolithic catalysts. *Chem. Eng. Sci.* **2013**, *87*, 51-66.
111. Moreno-Gonzalez, M.; Hueso, B.; Boronat, M.; Blasco, T.; Corma, A. Ammonia-Containing Species Formed in Cu-Chabazite As Per In Situ EPR, Solid-State NMR, and DFT Calculations. *J. Phys. Chem. Lett.* **2015**, *6*, 1011-1017.
112. Ruggeri, M. P.; Nova, I.; Tronconi, E.; Pihl, J. A.; Toops, T. J.; Partridge, W. P. In-situ DRIFTS measurements for the mechanistic study of NO oxidation over a commercial Cu-CHA catalyst. *Appl. Catal. B-Environ.* **2015**, *166*, 181-192.
113. Alvarado Ibarra, J.; Sotelo Lerma, M.; Meza Figueroa, D.; Maubert Franco, M.; Paz Moreno, F. A. Evaluating the Potential of a Natural Mexican Zeolite, Chabasita-Type, by Removal of Lead from Water. *Rev. Int. Contam. Ambient.* **2013**, *29*, 201-210.

114. Leyva-Ramos, R.; Monsivais-Rocha, J. E.; Aragon-Pina, A.; Berber-Mendoza, M. S.; Guerrero-Coronado, R. M.; Alonso-Davila, P.; Mendoza-Barron, J. Removal of ammonium from aqueous solution by ion exchange on natural and modified chabazite. *J. Environ. Manage.* **2010**, *91*, 2662-2668.
115. Yakout, S. M.; Borai, E. H. Adsorption behavior of cadmium onto natural chabazite: batch and column investigations. *Desalin. Water Treat.* **2014**, *52*, 4212-4222.
116. Zamzow, M.; Eichbaum, B.; Sandgren, K.; Shanks, D. Removal of Heavy-Metals and Other Cations from Waste-Water using Zeolites. *Sep. Sci. Technol.* **1990**, *25*, 1555-1569.
117. Ali, M.; Perzanowski, H.; Bukhari, A.; Alhaji, A. Nickel and Vanadyl Porphyrins in Saudi-Arabian Crude Oils. *Energy Fuels* **1993**, *7*, 179-184.
118. Stocker, M.; Tangstad, E.; Aas, N.; Myrstad, T. Quantitative determination of Ni and V in FCC catalysts monitored by ESR spectroscopy. *Catal. Lett.* **2000**, *69*, 223-229.
119. Kim, T.; Al-Mutairi, A.; Marafi, A. M. J.; Park, J.; Yoon, S.; Mochida, I. Characterization of metal complexes in Kuwait atmospheric residues. *Fuel Process Technol* **2014**, *126*, 497-503.
120. Zeng, Y.; Uden, P. High-Temperature Gas-Chromatography - Atomic-Emission Detection of Metalloporphyrins in Crude Oils. *HRC-J. High Resolut. Chromatogr.* **1994**, *17*, 223-229.
121. Hubaut, R.; Aissi, C.; Dejonghe, S.; Grimblot, J. ESR Identification of Vanadium Species Deposited on Al₂O₃ and MoS₂-Al₂O₃ Catalysts - Relevance to Catalytic Demetalation of Vanadyl Porphyrin. *J. Chim. Phys. Phys. -Chim. Biol.* **1991**, *88*, 1741-1755.
122. Boucher, L.; Katz, J. Infrared Spectra of Metalloporphyrins (4000-160 Cm⁻¹). *J. Am. Chem. Soc.* **1967**, *89*, 1340-&.
123. Mitchell, P. C. H.; Scott, C. E. Interaction of vanadium and nickel porphyrins with catalysts, relevance to catalytic demetallisation. *Catal. Today* **1990**, *7*, 467-477.

124. Barth, G.; Linder, R.; Bryson, C. Advances in Charge Neutralization for Xps Measurements of Nonconducting Materials. *Surf Interface Anal* **1988**, *11*, 307-311.
125. Karweik, D.; Winograd, N. X-Ray Photoelectron Spectroscopic Studies of Silver(iii) Octaethylporphyrin. *J. Am. Chem. Soc.* **1974**, *96*, 591-592.
126. Zaroni, R.; Boschi, T.; Licocchia, S.; Paolesse, R.; Tagliatesta, P. An Xps Study of Rh and Co Derivatives of Tetrapyrrole Macrocycles. *Inorg. Chim. Acta* **1988**, *145*, 175-177.
127. Karweik, D.; Winograd, N. Nitrogen Charge-Distributions in Free-Base Porphyrins, Metalloporphyrins, and their Reduced Analogs Observed by X-Ray Photoelectron-Spectroscopy. *Inorg. Chem.* **1976**, *15*, 2336-2342.
128. Kadish, K. M.; Smith, K. M.; Guillard, R. *The porphyrin handbook / editors, Karl M. Kadish, Kevin M. Smith, Roger Guillard*; San Diego : Academic Press, c2000: 2000; .
129. Wijesekera, T.; Dolphin, D. Some Preparations and Properties of Porphyrins. *Adv. Exp. Med. Biol.* **1985**, *193*, 229-266.
130. Abdo, S.; Cruz, M. I.; Fripiat, J. J. Metallation-De-Metallation Reaction of Tin Tetra(4-Pyridyl) Porphyrin in Na-Hectorite. *Clays Clay Miner.* **1980**, *28*, 125-129.
131. Wark, M.; Koch, M.; Bruckner, A.; Grunert, W. Investigation of zeolites by photoelectron and ion scattering spectroscopy - Part IV XPS studies of vanadium-modified zeolites. *J. Chem. Soc. Faraday T.* **1998**, *94*, 2033-2041.
132. Junaid, A. S. M.; Yin, H.; Koenig, A.; Swenson, P.; Chowdhury, J.; Burland, G.; McCaffrey, W. C.; Kuznicki, S. M. Natural zeolite catalyzed cracking-assisted light hydrocarbon extraction of bitumen from Athabasca oilsands. *Applied Catalysis A: General* **2009**, *354*, 44-49.
133. Gray, M. R. *Upgrading petroleum residues and heavy oils*; New York, NY (United States); Marcel Dekker Inc: 1994; .

134. Sadeghbeigi, R. *Fluid catalytic cracking handbook. [electronic resource] : an expert guide to the practical operation, design, and optimization of FCC units*; Oxford : Butterworth-Heinemann, 2012; 3rd ed: 2012; .
135. Zhang, J.; Shan, H.; Chen, X.; Liu, W.; Yang, C. Synergistic Process for High Nitrogen Content Feedstocks Catalytic Cracking: A Case Study of Controlling the Reactions of Nitrogen Compounds in Situ. *Ind Eng Chem Res* **2014**, *53*, 5718-5727.
136. Nur, H.; Ramli, Z.; Efendi, J.; Najati, A.; Rahman, A.; Chandren, S.; Yuan, L. S. Synergistic role of Lewis and Bronsted acidities in Friedel-Crafts alkylation of resorcinol over gallium-zeolite beta. *Catal. Commun.* **2011**, *12*, 822-825.
137. Almutairi, S. M. *The Role of Lewis and Brønsted Acidity for Alkane Activation Over Zeolites*, Technische Universiteit Eindhoven, Eindhoven, Netherlands, 2013.
138. Corma, A.; Wojciechowski, B. The Catalytic Cracking of Cumene. *Catal. Rev.* **1982**, *24*, 1-65.
139. Patrick, F.; Sugunan, S. Cracking of cumene on tungsten promoted ceria catalysts. *Reac. Kinet. Mech. Cat.* **2011**, *103*, 125-131.
140. Mavrodinova, V.; Popova, M.; Borbely, G.; Mihalyi, R.; Minchev, C. Transalkylation of toluene with cumene over zeolites Y dealuminated in solid-state. Part I. Effect of the alteration of Bronsted acidity. *Appl. Catal. A-Gen.* **2003**, *248*, 181-196.
141. Mavrodinova, V.; Popova, M.; Mihályi, R. M.; Pál-Borbély, G.; Minchev, C. Transalkylation of toluene with cumene over zeolites Y dealuminated in solid-state: Part II. Effect of the introduced Lewis acid sites. *Appl. Catal. A-Gen.* **2003**, *248*, 197-209.
142. Fukase, S.; Wojciechowski, B. The Cracking of Cumene on HZSM-5. *J. Catal.* **1986**, *102*, 452-455.

143. Corma, A.; Wojciechowski, B. Comparison of Hy and Lay Cracking Activity in Cumene Dealkylation. *J. Catal.* **1979**, *60*, 77-82.
144. Kissin, Y. V. Chemical Mechanisms of Catalytic Cracking Over Solid Acidic Catalysts: Alkanes and Alkenes. *Catalysis Reviews* **2001**, *43*, 85-146.
145. Williams, B.; Ji, W.; Miller, J.; Snurr, R.; Kung, H. Evidence of different reaction mechanisms during the cracking of n-hexane on H-USY zeolite. *Appl. Catal. A-Gen.* **2000**, *203*, 179-190.
146. Koyama, T.; Hayashi, Y.; Horie, H.; Kawauchi, S.; Matsumoto, A.; Iwase, Y.; Sakamoto, Y.; Miyaji, A.; Motokura, K.; Baba, T. Key role of the pore volume of zeolite for selective production of propylene from olefins. *Phys. Chem. Chem. Phys.* **2010**, *12*, 2541-2554.
147. Tukur, N.; Al-Khattaf, S. Catalytic cracking of n-dodecane and alkyl benzenes over FCC zeolite catalysts: Time on stream and reactant converted models. *Chem. Eng. Process* **2005**, *44*, 1257-1268.
148. Wu, G.; Katsumura, Y.; Matsuura, C.; Ishigure, K.; Kubo, J. Comparison of liquid-phase and gas-phase pure thermal cracking of n-hexadecane. *Ind. Eng. Chem. Res.* **1996**, *35*, 4747-4754.
149. Komatsu, T.; Ishihara, H.; Fukui, Y.; Yashima, T. Selective formation of alkenes through the cracking of n-heptane on Ca²⁺-exchanged ferrierite. *Appl. Catal. A-Gen.* **2001**, *214*, 103-109.
150. Abbot, J.; Wojciechowski, B. The Effect of Temperature on the Product Distribution and Kinetics of Reactions of Normal-Hexadecane on HY Zeolite. *J. Catal.* **1988**, *109*, 274-283.
151. Friette, V.; Weisz, P.; Golden, R. Catalysis by Crystalline Aluminosilicates .1. Cracking of Hydrocarbon Types Over Sodium and Calcium-X Zeolites. *J. Catal.* **1962**, *1*, 301-306.

152. Escobar, A. S.; Pereira, M. M.; Cerqueira, H. S. Effect of iron and calcium over USY coke formation. *Appl. Catal. A-Gen.* **2008**, *339*, 61-67.
153. Agudo, A.; Asensio, A.; Corma, A. Cracking of N-Heptane on a CrHNaY Zeolite Catalyst - the Network of the Reaction. *J. Catal.* **1981**, *69*, 274-282.
154. Rane, N.; Kersbulck, M.; van Santen, R. A.; Hensen, E. J. M. Cracking of n-heptane over Bronsted acid sites and Lewis acid Ga sites in ZSM-5 zeolite. *Micropor. Mesopor. Mat.* **2008**, *110*, 279-291.
155. Corma, A.; Wojciechowski, B. The Nature of the Active-Sites in the Reactions of Cumene on Hy and Lay Catalysts. *Can. J. Chem. Eng.* **1980**, *58*, 620-625.
156. Yaws, C. L.; Li, K. Y. Chapter 13 - Solubility parameter and liquid volume—Organic compounds. In *Thermophysical Properties of Chemicals and Hydrocarbons*; Yaws, C. L., Ed.; William Andrew Publishing: Norwich, NY, 2009; pp 597-643.